

Old Dominion University

ODU Digital Commons

Civil & Environmental Engineering Theses & Dissertations

Civil & Environmental Engineering

Fall 2015

Behavior and Strength of Pultruded FRP I-Section Columns Including Uniaxial and Biaxial Bending

Emad M. Amin

Old Dominion University, eamin002@odu.edu

Follow this and additional works at: https://digitalcommons.odu.edu/cee_etds



Part of the [Civil Engineering Commons](#), and the [Structural Engineering Commons](#)

Recommended Citation

Amin, Emad M.. "Behavior and Strength of Pultruded FRP I-Section Columns Including Uniaxial and Biaxial Bending" (2015). Master of Science (MS), Thesis, Civil & Environmental Engineering, Old Dominion University, DOI: 10.25777/jfirt-sj95
https://digitalcommons.odu.edu/cee_etds/4

This Thesis is brought to you for free and open access by the Civil & Environmental Engineering at ODU Digital Commons. It has been accepted for inclusion in Civil & Environmental Engineering Theses & Dissertations by an authorized administrator of ODU Digital Commons. For more information, please contact digitalcommons@odu.edu.

**BEHAVIOR AND STRENGTH OF
PULTRUDUD FRP I-SECTION
COLUMNS INCLUDING UNIAXIAL
AND BIAXIAL BENDING**

by

Emad M. Amin

BSc. Civil Engineering

A Thesis Submitted to the Faculty of Old Dominion
University in Partial Fulfillment of the
Requirements for the Degree of

MASTER OF SCIENCE

CIVIL ENGINEERING

OLD DOMINION UNIVERSITY

November 2015

Approved by:

Zia Razzaq (Director)

Chae Yunbyeong (Member)

Mojtaba Sirjani (Member)

ABSTRACT

BEHAVIOR AND STRENGTH OF PULTRUDED FRP I-SECTION COLUMN INCLUDING UNIAXIAL AND BIAXIAL BENDING

Emad M. Amin
Director: Dr. Zia Razzaq

This thesis presents the outcome of a study of the behavior and strength of pultruded glass fiber reinforced polymer (FRP) I-section columns including uniaxial and biaxial applied bending moments. Also included in the study is a critical assessment of ASCE-LRFD Pre-standard for pultruded FRP structures in view of the rigorous analysis presented herein. The theoretical solution is based on a system of three coupled differential equations of equilibrium combined with pinned flexural and torsional boundary conditions. Effects of induced warping due to second-order terms as well as initial out-of-straightness are accounted-for in the governing differential equations. Detailed investigations into the nonlinear response up to material cracking are conducted for centrally loaded column, uniaxially loaded beam-columns loaded about the cross-sectional minor axis and those loaded about the major axis with continuous lateral support, and biaxially loaded beam-columns. Serious flaws in the ASCE-LRFD Pre-Standard are found in light of the rigorous analysis presented in this thesis such as the strength prediction expressions for centrally loaded columns as well as those with uniaxial and biaxial bending. It is also found that induced warping normal stresses due to second-order torsional effects are not negligible. The results presented herein can aid in the development of accurate strength prediction formulae to replace the flawed ones in the ASCE-LRFD Pre-Standard.

ACKNOWLEDGMENTS

The author wishes to express his sincere appreciation to Professor Zia Razzaq, who supervised this thesis. Without his technical guidance and encouragement this thesis would not be possible. Special thanks are also extended to all of the professors, who provided their assistance to the author during his learning journey.

The author dedicates this work to his parents and family who have made huge contributions to his learning and ultimate success in his life. The patience and encouragement of the author's wife were also vital to completion of this work.

TABLE OF CONTENTS

Chapter	Page
1. INTRODUCTION	
1.1 Preliminary Remarks	7
1.2 Literature Review	8
1.3 Problem Definition	14
1.4 Objective and Scope	14
1.5 Assumptions and Conditions	15
2. ANALYSIS BASED ON DIFFERENTIAL EQUATIONS	
2.1 Column with Initial Out-of-Straightness	16
2.2 Uniaxially Loaded Beam-Column with Initial Out-of-Straightness.....	22
2.3 Biaxially Loaded Beam-Column with Initial Out-of-Straightness.....	24
3. ANALYSIS BASED ON ASCE-LRFD PRE-STANDARD	
3.1 Column with Initial Out-of-Straightness	27
3.2 Uniaxially Loaded Beam-Column with Initial Out-of-Straightness	30

	Page
3.3 Biaxially Loaded Beam-Column with Initial Out-of-Straightness	35
4. COMPARISON OF RESULTS AND DISCUSSION	
4.1 Column	36
4.2 Uniaxially Loaded Beam-Columns.....	38
4.3 Biaxially Loaded Beam-Columns.....	39
4.4 Critique of ASCE-LRDF Pre-Standard.....	39
5. CONCLUSIONS AND FUTURE RESEARCH	
5.1 Conclusions	42
5.2 Future research	43
REFERENCES	45
APPENDECIES	
Tables	46
Figures	107
C	177
VITA.....	184

CHAPTER 1

INTRODUCTION

1.1 Preliminary Remarks

The use of pultruded Fiber Reinforced Polymer (FRP) structural products has gained considerable momentum during the past couple of decades. Although a considerable body of literature related to the structural performance of FRP beams, columns, beam-columns, and panels exists, several crucial areas related to the study of the behavior and strength of such members is still quite deficient. One specific problem that has existed for a considerable period of time is the absence of reliable behavior and load prediction models and formulas in the form of a formal set of specifications for use in the analysis and design of FRP structural members. In 2010, the American Society of Civil Engineers (ASCE) produced a Load and Resistance Design Factor (LRFD) Pre-Standard to tentatively fill this need, however, it is both deficient and very flawed in certain areas.

The primary focus of this thesis is on determining the load-carrying capacity of centrally loaded Fiber Reinforced Polymer (FRP) columns, and both uniaxially and biaxially loaded beam-columns with geometric initial imperfections. The motivation of the study comes from the need to quantitatively assess the degree to which the ASCE-LRFD Pre-Standard is flawed in being able to predict the load-carrying capacities of such structural members. To achieve this, a finite-difference based numerical solution approach is used to solve governing

differential equations of equilibrium for such members in the presence of member geometric imperfections.

The outcome of rigorous numerical analysis of the governing differential equations with appropriate flexural and torsional boundary conditions is presented in the form of load-deflection relations, stiffness degradation curves, load-moment interaction curves, and member load-carrying capacities. A comparison of the results is then made with those based on the ASCE-LRFD Pre-Standard.

1.2 Literature Review

Presented below is a brief of publications relevant to the subject discussed in present study. To the best of the author's knowledge, no similar study was published before.

To measure the short-term critical loading and compare it with the theoretical critical loading for a pultruded I-beam under linear elastic lateral-torsional buckling. For I-beam simply supported about the major axis, and fixed about the minor axis at both ends which causes restrained warping and twisting for the member. The load is applied at the central point to the top flange. The critical loads calculated using finite-difference method are more realistic. Finite-difference method was used to derive the governing differential equations of the thin-walled theory. (Mottram, 1992)

FRP sections are suitable for the application in the construction field because they can be produced with different cross-sections and lengths. Their high corrosion resistance makes FRP much appreciated when used in high corrosive environments. However, design

criteria for this material are not fully developed. FRP tends to buckle easily because FRP members are composed of thin plate component. For this reason, in design, buckling is one of the main governing limits. The analytical study results relating to the buckling behavior for I-shape FRP compression member. Some studies adopted a design procedure similar to that used in AISC 360-10 with performing some minor modification. (Yoon, Jung and Jang, 1993)

A number of GRP pultruded I-section cantilever beams were selected to conduct a series of lateral buckling tests. The results of the theoretical loads calculated from approximate formulae, and numerical finite element eigenvalue method, were compared. The study suggests that linear buckling analysis gives inaccurate estimation for the critical loads and it is not recommended to be used in design. It is also suggested that initial out-of-straightness and pre-buckling deformation might be of value that must be included in the design formulas in order to get accurate critical load for pultruded GRP cantilever. (Brooks and Turvey, 1995)

Some studies present a comparison between experimental and analytical approach of the flexural-torsional buckling behavior of pultruded fiber reinforced plastic I-beam. Two pultruded FRP I-beams were tested under mid-span concentrated loads to measure their flexural-torsional buckling responses. Non-linear elastic theory was used to derive total potential energy equations for the instability of the FRP I-beams. The Rayleigh-Ritz method was used to solve the equilibrium equation in terms of the total potential energy. Some engineering equations were formulated to predict the critical flexural-torsional

buckling loads. The conclusions suggested a good agreement between the experimental results and finite-element analysis. (Davalos, Qiao, and Salim, 1997)

The behavior of polymeric composite columns was investigated. Twelve wide-flange columns manufactured by the pultrusion process are used to study the minor-axis buckling. Different parameters used mainly are heights and cross-sectional dimensions. Deformation and failure characteristics are presented. This study shows correlation between the maximum test loads and Euler critical buckling load. The differences between both loads are due to imperfection in the column specimens and the test rig. (Mottram, Brown, and Anderson, 2003)

Fiber Reinforced Polymer (FRP) is manufactured worldwide with different specifications. As of today, there is no approved American standards institute for structural design code for the pultruded profiles in the United States. Each manufacturer of pultruded profiles depends on its own design equations, design method, material properties, and safety factors for their FRP products. In structural engineering practice, there is a real need for standards to regulate the production and the design of pultruded reinforced fibers. This study suggests an appropriate way to find the resistance factors and a unified analytical equation for local and global buckling of concentrated axial loads for the FRP members that can be used in the future in the design code. The resistance factors are provided for different levels of structural reliability β , and for verities of nominal design properties of the FRP profiles. The Monte Carlo method was used to determine the resistance factors. Manufacturing design codes were used in calculating the resistance factor and a

comparison between both results was presented. (Vanevenhoven, Shield, and Bank, 2010)

Another paper study the effect of the unbraced length of a twenty six specimen of pultruded fiber reinforced plastic (PFRP) cantilever channel beams, on the lateral-torsional buckling behavior and the buckling moment of the beam. Comparisons were made between the buckling moments of the beams and the critical buckling moment, calculated using modified LRFD for the steel design equation. Depending on the range of the linear elastic response, the response curve was classified into two types: short beams and slender beams. Lateral-torsional buckling was the general mode of failure. (Thumrongvut, and Seangatith, 2011)

The lack of suitable design codes for pultruded fiber reinforced polymer has delayed the acceptance to use this material. Some of analytical and numerical structural design tools were developed recently that need to validate the accuracy of the results using additional and experimental data. This study is based on experimental data using first-order, buckling and post-buckling behaviors of pultruded FRP I-beams. At the first stage, test were conducted on small-scale specimens to determine the most relevant material mechanical properties. In the second stage, full scale pultruded I-beams were used with simply-supported boundary conditions that had varying spans under three points bending, and cantilever with varying spans with a tip point load applied at the end through the centroid. The cantilever was used to determine the failure from the lateral-torsional buckling. The study suggest that the instability is often governed by a large amount of deformations and/or local and global buckling due to low Young's modulus and high

strength of the fiber reinforced polymer. Due to low shear-to-Young's modulus ratio shear deformations are quite irrelevant. (Correia, Branco, Camotim, and Silvetre, 2011)

Lateral torsional buckling (LTB) resistance of Pultruded fiber reinforced polymer (FRP) I-beam is calculated using geometric non-linear finite element analysis. When initial out-of-straightness was associated with the lateral torsional buckling mode, this study proposes a data reduction method to determine the critical buckling load. This study used range of beam slenderness and initial out-of-straightness. To present the influence of changing load, height, or displacement boundary conditions on the member resistance, Eigenvalue finite element analysis was used. Comparing the predicted critical load of the beam with the elastic constant of either FRP or steel, it is found that the former has relatively larger effect on buckling strength with changing in load, height, and end warping fixity. The study suggests that the developed finite element method formulations is reliable for the design of FRP beams against lateral-torsional buckling failure.(Nguyen, Chan, and Mottram, 2013)

Using Galerkin method, this study represents the nonlinear governing equations of rotationally-restrained laminated composite plates with initial out-of-straightness. For post-buckling analysis, the governing equations were solved using Newton-Raphson method. The laminates used in this study are assumed to be symmetric and they are loaded in pure in-plane shear and compression. The deformation shape function of the restrained plates is obtained through a linear combination of vibration Eigen functions of simply supported and clamped beams along either the longitudinal or transverse direction of plates. This study suggests that the methods used are valid and effective for performing the

nonlinear analysis of laminates with all four edges elastically-restrained against rotation. A parameter study is used to validate the effect of rotational spring stiffness, material properties, and fiber orientation under pure in-plane shear as the loading ratio under combined shear and compression on the nonlinear static and post-buckling behavior of rotationally-restrained laminates. This study suggests that the solution for nonlinear static analysis of rotationally-restrained composite plates with imperfection is accurate and effective. (Qiao, and Chen, 2015)

To estimate shear and flexural properties of Pultruded Fiber-Reinforced Plastic (PFRP), usually three-and-four point scheme is used. The beam rigidities in Timoshenko beam model is found from the linear combinations of the experimental deflections. The parameter identification in Timoshenko model can be affected by many uncertainties. Wide-flange sections analyzed using new test configuration compared to Timoshenko model of three-and-four point schemes. The relative position of the applied load, using different span lengths and for the four-point scheme was investigated analyzing the influence of the load and deflection measurement errors, and providing the proper confidence intervals for the computed rigidities. (Minghini, Tullini, and Laudiero)

Fiber-reinforced plastic (FRP) beams and columns are being used for different structural applications where buckling is the main criteria in the design process. Processes developed models using local buckling modes under axial and shear loading, taking into account the interaction between the flange and the web. For some available cross-sections, observed behaviors are presented and predicted some experimental data. Developed failure envelopes for FRP I-shape and box shape beams and columns. This analysis method can

be used to predict the behavior of any new pultruded material. To analyze anisotropic flanges of I-beams and box-shape, the Rayleigh-Ritz method was used in this paper. The conclusion suggests using 45 degree angle-ply layers to improve the buckling strength of the columns. (Brbero, and Raftoyiannis)

1.3 Problem Definition

Five different pin-pin cases were studied and included in this thesis with different load combinations and different lengths with initial out-of-straightness. The structural element capacity for each case is calculated using finite difference method and compared to the capacity calculated using the equations used by the ASCE-LRFD Pre-Standard. The analysis are limited to elastic second-order analysis for IW660 and IW880 Pultex Wide Flange Sections. The lengths adopted are: 6, 12, and 18 feet, and the initial out-of-straightness are: $L/100000$, $L/1000$, $L/500$, and $L/250$ for each length. The axial load P increased from zero to the critical load P_E for each bending moment. Exact solution for the differential equations can be obtained easily for case 2.1. However, for cases 2.2 and 2.3, exact solutions are more complicated and for that reason, finite difference method only was used in these cases.

1.4 Objectives and Scope

The objective of this thesis is to calculate the capacity of the wide flange I-sections, by using the finite difference method, for different load combinations, lengths and initial out-of-straightness, and compare the results to those obtained from the equations used by

the ASCE-LRFD Pre-Standard. ASCE-LRFD Pre-Standard adopted amplification factors that were used to multiply the results obtained from the first-order analysis in order to reflect the effects of the second-order analysis.

IW660 and IW880 Pultex Wide Flange Sections were used. Minimum required characteristic mechanical properties for FRP composite shapes can be found in table 2.

1.5 Assumptions and Limitations

The following assumptions are made in the theoretical analysis:

1. The material is homogenous.
2. Plane cross section remains plane before and after deformation.
3. Residual stresses are neglected.
4. Both initial shape and deflection curves of the structural member are assumed to be sinusoidal.
5. The ends are pinned, prevented from translating with respect to each other.
6. The forces are only applied at the ends.
7. The differential equations are formulated on the deformed member.
8. All members are in braced-frame structural systems.

CHAPTER 2

ANALYSIS BASED ON DIFFERENTIAL EQUATIONS

2.1 Column with Initial Out-of-Straightness

Columns without residual stresses and with initial out-of-straightness for pultruded CFRP members, will fail when the fibers at the concave side starts to crush. According to this circumstances, a column with initial out-of-straightness carries a critical load less than that given by Euler's formula. The critical load of the column is closer to Euler's formula prediction for very long columns.

2.1.1 Major Axis Response

2.1.1. a Exact Solution

In this section, an exact solution is found for the differential equation. The relationship between load P versus total deflection in the middle of the span $V(\frac{L}{2})$ is drawn to define the behavior of wide flange pultruded CFRP column with initial out-of-straightness bent about the strong axis. Equation (2.1) is used to calculate the initial out-of-straightness along the span of the column.

$$v_i = \delta_{oy} \sin\left(\frac{\pi z}{L}\right) \quad (2.1)$$

v_i is deflection along the span assuming that the deflection curve is sinusoidal. Total deflection along the span V is obtained by adding deflection due to external loads v to the initial out-of-straightness v_i .

$$V(z) = v(z) + v_i \quad (2.2)$$

The general deflection equation for this case is.

$$E I_x \left(\frac{d^2 v}{dz^2} \right) + P V = 0 \quad (2.3)$$

$$E I_x \left(\frac{d^2 v}{dz^2} \right) + P v = - P \delta_{oy} \sin \left(\frac{\pi z}{L} \right) \quad (2.4)$$

The general solution for the above equation is.

Let

$$\lambda_x = \frac{P}{E I_x} \quad (2.5)$$

$$V(L) = C_1 \cos(z \sqrt{\lambda}) + C_2 \sin(z \sqrt{\lambda}) + \frac{\delta_{oy} \lambda L^2 \sin\left(\frac{\pi z}{L}\right)}{(\pi^2 - \lambda L^2)} \quad (2.6)$$

Using the boundary conditions for pin- pin column:

$$\Phi(0) = \Phi(L) = 0 \text{ and } \Phi''(0) = \Phi''(L) = 0$$

Solving eq. (2.6) for constants value $C_1 = 0$ and $C_2 = 0$.

Substituting C_1 and C_2 in equation (2.6), the total deflection in y-axis at the mid-span can be found using the below equation.

$$V\left(\frac{L}{2}\right) = - \frac{\delta_{oy}}{\left[1 - \left(\frac{PE}{P}\right)\right]} \quad (2.7)$$

Where P_E is Euler's critical load of the column, and is given in the below equation.

$$P_E = \frac{\pi^2 EI_x}{L^2} = (P_x)_{cr} \quad (2.8)$$

$$\sigma_{cr} = \pm \frac{P}{A} \pm \frac{PVC}{I_x} \quad (2.9)$$

Where

σ_{cr} : is the longitudinal compressive strength.

A: is the cross sectional area.

C: is $\frac{h}{2}$

The strength of the member can be calculated from equation (2.9). Lengths of: 6ft, 12ft, and 18ft are used, with δ_{oy} values of: L/100000, L/1000, L/500, and L/250 for each length.

2.1.1.b Finite-Difference Method

This method is one of the numerical methods used to solve problems with conditions that are very complicated. Numerical methods in general have the advantage that they can be programmed and handled easily. The basis of this method is the derivative consisting of the value of the function at that point and at several nearby points. Finite-Difference Method can be used as forward, backward, and central differences. Derivative expressions in terms of the value of the function at the pivotal point z and the point to the right is known as forward-finite-differences. Similarly, if the values of the function at the pivotal point z and the point to the left are used, this is known as backward-finite-differences. Expressions for the derivatives that involve both values of the function to the

left and right of the pivotal point z are called central-finite-differences. Central-finite-difference method is more accurate, and it is adopted in this thesis. The member is divided into twenty nodes as shown in figure (1), therefore $\Delta z = h = \frac{L}{20}$. The deflection in y -axis direction is labeled as V . The second order derivative expression is shown below.

$$\frac{d^2v}{dz^2} = \frac{v_{i-1} - 2v_i + v_{i+1}}{h^2} \quad (2.10)$$

Let

$$\lambda_x = \frac{h^2}{EI_x}$$

Equation (2.4) can be written as follows:

$$v_{i-1} + (\lambda_x P - 2)v_i + v_{i+1} = -\lambda_x P \delta_{o\gamma} \sin\left(\frac{\pi z}{L}\right) \quad (2.11)$$

Central-finite-difference method uses fictitious grid points beyond the support points. Applying equation (2.11) to the nodes along the span will give a series of equations that will be used to create a square matrix with number of rows and columns equal to the number of nodes.

To find $(P_x)_{cr}$ in this method, the stiffness degrading curve is plotted. $(P_x)_{cr}$ is the value of load P at the point $\frac{K_P}{K_o} = 0$. Figures 1, 2, and 3 shows the stiffness degradation curve for case 2.1.1.

2.1.2 Minor Axis Response

2.1.2.a Exact Solution

In this section, the wide flange pultruded CFRP section is bent about the minor axis.

The initial out-of-straightness is calculated using Equation (2.12)

$$u_i = \delta_{ox} \sin\left(\frac{\pi z}{L}\right) \quad (2.12)$$

The total deflection U is calculated using Equation (2.13)

$$U(z) = u(z) + u_i \quad (2.13)$$

The general differential equation for this case is

$$EI_Y \frac{d^2 u}{dz^2} + P U(z) = 0 \quad (2.14)$$

Using the same procedure in case 2.1.1.a, the total deflection in mid-span $U\left(\frac{L}{2}\right)$ is calculated as follows:

$$U\left(\frac{L}{2}\right) = -\frac{\delta_{ox}}{\left[1 - \left(\frac{P}{PE}\right)\right]} \quad (2.15)$$

Where PE is Euler's critical load of the column, and is given in the below equation.

$$P_E = \frac{\pi^2 EI_Y}{L^2} = (P_\gamma)_{cr} \quad (2.16)$$

$$\sigma_{cr} = \pm \frac{P}{A} \pm \frac{P U C}{I_Y} \quad (2.17)$$

Where

σ_{cr} : is the longitudinal compressive strength.

A: is the cross sectional area.

C: is $\frac{b}{2}$

Length of 6ft, 12ft, and 18ft are used, with δ_{ox} values of: L/100000, L/1000, L/500, and L/250 for each length.

2.1.2.b Finite-Difference Method

Using central-finite-difference method for twenty nodes, the second-order differential expression is as follows:

$$\frac{d^2u}{dz^2} = \frac{u_{i-1} - 2u_i + u_{i+1}}{h^2} \quad (2.18)$$

Finite-Difference formulation for this case is found by substituting equations (2.12) and (2.18) into equation (2.14).

$$EI_Y \frac{d^2u}{dz^2} + P u(z) = -P \delta_{ox} \sin\left(\frac{\pi z}{L}\right) \quad (2.19)$$

Let

$$\lambda_Y = \frac{(EI_Y)}{h^2}$$

Equation (2.19) after rearrangements is written as follows:

$$u_{i-1} + (\lambda_y P - 2)u_i + u_{i+1} = -\lambda_y P \delta_{ox} \sin\left(\frac{\pi z}{L}\right) \quad (2.20)$$

Equation (2.20) is applied for each node to construct member stiffness matrix. Lengths of: 6, 12, 18ft is used with deflections: $L/100000$, $L/1000$, $L/500$, and $L/250$ for each length.

2.2 Uniaxially Loaded Beam-Column with Initial out-of-straightness

The response of beam-column is different than the response of the columns and beams. The axial load P that can be supported by the column, is larger than the maximum axial load P can be supported by beam-column, allowing the member to support the applied bending moments M . Using same analogy, beam-columns carry smaller bending moments M than beams to spare part of the member's capacity to support the applied axial load P .

2.2.1 Major Axis Response

Applying different constant bending moments M_{ox} at the end of the member, with increasing the axial load P from zero to the critical load P_E . Different lengths L are used for each bending moment M_{ox} , and different deflections δ_{oy} for each length L . Due to the complexity of the exact solution, Finite-Difference method is used in this section and beyond. The Finite-Difference formula is shown below:

$$EI_x \frac{d^2 v}{dz^2} + Pv(z) = -M_{ox} - P\delta_{oy} \sin\left(\frac{\pi z}{L}\right) \quad (2.21)$$

Since

$$\frac{d^2 v}{dz^2} = \frac{v_{i-1} - 2v_i + v_{i+1}}{h^2}$$

Therefore Equation (2.21) can be written as follows:

$$v_{i-1} + (\lambda_x P - 2)v_i + v_{i+1} = -\lambda_x M_{ox} - \lambda_x P \delta_{oy} \sin\left(\frac{\pi z}{L}\right) \quad (2.22)$$

In which

$$\lambda_x = \frac{h^2}{EI_x}$$

The critical load for this case is calculated using the following equation:

$$\sigma_{cr} = \pm \frac{P}{A} \pm \frac{PVC}{I_x} \pm \frac{M_{ox}C}{I_x} \pm E \omega_n \varnothing \quad (2.23)$$

2.2.2 Minor Axis Response

The finite-Difference formulation in this case is shown as follows:

$$EI_y \frac{d^2 u}{dz^2} + Pu = -M_{oy} - P \delta_{ox} \sin\left(\frac{\pi z}{L}\right) \quad (2.24)$$

Substituting $\lambda_y = \frac{h^2}{EI_y}$ in equation (2.24) with rearrangement, the general Finite-

Difference equation that is used to formulate the member stiffness matrix can be written as follows:

$$u_{i-1} + (\lambda_y P - 2)u_i + u_{i+1} = -\lambda_y M_{oy} - \lambda_y P \delta_{ox} \sin\left(\frac{\pi z}{L}\right) \quad (2.25)$$

The critical load stress that the member can carry before crack occurs, can be calculated using the following equation

$$\sigma_{cr} = \pm \frac{P}{A} \pm \frac{PUC}{I_y} \pm \frac{M_y C}{I_y} \quad (2.26)$$

2.3 Biaxially Loaded Beam-Column with initial Out-of-Straightness

The theory of in-plane beam-column is used in the previous sections assuming that, all of the members in a structure lying in a single plane, with all of the loads applied in same plane. This assumption may not reflect that actual design loading. In actual structure, the beam-column takes in count bending moments acting about the principle axes of the cross section of the member, in addition to an axial compression or tension load. This type of loading known as biaxial loading.

The differential equations governing the elastic behavior of this type of loading is shown below:

$$B_x \frac{d^2v}{dz^2} + PV(z) + M_{oy}\Phi(z) = -M_{ox} \quad (2.27)$$

$$B_y \frac{d^2u}{dz^2} + PU(z) + M_{ox}\Phi(z) = M_{oy} \quad (2.28)$$

$$C_\omega \frac{d^4\Phi}{dz^4} - C_T \frac{d^2\Phi}{dz^2} + M_{ox} \frac{d^2u}{dz^2} + M_{oy} \frac{d^2v}{dz^2} = 0 \quad (2.29)$$

Where

Φ is the angle of twist.

B_x is the bending stiffness about x-axis, and define as: $B_x = EI_x$.

B_y is the bending stiffness about Y-axis, and define as: $B_y = EI_y$.

C_ω is the warping stiffness, and define as: $C_\omega EI_\omega$

C_T is the St. Venant stiffness, and define as: $C_T = GK_T$

G is the shear modulus.

K_T is the torsional constant, and define as: $K_T = \frac{1}{3} \sum b t^3$.

Finite-Difference formulation after rearrangements is as follow:

$$v_{i-1} - (\lambda_x P - 2)v_i + v_{i+1} + \lambda_x M_{oy} \Phi_i = -\lambda_x M_{ox} - \lambda_x \delta_{oy} P \sin\left(\frac{\pi z}{L}\right) \quad (2.30)$$

$$u_{i-1} + (\lambda_y P - 2)u_i + u_{i+1} + \lambda_y M_{ox} \Phi_i = \lambda_y M_{oy} - \lambda_y \delta_{ox} P \sin\left(\frac{\pi z}{L}\right) \quad (2.31)$$

$$C_1 \Phi_{i-2} - C_3 \Phi_{i-1} + C_4 \Phi_i - C_3 \Phi_{i+1} + C_1 \Phi_{i+2} + \frac{M_{ox}}{h^2} [u_{i-1} - 2u_i + u_{i+1}] + \frac{M_{oy}}{h^2} [v_{i-1} - 2v_i + v_{i+1}] = 0 \quad (2.32)$$

Where

$$C_1 = \frac{C\omega}{h^4}$$

$$C_2 = \frac{C\tau}{h^2}$$

$$C_3 = 4C_1 + C_2$$

$$C_4 = 6C_1 + 2C_2$$

The critical load strength can be calculated as follows:

$$\sigma_{cr} = \pm \frac{P}{A} \pm \frac{M\xi Y}{I_x} \pm \frac{PVY}{I_x} \pm \frac{M\eta X}{I_y} \pm \frac{PUX}{I_y} \pm E \omega_n \phi \quad (2.33)$$

Where

$$M_{\xi} = M_{ox} + \phi M_{oy}$$

$$M_{\eta} = M_{oy} - \phi M_{ox}$$

$$Y = \frac{d}{2}$$

$$X = \frac{b}{2}$$

CHAPTER 3

ANAYSIS BASED ON ASCE-LRFD PRE-STANDARD

This Pre-Standard was issued to design the structures constructed of Fiber-reinforced polymer composite structural shapes. ASCE-LRFD Pre-Standard adopted amplification factors that used to multiply the results obtained from the first-order analysis in order to reflect the effects of the second-order analysis.

3.1 Columns with Initial Out-of-Straightness

3.1.1 Major Axis Response

The equations used by ASCE-LRFD Pre-Standard to design the straight columns without initial out-of-straightness is as follows:

$$P_u \leq \lambda \Phi_c P_n \leq 0.7 \lambda F_c^c A_g \quad (3.1)$$

Where

$$\Phi_c = \Phi_c F_{cr} A_g$$

For I-shaped cross sections in which the x-axis and the y-axis are principle axes, $\Phi_c F_{cr}$ shall be taken as the smallest value of the following equations:

$$F_{crx} = \frac{\pi^2 E_c}{\left(K_x \frac{L_x}{r_x}\right)^2}, \quad \Phi_c = 0.7 \quad (3.2)$$

$$F_{cry} = \frac{\pi^2 E_c}{\left(K_y \frac{L_y}{r_y}\right)^2}, \quad \Phi_c = 0.7 \quad (3.3)$$

$$F_{crf} = \frac{G_{cr}}{\left(\frac{bt}{2t_f}\right)^2} \cdot \Phi_c = 0.8 \quad (3.4)$$

$$F_{crw} = \frac{\left(\frac{\pi^2}{6}\right) \left[\sqrt{(E_L w E_T w) + \nu_{LT} E_T w + 2G_{LT}} \right]}{\left(\frac{h}{tw}\right)^2}, \quad \Phi_c = 0.8 \quad (3.5)$$

Where

P_u = Required compression strength due to factored loads.

λ = Time effect factor. Assumed to be 1.0

P_n = Nominal axial compression strength

$\Phi_c F_{cr}$ = Factored critical stress

A_g = Gross area of the cross section

F_L^c = Minimum longitudinal compression material strength of all elements comprising the cross section.

E_L = Characteristic value of the longitudinal compression elastic modulus of the flange or web, whichever is smaller.

$\frac{KL}{r}$ = effective slenderness ratio.

F_{crx} = Elastic flexural buckling stress about x-axis.

F_{cry} = Elastic flexural buckling stress about y-axis.

F_{crf} = Local flange buckling stress.

F_{crw} = Local web buckling stress.

K_x = Effective length factor corresponding to x-axis.

K_y = Effective length factor corresponding to y-axis.

L = Laterally unbraced length of member.

r = radius of gyration.

E_{TW} = Elastic modulus of the web in the direction perpendicular to the pultrusion direction.

ν_{LT} = Poisson's Ratio

For columns with initial out-of-straightness, ASCE-LRDF Pre-Standard gives the following equations:

$$P_s \leq \Phi_o \frac{\pi^2 E_L}{\left(\frac{KL_e}{r}\right)^2} A_g \leq 0.3 F_c^c A_g \quad (3.6)$$

$$\Phi_o = 1 - 500 \left(\frac{\delta_o}{L}\right) \quad (3.7)$$

Where

P_s = Compression force due to serviceability load.

Φ_o = reduction factor that account for the initial out-of-straightness.

$\frac{\delta_o}{L}$ = initial out-of-straightness fraction guaranteed by pultrusion manufacturer.

ASCE-LRDF Pre-Standard considers structural members to be straight if the initial out-of-straightness is equal or less than L/500. Rejection of the structural members is solely related to excessive local deformations.

3.1.2 Minor Axis Response

The same procedure in subsection 3.1.1 is used to calculate the critical load for the column. Changes are required only for the limit $\frac{\pi^2 E_c}{\left(K \frac{L_e}{r_y}\right)^2}$. The slenderness ratio in this case is for the y-axis, while the rest of the equations remain unchanged.

3.2 Uniaxially Loaded Beam-Column with Initial Out-of-Straightness

3.2.1 Major Axis Response

The equation used by the ASCE-LRFD Pre-Standard to govern the interaction of bending moment and axial compression load for doubly symmetrical cross sections is as follows:

$$\frac{P_u}{P_c} + \frac{M_{ux}}{M_{ux}} \leq 1.0 \quad (3.8)$$

Where

P_u = required axial compression strength due to factored loads

$P_c = \lambda \phi \cdot P_n$ = available axial compressive strength.

M_u = required flexural strength due to factored loads.

$M_c = \lambda \phi_B M_n$ = available flexural strength.

ϕ_c = resistance factor, its 0.7 for compression rapture and global buckling, and 0.8 for local buckling.

ϕ_b = resistance factor, its 0.7 for lateral torsional buckling and web crippling, and 0.8 for local instability and web compression buckling.

λ = time effect factor, it is assumed to be 1.0.

P_c is calculated using the same procedure in subsection 3.1.1. $M_c = \lambda \phi M_n$ and shall be taken as the smallest strength obtained from these limits:

a. Due to material Rupture, the resistance factor ϕ_b is taken as 0.65.

M_n shall be the smallest value of equations (3.9), and (3.10):

$$M_n = \frac{F_L f (E_L f I_f + E_L w I_w)}{y_f E_L f} \quad (3.9)$$

$$M_n = \frac{F_L w (E_L f I_f + E_L w I_w)}{y_w E_L w} \quad (3.10)$$

Where

F_L = Characteristic longitudinal strength of flange

$F_L w$ = Characteristic longitudinal strength of web

$E_L f$ = Characteristic longitudinal modulus of flange

$E_L w$ = Characteristic longitudinal modulus of web

I_f = Moment of inertia of the flange

I_w = Moment of inertia of the web

y_f = Distance from the neutral axis to the extreme fibers of the flange.

y_w = Distance from the neutral axis to the extreme fibers of the web.

The Pre-Standard allows the use of the below equation if the longitudinal moduli of the flange and the web differs within 15 percent of each other:

$$M_n = \frac{F_L I_x}{y} \quad (3.11)$$

Where

F_L = Characteristic longitudinal strength of the member

I_x = Moment of inertia of the member about x-axis

y = Distance from the neutral axis to the extreme fibers of the member = $\frac{h}{2}$.

b. Due to Local Instability, the resistance fiber ϕb is taken as 0.8.

M_n shall be taken the smallest value of equations (3.12), and (3.13) below:

For the local buckling in the flange.

$$M_n = f_{cr} \frac{E_L f I_f + E_{LW} I_W}{y E_L f} \quad (3.12)$$

And

For the local buckling in the web.

$$M_n = f_{cr} \frac{(E_L f I_f + E_{LW} I_W)}{y E_{LW}} \quad (3.13)$$

Where:

f_{cr} = Critical buckling stress and shall be taken as the smallest value of equations (3.14), and (3.17) below:

Compression flange local buckling.

$$f_{cr} = \left(\frac{4(t_f)^2}{(b_f)^2} \right) \left[\frac{7}{12} \sqrt{\frac{E_L f E_T f}{1 + 4.1 \xi}} + G_{LT} \right] \quad (3.14)$$

With

$$\xi = \frac{E_T f (t f)^3}{6 b f K r} \quad (3.15)$$

$$K_r = \left(\frac{E_{TW} (t w)^3}{6 h} \right) \left[1 - \left[\left(\frac{48 (t f)^2 h^2 E_{LW}}{11.1 \pi^2 (t w)^2 (b f)^2 E_{L f}} \right) \left(\frac{G_{LT}}{1.25 \sqrt{E_{LW} E_{TW}} + E_{TW} \nu_{LT} + 2 G_{LT}} \right) \right] \right] \quad (3.16)$$

And

Compression web local buckling.

$$f_{cr} = \frac{11.1 \pi^2 (t w)^2}{12 h^2} \left(1.25 \sqrt{E_{LW} E_{TW}} + E_{TW} \nu_{LT} + 2 G_{LT} \right) \quad (3.17)$$

The Pre-Standard allows the use of the below equation when the elastic moduli of the flange and the web differs within 15 percent of each other:

$$M_n = \frac{f_{cr} I_x}{y} \quad (3.18)$$

Where

I_x = moment of inertia about the x-axis

y = Distance from the neutral axis to the extreme fibers of the member, $y = \frac{h}{2}$.

In this thesis an assumption is made that the longitudinal modulus of elasticity of the flange $E_{L f}$ is equal to the longitudinal modulus of elasticity of the web $E_{L w}$. In this case it is allowed to use equation (3.11) and (3.18)

c. Due to Lateral-Torsional Buckling, the resistance factor ϕ shall be taken

0.7. The equation for the I-Shapes is as follows:

$$M_n = C_b \sqrt{\left(\frac{\pi^2 E_{L f} I_y D_j}{L^2} + \frac{\pi^4 (E_{L f})^2 I_y C_w}{L^4} \right)} \quad (3.19)$$

Where

D_j = Torsional rigidity of an open section. $D_j = G_{LT} \sum_i \frac{1}{3} b_i t_i^3$

$$C_w = \text{Warping constant. } C_w = \frac{t f h^2 (b f)^3}{24} .$$

$$C_b = \text{Moment modification factor. } C_b = \frac{12.5 M_{max}}{2.5 M_{max} + 3 M_A + 4 M_B + 3 M_C} \leq 3.0. \quad C_b$$

assumed to be 1.

3.2.2 Minor Axis Response

The governing equation in this case is:

$$\frac{P_u}{P_c} + \frac{M_{uy}}{M_{cy}} \leq 1.0 \quad (3.20)$$

Equation (3.11) is changed about the minor axis as follows:

$$M_n = \frac{F_L I_y}{y} \quad (3.21)$$

And, equation (3.13) is changed about y-axis as follows:

$$M_n = \frac{f_{cr} I_y}{y} \quad (3.21)$$

f_{cr} in the above equation, is the value of the equation below:

For compression flange local buckling.

$$f_{cr} = \frac{4(t f)^2}{(b f)^2} G_{LT} \quad (3.22)$$

3.3 Biaxially Loaded Beam-Column with Initial Out-of-Straightness

The equation below governs the interaction of flexural and compression loads in doubly symmetric members:

$$\frac{P_u}{P_c} + \frac{M_{ux}}{M_{cx}} + \frac{M_{uy}}{M_{cy}} \leq 1.0 \quad (3.23)$$

Same procedures in subsections 3.1 and 3.2 is used to calculate P_c , M_{cx} , and M_{cy} .

CHAPTER 4

COMPARISON OF RESULTS AND DISCUSSION

4.1 Columns

Tables 16 through 27 list the load-deflection values for different lengths and initial out-of-straightness for section IW660 column. The comparison will be limited to initial out-of-straightness of $L/500$ and $L/100000$ due to the assumption of ASCE Pre Standard which indicates that “compression members shall be considered to be straight if the variation in straightness is equal to or less than $1/500$ of the length in the axial direction between points that are laterally supported. Excessive local deformations shall be cause for rejection”.

Figure 59 shows the load-slenderness ratio for section IW660 column, major axis response with initial out-of-straightness $L/500$ using finite-difference method. This curve shows that cracking of the extreme fibers occurs before reaching the buckling load. The strength of the member decreases as the slenderness ratio increases to reach the maximum value of 40. Figure 60 shows the major axis response for section IW660 column for initial out-of-straightness $L/100000$. In this case, cracking is in control for short columns, and at slenderness ratio 31.325 buckling controls. Figure 61 shows the comparison between both cases for the major axis response. Similarly, Figure 71 shows the minor axis response for initial out-of-straightness of $L/500$ and Figure 72 shows the minor axis response with initial out-of-straightness of $L/100000$ for section IW660. For section WI880 Figures 129, 130, and 131 show the load-slenderness ratio relation. ASCE Pre-Standard use Equation 3.1 to design the straight columns without counting for the initial out-of-straightness while

Equation 3.6 is used to count for the initial out-of-straightness by using reduction factor (Φ_0). The reduction factor (Φ_0) must be calculated from Equation 3.7, this Equation is problematic for initial out-of-straightness equal to $L/500$ and smaller. For initial out-of-straightness $L/500$ equation 3.7 gives zero reduction factor, and this will lead to critical load strength equals to zero in equation 3.6. For deflections smaller than $L/500$, equation 3.7 results in negative reduction factor value, and this leads to negative critical load strength. Figure 64 shows the comparison between finite-difference method and ASCE Pre-Standard for IW660 column for initial out-of-straightness $L/500$ major axis response. ASCE Pre-Standard uses a small percentage of the theoretical strength of the member to the conservative side but in the other hand assumes that the member is stable pass slenderness ratio of value 40 while finite-difference method analysis shows that the member is unstable beyond this value. The strength of the member calculated using Equation 3.6 is shown to be zero. Figure 64 shows the comparison for section IW660 for initial out-of-straightness $L/100000$, member strength calculated from Equation 3.6 in this case is higher than that calculated from Equation 3.1. For section IW880, Figures 134 and 135 show the curves for ASCE Pre-Standards and finite-difference method for the major axis response, Figures 141 and 142 show the curves for the minor axis response. Finite-difference method analysis shows this section cannot be used for slenderness value larger than 53 while the equations from ASCE Pre-Standard show the member is still stable.

4.2 Uniaxially Loaded Beam-Columns

The load-moment interaction curves for IW660 are shown in Figures 66 and 67 for the major axis response using finite-difference method. Figure 68 shows the comparison between initial out-of-straightness of L/500 and L/100000. Comparing both curves of initial out-of-straightness of L/500 and L/100000 show that the section with L/500 initial out-of-straightness can tolerate less ultimate moment for the same load. For example, for $P_u/\Phi_c P_n = 0.6$, the ratio of $M_u/\Phi_c M_n$ for L/500 is 0.261 while for L/100000 is 0.335. Another example for $P_u/\Phi_c P_n = 0.7$, the ratio of $M_u/\Phi_c M_n$ for L/500 is 0.124 while for L/100000 is 0.2169. For section IW880, Figures 146 and 147 show the load-moment interaction, and the comparison between initial out-of-straightness L/500 and L/100000 is presented in Figure 148. For $P_u/\Phi_c P_n = 0.6$, the ratio of $M_u/\Phi_c M_n$ for L/500 is 0.34 and for L/100000 is 0.38. Figure 152 presents the comparison between L/500 and L/100000 for section IW880 for the minor axis response. For this case, $P_u/\Phi_c P_n = 0.6$ $M_u/\Phi_c M_n$ for L/500 is 0.22 and for L/100000 is 0.335. ASCE Pre-Standard gives load-moment interaction equations 3.8 and 3.20 for major and minor response respectively. Figure 69 represents the comparison between load-interaction curves for finite-difference method and ASCE Pre-Standard for IW660 for the major axis response. For $P_u/\Phi_c P_n = 0.6$ the ratio of $M_u/\Phi_c M_n$ for L/500 from the finite difference method is 0.261 while that from ASCE Pre-Standard is 0.4. Finite-difference method for section IW660 and initial out-of-straightness of L/500 gives $M_u/\Phi_c M_n=0$ when ASCE Pre-Standard gives 0.2 for $P_u/\Phi_c P_n =0.8$. Results obtained from the ASCE Pre-Standard are less conservative and reduction factors should be used to minimize the error.

4.3 Biaxially Loaded Beam-Columns

Load-moment interaction curves for biaxial response using finite-difference method is shown in Figures 156 and 157 for initial out-of-straightness of $L/500$ and $L/100000$ respectively. Comparing $L/500$ to $L/100000$, for $L/500$, ratio $M_{ux}/\Phi_b M_{nx}=0$ and $P_u/\Phi_c P_n=0.8$ the value of $M_{uy}/\Phi_b M_{ny}=0.7$ while it is 0.82 for $L/100000$. Comparing both figures leads to a conclusion that $L/100000$ can tolerate higher moments for the same load ratio. For $L/500$ the ratio $M_{ux}/\Phi_b M_{nx}=0.6$ and ratio $P_u/\Phi_c P_n=0.2$ the ratio $M_{uy}/\Phi_b M_{ny}=1.8$ compared to 1.9 for $L/100000$. ASCE Pre Standard adopts Equation 3.23 to describe the load-moment interaction in the biaxial response. Figure 158 represents the interaction curves for different values of load ratios. For ratio $M_{ux}/\Phi_b M_{nx}=0.6$ and ratio $P_u/\Phi_c P_n=0.2$ the ratio $M_{uy}/\Phi_b M_{ny}=0.2$. For smaller values of $M_{ux}/\Phi_b M_{nx}$ for example 0.1 and ratio $P_u/\Phi_c P_n=0.4$ the ratio $M_{uy}/\Phi_b M_{ny}=0.5$ for $L/500$ and 0.45 for $L/100000$ using finite-difference method, while it is 0.5 using ASCE Pre Standard. In this case there are no significant differences between all studied cases.

4.4 Critique of ASCE-LRDF Pre-Standard

In columns, ASCE Pre Standard underestimates the member strength and it is very conservative, however, it is wrongly assume that the member is still stable when the calculations from the finite-difference method show that the member is no longer stable. Load-deflection calculations from the finite-difference method show larger deflection values for initial out-of-straightness of value $L/500$ than those of $L/100000$ for the same load value indicating that the assumption made by ASCE Pre Standard to consider columns with initial out-of-straightness of $L/500$ are straight members is wrong. Equation 3.7 to

calculate the deflection is also wrong for initial out-of-straightness values of $L/500$ and smaller. For initial out-of-straightness of value $L/500$, Equation 3.6 will have zero strength value, and for initial out-of-straightness smaller than $L/500$ will result in negative member strength value in Equation 3.7. ASCE Pre Standard should state that this equation is invalid for initial out-of-straightness of $L/500$ and less. Although Equation 3.7 is used for columns with initial out-of-straightness, it gave results higher than Equation 3.1 which is used for perfect columns. The column section 3 and 4 in ASCE Pre-Standard used to design tension and compression members are ambiguous. Equations 3.1 and 3.7 should be re-written as follows:

Compression members without initial out-of-straightness shall be designed such that P_u is the smaller value of:

$$P_u = \lambda \Phi_c P_n$$

$$P_u = 0.7 \lambda F_c A_g$$

Compression members with initial out-of-straightness shall be designed such that P_s is the smaller value of:

$$P_s = \Phi_o \frac{\pi^2 E I}{\left(\frac{KL_e}{r}\right)^2} A_g$$

$$P_s = 0.3 F_c A_g$$

For $\delta_o > L/500$

$$\Phi_o = 1 - 500 \left(\frac{\delta_o}{L} \right)$$

Compression member strength shall be the smallest value of P_u and P_s .

In case of the uniaxial beam-column response, ASCE Pre Standard gave higher results than those calculated using finite-difference method. ASCE Pre Standard is less conservative and must use reduction factors to reduce the results. Finally, in biaxial loaded members, the results from both finite-difference method and ASCE Pre Standard were close. Although the results from ASCE Pre Standard are slightly higher in some cases but no significant differences were found.

CHAPTER 5

CONCLUSIONS AND FUTURE RESEARCH

5.1 Conclusions

The following conclusions are drawn for the investigation related to FRP members presented in this thesis:

- 1- The finite-difference method used for solving the governing differential equations of equilibrium for columns and beam-columns with initial imperfection provided is a computationally efficient procedure for determining the load-carrying capacities.
- 2- With smaller cross sections, both minor and major axis peak load values are found to be less for columns with initial imperfection than those for nearly perfect ones, and the peak loads for imperfect columns are always associated with material cracking.
- 3- For nearly perfect columns with smaller cross sections, the peak load is governed by either axial crushing or elastic instability without cracking.
- 4- With larger cross sections, both major and minor axis differences in peak load values are found to be small for both imperfect and nearly perfect columns, and the peak load is governed by either axial crushing, elastic instability, or cracking.

- 5- For nearly perfect beam-column, both major and minor axis peak load values are found to be less for members with initial imperfection than those for nearly perfect ones.
- 6- For uniaxially and biaxially loaded members, warping stresses are found to be significant using the finite-difference method, however, they are neglected in ASCE-LRFD Pre-Standard.
- 7- Based on rigorous finite-difference analysis presented, it is found that for centrally loaded columns with small to medium slenderness, ASCE-LRFD Pre-Standard grossly underestimates the peak load while giving completely erroneous estimates when slenderness is relatively large.
- 8- For both uniaxially and biaxially loaded beam-columns, ASCE-LRFD overestimates the ultimate loads and moments when compared with the values obtained using the finite-difference

5.2 Future Research

It is known that the initial out-of-straightness and residual stresses caused by unavoidable manufacturing process. The combined influence may be considerable for the axially loaded columns for future research.

The present study was made to determine whether the formulas used in the ASCE-LRFD Pre-Standard lead to conservative results comparing to the theoretical analysis.

This study used wide flange I-section. Different cross sections can be used in future to compare the critical load.

The present study was made on pinned-pinned members. Different boundary conditions can be used to determine the influence of the warping stress.

REFERENCES

1. *Pre-Standard for Load & Resistance Factor Design (LRFD) of Pultruded Fiber Reinforced Polymer (FRP) Structures* (Final ed.). (2010). American Society of Civil Engineers.
2. *The Pultex Pultrusion Design Manual* (Imperial Version). (2004) Creative Pultrusions, Inc.
3. Galambos, T. (1968). *Structural members and frames*. Englewood Cliffs, N.J.: Prentice-Hall.
4. Timoshenko, S., & Gere, J. (1961). *Theory of elastic stability* (2nd ed., Dover ed.). Mineola, N.Y.: Dover Publications
5. Ziemian, R. (2010). *Guide to stability design criteria for metal structures*(6th ed.). Hoboken, N.J.: John Wiley & Sons.
6. *Steel construction manual* (14.th ed.). (2011). Milwaukee, Wis: AISC.
7. Chen, W., & Atsuta, T. (1976). *Space behavior and design* (Vol. 1). New York u.a.: McGraw-Hill
8. Chen, W., & Atsuta, T. (1977). *Space behavior and design* (Vol. 2). New York u.a.: McGraw-Hill
9. Mottram, J. (n.d.). Lateral-torsional buckling of a pultruded I-beam. *Composites*, 81-92.
10. Yoon, S., Jung, J., & Jang, W. (1993). Elastic Web Buckling Strength of Pultruded Flexural Members. *KEM Key Engineering Materials*, 621-626.
11. Turvey, G., & Brooks, R. (1995). Semi-rigid—simply supported shear deformable pultruded GRP beams subjected to end moment loading:

Comparison of measured and predicted deflections. *Composite Structures*, 263-277

12. Davalos, J., Qiao, P., & Salim, H. (1997). Flexural-torsional buckling of pultruded fiber reinforced plastic composite I-beams: Experimental and analytical evaluations. *Composite Structures*, 241-250.
13. Mottram, J., Brown, N., & Anderson, D. (2003). Buckling characteristics of pultruded glass fibre reinforced plastic columns under moment gradient. *Thin-Walled Structures*, 619-638.
14. Vanevenhoven, L., Shield, C., & Bank, L. (2010). Closure to “LRFD Factors for Pultruded Wide-Flange Columns” by Linda M. Vanevenhoven, Carol K. Shield, and Lawrence C. Bank. *Journal of Structural Engineering J. Struct. Eng.*, 659-660.
15. Thumrongvut, J., & Seangatith, S. (2011). Responses of PFRP Cantilevered Channel Beams under Tip Point Loads. *KEM Key Engineering Materials*, 578-583.
16. Correia, J., Branco, F., Silva, N., Camotim, D., & Silvestre, N. (2011). First-order, buckling and post-buckling behaviour of GFRP pultruded beams. Part 1: Experimental study. *Computers & Structures*, 2052-2064
17. Nguyen, T., Chan, T., & Mottram, J. (2013). Lateral–Torsional Buckling design for pultruded FRP beams. *Composite Structures*, 782-793.
18. Chen, Q., & Qiao, P. (2015). Post-buckling analysis of composite plates under combined compression and shear loading using finite strip method. *Finite Elements in Analysis and Design*, 33-42.

19. Minghini, F., Tullini, N., & Laudiero, F. (n.d.). Elastic buckling analysis of pultruded FRP portal frames having semi-rigid connections. *Engineering Structures*, 292-299.
20. Barbero, E., & Raftoyiannis, I. (n.d.). Lateral and distortional buckling of pultruded I-beams. *Composite Structures*, 261-268.

Appendix A

Tables

Table 1. IW 660- Pultex Wide Flange section

Depth (h)	Width (d)	Thick (t)	Area	I_x	S_x	r_x	I_y	S_y	r_y	C_{vv}	
in	in	in	in ²	in ⁴	in ³	in	in ⁴	in ³	in	in ⁶	
6.00	6.00	0.375	6.57	40.76	13.59	2.49	13.32	4.44	1.42	119.84	IW660
8.00	8.00	0.5	11.67	128.81	32.2	3.32	42.09	10.52	1.9	673.41	IW880

Table 2. Mechanical properties IW660 Wide-Flange

Mechanical Property	Minimum Requirement
Longitudinal Tensile Strength	30000 psi
Longitudinal Tensile Modulus	3000000 psi
Longitudinal Compressive Strength	30000 psi
Longitudinal Compressive Modulus	3000000 psi
In-Plane Shear Strength	8000 psi
In-Plane Shear Modulus	400000 psi
Minimum Numbers of Tests	10

Table 3. IW660 column major axis response L=6ft.

P (K)	$\frac{KP}{K_0}$
0	1
25	0.8328
50	0.6828
75	0.5487
100	0.4293
125	0.3235
150	0.2303
175	0.1486
200	0.0775
225	0.0162
250	-0.0361

Table 4. IW660 column major axis response. L=12ft.

P (K)	$\frac{KP}{K_0}$
0	1
5	0.8648
10	0.7408
15	0.6273
20	0.5237
25	0.4293
30	0.3436
35	0.2661
40	0.1963
45	0.1336
50	0.0775
55	0.0278
60	-0.0162

Table 5. IW660 column major axis response. L=18ft.

P (K)	$\frac{KP}{K_0}$
0	1
3	0.8202
6	0.6603
9	0.5187
12	0.394
15	0.2848
18	0.1897
21	0.1076
24	0.0372
27	-0.0223
30	-0.0722

Table 6. IW660 column minor axis response, L=6ft.

P (K)	$\frac{KP}{K_0}$
0	1
5	0.8956
10	0.7978
15	0.7063
20	0.6208
25	0.5411
30	0.4669
35	0.3979
40	0.3339
45	0.2746
50	0.2199
55	0.1694
60	0.123
65	0.0805
70	0.0416
75	0.0062
80	-0.026

Table 7. IW660 column minor axis response. L=12ft.

P (K)	$\frac{KP}{K_0}$
0	1
2	0.8361
4	0.6887
6	0.5566
8	0.4387
10	0.3339
12	0.2413
14	0.1598
16	0.0887
18	0.027
20	-0.026

Table 8. IW660 column minor axis response. L=18ft.

P (K)	$\frac{KP}{K_0}$
0	1
1	0.8168
2	0.6543
3	0.5108
4	0.3847
5	0.2746
6	0.1792
7	0.097
8	0.027
9	-0.032

**Table 9. IW660 uniaxial beam-column major axis response.
L=6ft.**

P (K)	$\frac{KP}{K_0}$
0	1
20	0.8648
40	0.7408
60	0.6273
80	0.5237
100	0.4293
120	0.3436
140	0.2661
160	0.1963
180	0.1336
200	0.0775
220	0.0278
240	-0.0162

Table 10. IW660 uniaxial beam-column major axis response

L=12ft

P (K)	$\frac{KP}{K_0}$
0	1
5	0.8648
10	0.7408
15	0.6273
20	0.5237
25	0.4293
30	0.3436
35	0.2661
40	0.1963
45	0.1336
50	0.0775
55	0.0278
60	-0.0162

**Table 11. IW660 uniaxial beam-column major axis response
L=18ft.**

P (K)	$\frac{KP}{K_0}$
0	1
2.5	0.8487
5	0.7115
7.5	0.5873
10	0.4754
12.5	0.3748
15	0.2848
17.5	0.2046
20	0.1336
22.5	0.071
25	0.0162
27.5	-0.0313
30	-0.0722

**Table 12. IW660 uniaxial beam-column minor axis response.
L=6ft.**

P (K)	$\frac{KP}{K_0}$
0	1
10	0.7978
20	0.6208
30	0.4669
40	0.3339
50	0.2199
60	0.123
70	0.0416
80	-0.026
90	-0.081

**Table 13. IW660 uniaxial beam-column minor axis response
L=12ft.**

P (K)	$\frac{KP}{K_0}$
0	1
2	0.8361
4	0.6887
6	0.5566
8	0.4387
10	0.3339
12	0.2413
14	0.1598
16	0.0887
18	0.027
20	-0.026

**Table 14. IW660 uniaxial beam-column minor axis response
L=18ft.**

P (K)	$\frac{KP}{K_0}$
0	1
1	0.8168
2	0.6543
3	0.5108
4	0.3847
5	0.2746
6	0.1792
7	0.097
8	0.027
9	-0.032

**Table 15. IW660 biaxial beam-column major axis response
L=6ft**

P(K)	$\frac{KP}{K_0}$
0	1
10	0.742
20	0.5358
30	0.3728
40	0.2459
50	0.1486
60	0.0757
70	0.0225
80	-0.0149
90	-0.0396

**Table 16. IW660 column major axis response- Exact solution
L=6ft.**

	L/100000	L/1000	L/500	L/250
δ_{oy} (in)	0.00072	0.072	0.144	0.288

P (k)	V (in)	V (in)	V (in)	V (in)
0	0.00072	0.072	0.144	0.288
23.2804	0.0008	0.08	0.16	0.32
46.5608	0.0009	0.09	0.18	0.36
69.8412	0.001029	0.103	0.206	0.411
93.1216	0.0012	0.12	0.24	0.48
116.402	0.00144	0.144	0.288	0.576
139.6824	0.0018	0.18	0.36	0.72
162.9628	0.0024	0.24	0.48	0.96
186.2432	0.0036	0.36	0.72	1.44
209.5236	0.0072	0.72	1.44	2.88
214.5236	0.009169	0.917	1.834	3.668
219.5236	0.012622	1.262	2.524	5.049
224.5236	0.020243	2.024	4.049	8.097
229.5236	0.051099	5.11	10.22	20.44
230	0.059781	5.978	11.956	23.913
231	0.092922	9.292	18.584	37.169
231.5	0.128556	12.856	25.711	51.422
232	0.208517	20.852	41.703	83.407
232.5	0.551626	55.163	110.325	220.65
232.7	1.613844	161.384	322.769	645.538
232.75	3.111942	311.194	622.388	1244.777
232.804	∞	∞	∞	∞

Table 17. IW660 column major axis response- FDM. L=6ft.

	L/100000	L/1000	L/500	L/250
δ_{oy} (in)	0.00072	0.072	0.144	0.288

P (k)	V (in)	V (in)	V (in)	V (in)
0	0.00072	0.072	0.144	0.288
23.2804	0.00073	0.073	0.1461	0.2921
46.5608	0.0009	0.09	0.1801	0.3602
69.8412	0.001029	0.1029	0.2059	0.4118
93.1216	0.001202	0.1202	0.2403	0.4807
116.402	0.001443	0.1443	0.2886	0.5772
139.6824	0.00182	0.1806	0.3611	0.7222
162.9628	0.00242	0.2412	0.4823	0.9646
186.2432	0.00362	0.363	0.726	1.452
209.5236	0.00732	0.7336	1.4672	2.9344
214.5236	0.00942	0.9396	1.8793	3.7586
219.5236	0.01302	1.3066	2.6133	5.2265
224.5236	0.02142	2.144	4.288	8.576
229.5236	0.05972	5.9699	11.9398	23.8795
230	0.07192	7.1928	17.3857	28.7713
231	0.12622	12.619	25.2381	50.4761
231.4	0.18072	18.077	36.1451	72.2901
231.8	0.31832	31.8271	63.6541	127.3083
232.2	1.33212	133.2091	266.4181	532.8363
232.25	2	221.342	442.6839	885.3678
232.8039	∞	∞	∞	∞

**Table 18. IW660 column major axis response-Exact Solution.
L=12ft.**

	L/100000	L/1000	L/500	L/250
δ_{oy} (in)	0.00144	0.144	0.288	0.576

P (k)	V (in)	V (in)	V (in)	V (in)
0	0.001	0.144	0.288	0.576
10	0.002	0.174	0.348	0.695
20	0.002	0.219	0.439	0.878
30	0.003	0.297	0.594	1.189
40	0.005	0.46	0.921	1.842
50	0.01	1.022	2.044	4.088
52	0.014	1.352	2.703	5.406
54	0.02	1.995	3.99	7.98
56	0.038	3.808	7.616	15.231
57	0.07	6.978	13.957	27.914
58	0.417	41.703	83.407	166.813
58.1	0.83	83.008	166.015	332.031
58.15	1.644	164.443	328.885	657.77
58.175	3.228	322.769	645.538	1291.075
58.201	∞	∞	∞	∞

Table 19. IW660 column major axis response-FDM. L=12ft.

	L/100000	L/1000	L/500	L/250
δ_{oy} (in)	0.00144	0.144	0.288	0.576

P (k)	V (in)	V (in)	V (in)	V (in)
0	0.00144	0.144	0.288	0.576
10	0.001739	0.1739	0.3479	0.6958
20	0.002196	0.2196	0.4393	0.8785
30	0.00294	0.2978	0.5957	1.1914
40	0.00464	0.4626	0.9251	1.8502
50	0.01034	1.0349	2.0699	4.1397
52	0.01374	1.3753	2.7506	5.5012
54	0.02054	2.0492	4.0985	8.1969
56	0.04014	4.0183	8.0367	16.0733
57	0.07734	7.7342	15.4684	30.9368
58	1.02754	102.757	205.514	411.0279
58.05	2.66414	266.4181	532.8363	1065.676
58.201	∞	∞	∞	∞

**Table 20. IW660 column major axis response-Exact Solution.
L=18ft.**

	L/100000	L/1000	L/500	L/250
δ_{oy} (in)	0.00216	0.216	0.432	0.864

P (k)	V (in)	V (in)	V (in)	V (in)
0	0.002	0.216	0.432	0.864
2.5	0.002	0.239	0.478	0.956
5	0.003	0.268	0.536	1.071
7.5	0.003	0.304	0.608	1.217
10	0.004	0.352	0.704	1.409
12.5	0.004	0.418	0.836	1.672
15	0.005	0.514	1.028	2.057
17.5	0.007	0.668	1.336	2.671
20	0.01	0.952	1.905	3.809
22.5	0.017	1.659	3.319	6.638
25	0.064	6.444	12.887	25.775
25.2	0.084	8.376	16.751	33.502
25.4	0.12	11.962	23.924	47.847
25.6	0.209	20.919	41.837	83.675
25.7	0.334	33.438	66.875	133.751
25.8	0.833	83.273	166.546	333.093
25.82	1.186	118.637	237.273	474.546
25.84	2.062	206.204	412.409	824.818
25.86	7.874	787.398	1574.795	3149.591
25.8671	∞	∞	∞	∞

Table 21. IW660 column major axis response-FDM. L=18ft.

	L/100000	L/1000	L/500	L/250
δ_{oy} (in)	0.00216	0.216	0.432	0.864

P (k)	V (in)	V (in)	V (in)	V (in)
0	0.00216	0.216	0.432	0.864
2.5	0.002392	0.2392	0.4783	0.9566
5	0.002679	0.2679	0.5358	1.0716
7.5	0.003045	0.3045	0.6089	1.2178
10	0.00356	0.3526	0.7052	1.4104
12.5	0.00416	0.4188	0.8376	1.6752
15	0.00516	0.5156	1.0312	2.0625
17.5	0.00666	0.6707	1.3413	2.6826
20	0.00956	0.959	1.9181	3.8362
22.5	0.01686	1.6825	3.3651	6.7301
25	0.06846	6.8503	13.7006	27.4012
25.2	0.09086	9.0818	18.1637	36.3273
25.4	0.13466	13.4697	26.9394	53.8788
25.6	0.26056	26.061	52.122	104.2439
25.7	0.48936	48.931	97.862	195.7241
25.75	0.87186	87.1867	174.3735	348.747
25.8	3.99626	399.6272	799.2544	1598.464
25.81	6.22816	622.8193	1245.632	2491.264
25.8671	∞	∞	∞	∞

**Table 22. IW660 column minor axis response-Exact Solution.
L=6ft.**

	L/100000	L/1000	L/500	L/250
δ_{ox} (in)	0.00072	0.072	0.144	0.288

P (k)	U (in)	U (in)	U (in)	U (in)
0	0.00072	0.072	0.144	0.288
5	0.000771	0.077	0.154	0.308
10	0.000829	0.083	0.166	0.332
15	0.000897	0.09	0.179	0.359
20	0.000977	0.098	0.195	0.391
25	0.001072	0.107	0.214	0.429
30	0.001189	0.119	0.238	0.476
35	0.001333	0.133	0.267	0.533
40	0.001518	0.152	0.304	0.607
45	0.001763	0.176	0.353	0.705
50	0.0021	0.21	0.42	0.84
55	0.002599	0.26	0.52	1.039
60	0.003407	0.341	0.681	1.363
65	0.004945	0.494	0.989	1.978
70	0.009012	0.901	1.802	3.605
75	0.050803	5.08	10.161	20.321
75.2	0.062373	6.237	12.475	24.949
75.4	0.080767	8.077	16.153	32.307
75.6	0.114547	11.455	22.909	45.819
76.0782	∞	∞	∞	∞

Table 23. IW660 column minor axis response-FDM. L=6ft.

	L/100000	L/1000	L/500	L/250
δ_{ox} (in)	0.00072	0.072	0.144	0.288

P (k)	U (in)	U (in)	U (in)	U (in)
0	0.00072	0.072	0.144	0.288
5	0.000771	0.0771	0.1542	0.3083
10	0.000829	0.0829	0.1658	0.3317
15	0.000897	0.0897	0.1795	0.3589
20	0.000978	0.0978	0.1955	0.391
25	0.001073	0.1073	0.2147	0.4294
30	0.00119	0.119	0.2381	0.4761
35	0.001336	0.1336	0.2672	0.5343
40	0.001522	0.1522	0.3043	0.6087
45	0.00172	0.1768	0.3536	0.7071
50	0.00212	0.2109	0.4218	0.8435
55	0.00262	0.2613	0.5226	1.0451
60	0.00342	0.3433	0.6866	1.3733
65	0.00502	0.5005	1.001	2.002
68.47038	0.00732	0.7336	1.4672	2.9344
69.47038	0.00852	0.8473	1.6946	3.3892
70.47038	0.01002	1.0027	2.0055	4.0109
71.47038	0.01232	1.228	2.456	4.9119
72.47038	0.01582	1.5838	3.1675	6.335
73.47038	0.02232	2.2298	4.4596	8.9192
74.47038	0.03762	3.766	7.5319	15.0639
75.47038	0.12102	12.1066	24.2133	48.4265
76.0782	∞	∞	∞	∞

**Table 24. IW660 column minor axis response-Exact Solution.
L=12ft.**

	L/100000	L/1000	L/500	L/250
δ_{ox} (in)	0.00144	0.144	0.288	0.576

P (k)	U (in)	U (in)	U (in)	U (in)
0	0.00144	0.144	0.288	0.576
2	0.001609	0.160922	0.321843	0.643687
4	0.001824	0.18235	0.3647	0.7294
6	0.002104	0.210362	0.420723	0.841447
8	0.002485	0.248541	0.497083	0.994166
10	0.003037	0.303653	0.607306	1.214613
12	0.003902	0.39017	0.780339	1.560678
14	0.005456	0.54563	1.091259	2.182518
16	0.00907	0.907028	1.814055	3.62811
18	0.026863	2.686298	5.372595	10.74519
18.2	0.033419	3.341852	6.683704	13.36741
18.4	0.044207	4.420651	8.841303	17.68261
18.6	0.06528	6.527981	13.05596	26.11192
18.8	0.124747	12.47467	24.94934	49.89867
19.01955	∞	∞	∞	∞

Table 25. IW660 column minor axis response-FDM.L=12ft.

	L/100000	L/1000	L/500	L/250
δ_{ox} (in)	0.00144	0.144	0.288	0.576

P (k)	U (in)	U (in)	U (in)	U (in)
0	0.00144	0.144	0.288	0.576
2	0.00161	0.161	0.3219	0.6438
4	0.001825	0.1825	0.3649	0.7298
6	0.002106	0.2106	0.4211	0.8422
8	0.00244	0.2489	0.4978	0.9957
10	0.00304	0.3043	0.6087	1.2174
12	0.00394	0.3915	0.7831	1.5662
14	0.00544	0.5488	1.0976	2.1951
16	0.00914	0.917	1.8341	3.6681
18	0.02784	2.7876	5.5752	11.1505
18.2	0.03504	3.502	7.0039	14.0078
18.4	0.04704	4.7085	9.4171	18.8342
18.6	0.07184	7.1836	14.3672	28.7345
18.8	0.15144	15.148	30.2888	60.5777
19.01955	∞	∞	∞	∞

**Table 26. IW660 column minor axis response- Exact solution.
L=18ft.**

	L/100000	L/1000	L/500	L/250
δ_{ox} (in)	0.00216	0.216	0.432	0.864

P (k)	U (in)	U (in)	U (in)	U (in)
0	0.00216	0.216	0.432	0.864
0.8453	0.0024	0.24	0.479999	0.959998
1.6906	0.0027	0.269999	0.539998	1.079996
2.5359	0.003086	0.308569	0.617139	1.234277
3.3812	0.0036	0.359996	0.719992	1.439985
4.2265	0.00432	0.431993	0.863986	1.727973
5.0718	0.0054	0.539987	1.079974	2.159949
5.9171	0.0072	0.719973	1.439947	2.879894
6.7624	0.010799	1.079932	2.159864	4.319727
7.6077	0.021597	2.159693	4.319387	8.638773
7.8	0.027956	2.795565	5.59113	11.18226
8	0.040294	4.029447	8.058893	16.11779
8.2	0.072131	7.213101	14.4262	28.8524
8.3	0.119234	11.92344	23.84688	47.69376
8.35	0.17704	17.70403	35.40806	70.81612
8.4	0.34364	34.36401	68.72803	137.4561
8.453133	∞	∞	∞	∞

Table 27. IW660 column minor axis-FDM. L=18ft.

	L/100000	L/1000	L/500	L/250
δ_{ox} (in)	0.00216	0.216	0.432	0.864

P (k)	U (in)	U (in)	U (in)	U (in)
0	0.00216	0.216	0.432	0.864
0.4	0.002268	0.2268	0.4535	0.907
0.8	0.002386	0.2386	0.4773	0.9545
1.2	0.002518	0.2518	0.5036	1.0073
1.6	0.002666	0.2666	0.5331	1.0662
2	0.002831	0.2831	0.5662	1.1325
2.4	0.003019	0.3019	0.6038	1.2076
2.8	0.00326	0.3233	0.6466	1.2933
3.2	0.00346	0.348	0.696	1.3921
3.6	0.00376	0.3768	0.7536	1.5072
4	0.00406	0.4108	0.8216	1.6431
4.4	0.00456	0.4515	0.903	1.806
4.8	0.00506	0.5012	1.0023	2.0047
5.2	0.00566	0.5631	1.1262	2.2525
5.6	0.00646	0.6426	1.2851	2.5702
6	0.00746	0.7481	1.4961	2.9923
6.4	0.00896	0.8941	1.7901	3.5802
6.8	0.01116	1.1139	2.2279	4.4557
7.2	0.01476	1.4745	2.949	5.898
7.6	0.02176	2.1444	4.3604	8.7207
8	0.04186	4.1814	8.3629	16.7257
8.4	0.50946	50.9449	101.8897	203.7794
8.453133	∞	∞	∞	∞

**Table 28. IW660 uniaxial beam-column major axis response
 $M_{ox}=0$, $L=6ft$.**

	L/100000	L/1000	L/500	L/250
δ_{oy}	0.00072	0.072	0.144	0.288

P (k)	V (in)	V (in)	V (in)	V (in)
0	0.00072	0.072	0.144	0.288
10	0.000752	0.0752	0.1505	0.301
20	0.000788	0.0788	0.1576	0.3151
30	0.000827	0.0827	0.1654	0.3307
40	0.00087	0.087	0.1739	0.3479
50	0.000917	0.0917	0.1835	0.367
60	0.000971	0.0971	0.1941	0.3883
70	0.00103	0.103	0.2061	0.4122
80	0.001098	0.1098	0.2196	0.4393
90	0.001175	0.1175	0.2351	0.4701
100	0.001264	0.1264	0.2528	0.5056
110	0.001367	0.1367	0.2735	0.547
120	0.001489	0.1489	0.2978	0.5957
130	0.001635	0.1635	0.3269	0.6539
140	0.00182	0.1812	0.3624	0.7247
150	0.00202	0.2032	0.4064	0.8127
160	0.00232	0.2313	0.4626	0.9251
170	0.00272	0.2684	0.5368	1.0736
180	0.00322	0.3197	0.6394	1.2787
190	0.00392	0.3952	0.7904	1.5808
200	0.00522	0.5175	1.0349	2.0699
210	0.00752	0.7493	1.4985	2.997
220	0.01362	1.3571	2.7143	5.4285
230	0.07192	7.1928	14.3857	28.7713
231	0.12622	12.619	25.2381	50.4761
232	0.51382	51.3785	102.757	205.514
232.25	2.21342	221.342	442.6839	885.3678
232.3	6.54112	654.1096	1308.244	2616.488
232.8039	∞	∞	∞	∞

**Table 29. IW660 uniaxial beam-column major axis response
 $M_{ox}=16.304$ K-in., $L=6$ ft.**

	L/100000	L/1000	L/500	L/250
δ_{oy}	0.00072	0.072	0.144	0.288

P (k)	V (in)	V (in)	V (in)	V (in)
0	0.00072	0.072	0.144	0.288
10	0.09022	0.1647	0.24	0.3904
20	0.09462	0.1726	0.2514	0.4089
30	0.09942	0.1812	0.2639	0.4293
40	0.10462	0.1908	0.2777	0.4517
50	0.11052	0.2014	0.2931	0.4766
60	0.11712	0.2132	0.3103	0.5044
70	0.12442	0.2265	0.3295	0.5356
80	0.13282	0.2415	0.3513	0.5709
90	0.14218	0.2586	0.3762	0.6112
100	0.15322	0.2784	0.4048	0.6576
110	0.16592	0.3013	0.4381	0.7116
120	0.18092	0.3284	0.4773	0.7751
130	0.19892	0.3607	0.5242	0.8511
140	0.22072	0.4001	0.5812	0.9436
150	0.24782	0.449	0.6522	1.0585
160	0.28242	0.5114	0.7427	1.2053
170	0.32822	0.5939	0.8623	1.3991
180	0.39142	0.7079	1.0276	1.667
190	0.48452	0.8758	1.271	2.0614
200	0.63532	1.1476	1.6651	2.7
210	0.92112	1.6629	2.4121	3.9106
220	1.67072	3.0143	4.3715	7.0857
230	8.86732	15.9883	23.1811	37.5667
231	15.55902	28.0518	40.6709	65.9089
232	63.35752	114.2222	165.6007	268.3577
232.3	806.6504	1454.172	2108.344	3416.588
232.8039	∞	∞	∞	∞

Table 30. IW660 uniaxial beam-column major axis response.
 $M_{ox}=32.608.$, $L=6ft.$

	L/100000	L/1000	L/500	L/250
δ_{oy}	0.00072	0.072	0.144	0.288

P (k)	V (in)	V (in)	V (in)	V (in)
0	0.00072	0.072	0.144	0.288
10	0.17972	0.2542	0.3294	0.4799
20	0.18842	0.2664	0.3452	0.5027
30	0.19792	0.2798	0.3625	0.5278
40	0.20842	0.2946	0.3815	0.5555
50	0.22012	0.311	0.4027	0.5862
60	0.23322	0.3293	0.4264	0.6205
70	0.24782	0.3499	0.4529	0.659
80	0.26442	0.3732	0.483	0.7026
90	0.28342	0.3997	0.5173	0.7523
100	0.30512	0.4303	0.5567	0.8095
110	0.33052	0.4659	0.6026	0.8761
120	0.36042	0.5078	0.6567	0.9546
130	0.39612	0.5579	0.7214	1.0484
140	0.43962	0.6189	0.8001	1.1625
150	0.49362	0.6948	0.8979	1.3043
160	0.56262	0.7915	1.0228	1.4854
170	0.65372	0.9194	1.1878	1.7246
180	0.77962	1.0961	1.4158	2.0552
190	0.96512	1.3564	1.7516	2.542
200	1.26542	1.7777	2.2952	3.3301
210	1.83472	2.5765	3.3258	4.8243
220	3.32792	4.6715	6.0286	8.7429
230	17.66282	24.7837	31.9765	46.3622
231	30.99172	43.4847	56.1037	81.3417
232	126.2012	177.0659	228.4444	331.2014
232.3	1606.801	2254.372	2908.444	4216.688
232.8039	∞	∞	∞	∞

Table 31. IW660 uniaxial beam-column major axis response.
 $M_{ox}=65.216$ K-in., $L=6$ ft.

	L/100000	L/1000	L/500	L/250
δ_{oy}	0.00072	0.072	0.144	0.288

P (k)	V (in)	V (in)	V (in)	V (in)
0	0.00072	0.072	0.144	0.288
10	0.35872	0.4332	0.5084	0.6589
20	0.37602	0.454	0.5328	0.6903
30	0.39502	0.4769	0.5596	0.7249
40	0.41602	0.5022	0.5891	0.7631
50	0.43942	0.5302	0.622	0.8055
60	0.46542	0.5615	0.6586	0.8527
70	0.49472	0.5967	0.6998	0.9059
80	0.52782	0.6365	0.7463	0.966
90	0.56562	0.6819	0.7995	1.0345
100	0.60902	0.7342	0.8606	1.1134
110	0.65972	0.795	0.9318	1.2053
120	0.71932	0.8667	1.0156	1.3135
130	0.79062	0.9524	1.1159	1.4428
140	0.87732	1.0567	1.2379	1.6002
150	0.98522	1.1863	1.3895	1.7959
160	1.12282	1.3518	1.5831	2.0457
170	1.30472	1.5704	1.8388	2.3756
180	1.55612	1.8726	2.1923	2.8317
190	1.92632	2.3176	2.7128	3.5033
200	2.52572	3.038	3.5555	4.5904
210	3.66202	4.4038	5.153	6.6516
220	6.64232	7.9859	9.343	12.0573
230	35.25372	42.3746	49.5674	63.9531
231	61.85742	74.3503	86.9693	112.2074
232	251.8886	302.7533	354.1318	456.8888
232.3	3207.011	3854.572	4508.644	5816.888
232.8039	∞	∞	∞	∞

Table 32. IW660 uniaxial beam-column major axis response.
 $M_{ox}=97.824K\text{-in.}$, $L=6\text{ft}$

	L/100000	L/1000	L/500	L/250
δ_{oy}	0.00072	0.072	0.144	0.288

P (k)	V (in)	V (in)	V (in)	V (in)
0	0.00072	0.072	0.144	0.288
10	0.53762	0.6121	0.6874	0.8379
20	0.56362	0.6416	0.7204	0.878
30	0.59212	0.674	0.7567	0.922
40	0.62362	0.7098	0.7967	0.9707
50	0.65862	0.7495	0.8412	1.0247
60	0.69772	0.7938	0.8908	1.085
70	0.74152	0.8436	0.9466	1.1527
80	0.79112	0.8999	1.0097	1.2293
90	0.84782	0.9641	1.0817	1.3167
100	0.91292	1.0381	1.1645	1.4173
110	0.98882	1.1242	1.2609	1.5344
120	1.07822	1.2256	1.3746	1.6724
130	1.18502	1.3469	1.5104	1.8373
140	1.31512	1.4945	1.6756	2.038
150	1.47672	1.6779	1.8811	2.2875
160	1.68312	1.9121	2.1434	2.6059
170	1.95572	2.2214	2.4898	3.0266
180	2.33262	2.6491	2.9688	3.6081
190	2.88762	3.2788	3.674	4.4645
200	3.78602	4.2983	4.8158	5.8507
210	5.48932	6.2311	6.9803	8.4788
220	9.95672	11.3003	12.6574	15.3717
230	52.84452	59.9655	67.1583	81.5439
231	92.72302	105.2159	117.8349	143.073
232	377.576	428.4407	479.8192	582.5762
232.3	4807.201	5453.772	6108.844	7417.088
232.8039	∞	∞	∞	∞

Table 33. IW660 uniaxial beam-column major axis response.
 $M_{ox}=0$, $L=12ft$.

	L/100000	L/1000	L/500	L/250
δ_{oy}	0.00144	0.144	0.288	0.576

P (k)	V (in)	V (in)	V (in)	V (in)
0	0.00144	0.144	0.288	0.576
3	0.001518	0.1518	0.3037	0.6074
6	0.001606	0.1606	0.3212	0.6424
9	0.001704	0.1704	0.3408	0.6816
12	0.001815	0.1815	0.363	0.726
15	0.001941	0.1941	0.3883	0.7766
18	0.002087	0.2087	0.4173	0.8347
21	0.002256	0.2256	0.4511	0.9022
24	0.00244	0.2454	0.4908	0.9816
27	0.00274	0.2691	0.5381	1.0764
30	0.00294	0.2978	0.5957	1.1914
33	0.00334	0.3335	0.6669	1.3339
36	0.00374	0.3788	0.7575	1.5151
39	0.00434	0.4383	0.8766	1.7533
42	0.00524	0.5201	1.0402	2.0803
45	0.00644	0.6394	1.2787	2.5574
48	0.00834	0.8296	1.6592	3.3185
51	0.01184	1.1811	2.3622	4.7243
54	0.02054	2.0492	4.0985	8.1969
57	0.07734	7.7342	15.4684	30.9368
57.2	0.09494	9.4892	18.9784	37.9568
57.4	0.12274	12.2744	24.5489	49.0978
57.6	0.17374	17.374	34.748	69.496
57.8	0.29724	29.7225	59.4451	118.8902
58	1.02754	102.757	205.514	411.0279
58.20097	∞	∞	∞	∞

Table 34. IW660 uniaxial beam-column major axis response.
 $M_{ox}=16.304$ K-in., $L=12$ ft.

	L/100000	L/1000	L/500	L/250
δ_{oy}	0.00144	0.144	0.288	0.576

P (k)	V (in)	V (in)	V (in)	V (in)
0	0.00144	0.144	0.288	0.576
3	0.36274	0.5131	0.665	0.9686
6	0.38424	0.5432	0.7038	1.025
9	0.40824	0.5769	0.7474	1.0882
12	0.43544	0.6151	0.7966	1.1596
15	0.46644	0.6586	0.8527	1.241
18	0.50204	0.7086	0.9173	1.3346
21	0.54344	0.7667	0.9923	1.4434
24	0.59214	0.8351	1.0805	1.5713
27	0.65024	0.9166	1.1857	1.7239
30	0.72074	1.0156	1.3135	1.9092
33	0.80824	1.1383	1.4718	2.1387
36	0.91944	1.2944	1.6732	2.4307
39	1.06564	1.4996	1.9379	2.8145
42	1.26644	1.7813	2.3014	3.3416
45	1.55934	2.1923	2.8317	4.1104
48	2.02664	2.8479	3.6775	5.3368
51	2.88984	4.0591	5.2402	7.6024
54	5.02234	7.0511	9.1003	13.1988
57	18.98694	26.6438	34.378	49.8464
57.2	23.29794	32.6922	42.1814	61.1598
57.4	30.13964	42.2913	54.5657	79.1146
57.6	42.66624	59.8665	77.2405	111.9884
57.8	72.99934	102.4247	132.1472	191.5923
58	252.4024	354.1318	456.8888	662.4028
58.20097	∞	∞	∞	∞

Table 35. IW660 uniaxial beam-column major axis response.
 $M_{ox}=32.608$ K-in., $L=12$ ft.

	L/100000	L/1000	L/500	L/250
δ_{oy}	0.00144	0.144	0.288	0.576

P (k)	V (in)	V (in)	V (in)	V (in)
0	0.00144	0.144	0.288	0.576
3	0.72404	0.8744	1.0262	1.3299
6	0.76684	0.9258	1.0864	1.4076
9	0.81484	0.9835	1.1539	1.4947
12	0.86904	1.0487	1.2302	1.5932
15	0.93084	1.1231	1.3172	1.7055
18	1.00644	1.2086	1.4172	1.8346
21	1.08464	1.3079	1.5335	1.9846
24	1.18184	1.4248	1.6702	2.161
27	1.29784	1.5642	1.8333	2.3715
30	1.43864	1.7335	2.0313	2.627
33	1.61314	1.9432	2.2767	2.9436
36	1.83504	2.2101	2.5888	3.3464
39	2.12694	2.5608	2.9991	3.8758
42	2.52764	3.0425	3.5626	4.6028
45	3.11224	3.756	4.3846	5.6633
48	4.04494	4.8662	5.6959	7.3551
51	5.76794	6.9372	8.1183	10.4804
54	10.02414	12.0529	14.1021	18.2006
57	37.89644	45.5533	53.2876	68.756
57.2	46.50094	55.8952	65.3844	84.3628
57.4	60.15644	72.3082	84.5826	109.1315
57.6	85.15864	102.3589	119.7329	154.4809
57.8	145.7015	175.1269	204.8494	264.2945
58	503.7772	605.5066	708.2636	913.7776
58.20097	∞	∞	∞	∞

Table 36. IW660 uniaxial beam-column major axis response.
 $M_{ox}=65.316$ K-in., $L=12$ ft.

	L/100000	L/1000	L/500	L/250
δ_{oy}	0.00144	0.144	0.288	0.576

P (k)	V (in)	V (in)	V (in)	V (in)
0	0.00144	0.144	0.288	0.576
3	1.44654	1.5969	1.7487	2.0524
6	1.53204	1.691	1.8516	2.1727
9	1.62784	1.7966	1.967	2.3108
12	1.73624	1.916	2.0975	2.4605
15	1.85984	2.052	2.2461	2.6344
18	2.00544	2.2085	2.4171	2.8345
21	2.16694	2.3903	2.6158	3.0669
24	2.36114	2.6041	2.8495	3.3403
27	2.59294	2.8593	3.1284	3.6666
30	2.87424	3.1691	3.4669	4.0626
33	3.22284	3.553	3.8865	4.5534
36	3.66634	4.0414	4.4201	5.1777
39	4.24944	4.6833	5.1217	5.9983
42	5.05004	5.565	6.085	7.1252
45	6.21814	6.8511	7.4905	8.7692
48	8.08154	8.9029	9.7325	11.3917
51	11.52404	12.6933	13.8744	16.2366
54	20.02784	22.0565	24.1058	28.2042
57	75.71564	83.3725	91.1067	106.5751
57.2	92.90694	102.3013	111.7905	130.7647
57.4	120.1901	132.3419	144.6163	169.1652
57.6	170.1436	187.3439	204.7179	239.4658
57.8	291.1058	320.5312	350.2537	409.6988
58	1006.501	1108.244	1210.988	1416.576
58.20097	∞	∞	∞	∞

**Table 37. IW660 uniaxial beam-column major axis response.
 $M_{ox}=0$ K-in., L=18ft.**

	L/100000	L/1000	L/500	L/250
δ_{oy}	0.00216	0.216	0.432	0.864

P (k)	V (in)	V (in)	V (in)	V (in)
0	0.00216	0.216	0.432	0.864
1	0.002247	0.2247	0.4494	0.8988
2	0.002341	0.2341	0.4683	0.9366
3	0.002444	0.2444	0.4888	0.9776
4	0.002556	0.2556	0.5112	1.0224
5	0.002679	0.2679	0.5358	1.0716
7.5	0.003045	0.3045	0.6089	1.2178
10	0.00356	0.3526	0.7052	1.4104
12.5	0.00416	0.4188	0.8376	1.6752
15	0.00516	0.5156	1.0312	2.0625
17.5	0.00666	0.6707	1.3413	2.6826
20	0.00956	0.959	1.9181	3.8362
22.5	0.01686	1.6825	3.3651	6.7301
25	0.06846	6.8503	13.7006	27.4012
25.2	0.09086	9.0818	18.1637	36.3273
25.4	0.13466	13.4697	26.9394	53.8788
25.6	0.26056	26.061	52.122	104.2439
25.8	3.99626	399.6272	799.2544	1598.464
25.8671	∞	∞	∞	∞

Table 38. IW660 uniaxial beam-column major axis response.
 $M_{ox}=16.304$ K-in., $L=18$ ft.

	L/100000	L/1000	L/500	L/250
δ_{oy}	0.00216	0.216	0.432	0.864

P (k)	V (in)	V (in)	V (in)	V (in)
0	0.00216	0.216	0.432	0.864
1	0.80386	1.0264	1.2511	1.7005
2	0.83856	1.0703	1.3045	1.7727
3	0.87616	1.1181	1.3625	1.8513
4	0.91726	1.1703	1.4259	1.9372
5	0.96236	1.2276	1.4955	2.0312
7.5	1.09666	1.398	1.7025	2.3114
10	1.27346	1.6225	1.9751	2.6803
12.5	1.51676	1.9314	2.3501	3.1877
15	1.87266	2.3831	2.8988	3.93
17.5	2.44286	3.1068	3.7775	5.1188
20	3.50366	4.4531	5.4122	7.3303
22.5	6.16556	7.8312	9.5137	12.8788
25	25.18066	31.9624	38.8127	52.5133
25.2	33.39186	42.3828	51.4647	69.6283
25.4	49.53746	62.8725	76.3422	103.2815
25.6	95.86866	121.669	147.73	199.852
25.8	1470.502	1866.116	2265.732	3064.964
25.8671	∞	∞	∞	∞

Table 39. IW660 uniaxial beam-column major axis response.
 $M_{ox}=32.608$ K-in., $L=18$ ft.

	L/100000	L/1000	L/500	L/250
δ_{oy}	0.00216	0.216	0.432	0.864

P (k)	V (in)	V (in)	V (in)	V (in)
0	0.00216	0.216	0.432	0.864
1	1.60556	1.828	2.0527	2.5021
2	1.67466	1.9065	2.1406	2.6089
3	1.74986	1.9918	2.2363	2.7251
4	1.83196	2.0851	2.3407	2.8519
5	1.92206	2.1872	2.4551	2.9909
7.5	2.19016	2.4916	2.7961	3.405
10	2.54336	2.8924	3.245	3.95
12.5	3.02926	3.4439	3.8627	4.7003
15	3.74026	4.2507	4.7663	5.7975
17.5	4.87906	5.543	6.2137	7.555
20	6.99776	7.9472	8.9063	10.8244
22.5	12.31416	13.9799	15.6624	19.0275
25	50.29276	57.0745	63.9248	77.6254
25.2	66.69276	75.6838	84.7657	102.9293
25.4	98.94026	112.5289	125.7449	152.6843
25.6	191.4768	217.2771	243.3381	295.4601
25.8	2936.902	3332.516	3732.132	4531.464
25.8671	∞	∞	∞	∞

Table 40. IW660 uniaxial beam-column major axis response.
 $M_{ox}=65.216$ K-in., $L=18$ ft.

	L/100000	L/1000	L/500	L/250
δ_{oy}	0.00216	0.216	0.432	0.864

P (k)	V (in)	V (in)	V (in)	V (in)
0	0.00216	0.216	0.432	0.864
1	3.20886	3.4313	3.656	4.1054
2	3.34706	3.5788	3.813	4.2811
3	3.49736	3.7393	3.9837	4.4725
4	3.66146	3.9145	4.1701	4.6813
5	3.84136	4.1066	4.3745	4.9103
7.5	4.37736	4.6788	4.9832	5.5921
10	5.08316	5.4322	5.7848	6.49
12.5	6.05446	6.469	6.8878	7.7254
15	7.47526	7.9857	8.5014	9.5326
17.5	9.75136	10.4153	11.086	12.4273
20	13.98596	14.9354	15.8945	17.8126
22.5	24.61156	26.2773	27.9598	31.3249
25	100.517	107.2987	114.149	127.8496
25.2	133.2948	142.2858	151.3676	169.5313
25.4	197.7458	211.0808	224.5505	251.4899
25.6	382.6929	408.4932	434.5542	486.6762
25.8	5869.902	6265.416	6665.032	7464.364
25.8671	∞	∞	∞	∞

Table 41. IW660 uniaxial beam-column minor axis response.
 $M_{oy}=0$ K-in., $L=6$ ft.

δ_{ox}	0.00072	0.072	0.144	0.288
P (K)	U (in)	U (in)	U (in)	U (in)
0	0.00072	0.072	0.144	0.288
2.5	0.000745	0.0745	0.1489	0.2978
5	0.000771	0.0771	0.246	0.3083
10	0.000829	0.0829	0.1658	0.3317
15	0.000897	0.0897	0.1795	0.3589
20	0.000978	0.0978	0.1955	0.391
25	0.001073	0.1073	0.2147	0.4294
30	0.00119	0.119	0.2381	0.4761
35	0.001336	0.1336	0.2672	0.5343
40	0.001522	0.1522	0.3043	0.6087
45	0.00172	0.1768	0.3536	0.7071
50	0.00212	0.2109	0.4218	0.8435
55	0.00262	0.262	0.5226	1.1451
60	0.00342	0.3433	0.6866	1.3733
65	0.00502	0.5005	1.001	2.002
70	0.00922	0.9231	1.8462	3.6923
72	0.01392	1.3938	2.7876	6.16
73	0.01872	1.8708	3.7417	7.4833
74	0.02842	2.8443	5.589	11.377
75	0.05932	5.9295	11.8589	23.7179
75.9	2.49612	249.6101	499.2202	998.4403
76.0782	∞	∞	∞	∞

Table 42. . IW660 uniaxial beam-column minor axis response.
 $M_{oy}=5.328$ K-in., $L=6$ ft.

δ_{ox}	0.00072	0.072	0.144	0.288
---------------	---------	-------	-------	-------

P (K)	U (in)	U (in)	U (in)	U (in)
0	0.00072	0.072	0.144	0.288
2.5	0.08922	0.163	0.2374	0.3863
5	0.09252	0.1688	0.2459	0.4
10	0.09972	0.1818	0.2647	0.4305
15	0.10802	0.1969	0.2866	0.4661
20	0.11792	0.2147	0.3124	0.5079
25	0.12972	0.236	0.3434	0.5581
30	0.14412	0.262	0.381	0.6191
35	0.16202	0.2943	0.4279	0.695
40	0.18492	0.3356	0.4878	0.7921
45	0.21532	0.3903	0.5671	0.9206
50	0.25732	0.4661	0.6769	1.0987
55	0.31942	0.5781	0.8394	1.3619
60	0.42062	0.7605	1.1038	1.7904
65	0.61442	1.1099	1.6104	2.6114
70	1.13552	2.0493	2.9724	4.8186
72	1.71602	3.0959	4.4897	7.2773
73	2.30422	4.1564	6.0272	9.7689
74	3.50472	6.3205	9.1648	14.8533
75	7.08772	13.1796	19.109	30.968
75.9	307.8183	554.9323	804.5424	1303.788
76.0782	∞	∞	∞	∞

Table 43. IW660 uniaxial beam-column minor axis response.
 $M_{oy}=10.626$ K-in., $L=6$ ft.

δ_{ox}	0.00072	0.072	0.144	0.288
---------------	---------	-------	-------	-------

P (K)	U (in)	U (in)	U (in)	U (in)
0	0.00072	0.072	0.144	0.288
2.5	0.17782	0.2515	0.326	0.4749
5	0.18422	0.2605	0.3375	0.4918
10	0.19852	0.2806	0.3636	0.5294
15	0.21522	0.304	0.3938	0.5732
20	0.23492	0.3316	0.4294	0.6249
25	0.25842	0.3647	0.472	0.6867
30	0.28712	0.4049	0.524	0.762
35	0.32272	0.455	0.5886	0.8557
40	0.36842	0.519	0.6712	0.9756
45	0.42882	0.6038	0.7806	1.1341
50	0.55252	0.7213	0.9321	1.3539
55	0.63622	0.8949	1.1562	1.6787
60	0.83772	1.1776	1.5209	2.2076
65	1.22372	1.7193	2.2198	3.2207
70	2.26172	3.1756	4.0987	5.9448
72	3.41802	4.7979	6.1917	8.9793
73	4.58982	6.4419	8.3127	12.0544
74	6.98092	9.7967	12.641	18.3295
75	14.55952	20.4297	26.3591	38.2181
75.9	613.1406	860.2546	1109.844	1609.088
76.0782	∞	∞	∞	∞

Table 44. IW660 uniaxial beam-column minor axis response.
 $M_{oy}=21.312$ K-in., $L=6$ ft.

δ_{ox}	0.00072	0.072	0.144	0.288
P (K)	U (in)	U (in)	U (in)	U (in)
0	0.00072	0.072	0.144	0.288
2.5	0.35482	0.4285	0.503	0.6519
5	0.36762	0.444	0.521	0.6752
10	0.39622	0.4783	0.5613	0.7271
15	0.42952	0.5184	0.6081	0.7875
20	0.46882	0.5655	0.6633	0.8588
25	0.51572	0.622	0.7294	0.9441
30	0.57292	0.6908	0.8098	1.0479
35	0.64422	0.7764	0.91	1.1772
40	0.73522	0.8859	1.0381	1.3424
45	0.85582	1.0308	1.2076	1.5611
50	1.02282	1.2316	1.4425	1.8643
55	1.26982	1.5285	1.7898	2.3123
60	1.67202	2.0119	2.3552	3.0419
65	2.44252	2.938	3.4385	4.4395
70	4.51422	5.4281	6.3512	8.1973
72	6.82212	8.202	9.5958	12.3834
73	9.16082	11.013	12.8838	16.6255
74	13.93342	16.7492	19.5935	25.282
75	29.05962	34.9298	40.8593	52.7183
75.9	1223.801	1470.872	1720.544	2219.688
76.0782	∞	∞	∞	∞

Table 45. IW660 uniaxial beam-column minor axis response.
 $M_{oy}=0$ K-in., $L=12$ ft.

δ_{ox}	0.00144	0.144	0.288	0.576
---------------	---------	-------	-------	-------

P (K)	U (in)	U (in)	U (in)	U (in)
0	0.00144	0.144	0.288	0.576
1	0.00152	0.152	0.304	0.608
2	0.001608	0.161	0.3219	0.6438
4	0.001825	0.1825	0.3649	0.7298
6	0.002106	0.2106	0.4211	0.8422
8	0.00244	0.2489	0.4978	0.9957
10	0.00304	0.3043	0.6087	1.2174
12	0.00394	0.3915	0.7831	1.5662
14	0.00544	0.5488	1.0976	2.1951
16	0.00914	0.917	1.8341	3.6681
17	0.01384	1.3801	2.7601	5.5203
18	0.02784	2.7876	5.5752	11.1505
18.5	0.05684	5.6885	11.377	22.7541
18.9	0.33964	33.9632	67.9265	135.8529
19.01955	∞	∞	∞	∞

Table 46. IW660 uniaxial beam-column minor axis response.
 $M_{oy}=5.328$ K-in., $L=12$ ft.

δ_{ox}	0.00144	0.144	0.288	0.576
---------------	---------	-------	-------	-------

P (K)	U (in)	U (in)	U (in)	U (in)
0	0.00144	0.144	0.288	0.576
1	0.36324	0.5137	0.6657	0.9697
2	0.38514	0.5445	0.7054	1.0273
4	0.43774	0.6184	0.8008	1.1657
6	0.50664	0.7151	0.9257	1.3468
8	0.60074	0.8472	1.0961	1.5939
10	0.73674	1.0381	1.3424	1.9511
12	0.95084	1.3384	1.73	2.5131
14	1.33684	1.8802	2.429	3.5265
16	2.24134	3.1492	4.0662	5.9003
17	3.37864	4.7449	6.125	8.8851
18	6.83604	9.5958	12.3834	17.9587
18.5	13.90748	19.5935	25.282	36.659
18.9	83.41634	117.0399	151.0031	218.9296
19.01955	∞	∞	∞	∞

Table 47. IW660 uniaxial beam-column minor axis response.
 $M_{oy}=10.656$ K-in., $L=12$ ft.

δ_{ox}	0.00144	0.144	0.288	0.576
---------------	---------	-------	-------	-------

P (K)	U (in)	U (in)	U (in)	U (in)
0	0.00144	0.144	0.288	0.576
1	0.72484	0.8753	1.0274	1.3314
2	0.76864	0.928	1.0889	1.4108
4	0.87374	1.0543	1.2368	1.6017
6	1.01124	1.2197	1.4303	1.8514
8	1.19894	1.4454	1.6943	2.1922
10	1.47044	1.7718	2.0761	2.6848
12	1.89774	2.2853	2.6769	3.46
14	2.66824	3.2116	3.7603	4.8579
16	4.47344	5.3813	6.2983	8.1324
17	6.74344	8.1097	9.4898	12.2499
18	13.64424	16.404	19.1916	24.7669
18.5	27.86684	33.4984	39.1869	50.564
18.9	166.4929	200.1166	234.0798	302.0063
19.01955	∞	∞	∞	∞

Table 48. IW660 uniaxial beam-column minor axis response.
 $M_{oy}=21.312$ K-in., $L=12$ ft.

δ_{ox}	0.00144	0.144	0.288	0.576
---------------	---------	-------	-------	-------

P (K)	U (in)	U (in)	U (in)	U (in)
0	0.00144	0.144	0.288	0.576
1	1.44824	1.5987	1.7507	2.0547
2	1.53564	1.695	1.8559	2.1779
4	1.74554	1.9262	2.1087	2.4736
6	2.02034	2.2288	2.4394	2.8605
8	2.39544	2.6419	2.8908	3.3887
10	2.93794	3.2392	3.5436	4.1523
12	3.79144	4.1791	4.5707	5.3538
14	5.33104	5.8744	6.4231	7.5207
16	8.93764	9.8455	10.7626	12.5966
17	13.47314	14.8394	16.2194	18.9796
18	27.26064	30.0204	32.808	38.3832
18.5	55.67674	61.3083	66.9969	78.3739
18.9	332.6463	366.2699	400.2331	468.1596
19.01955	∞	∞	∞	∞

Table 49. IW660 uniaxial beam-column minor axis response.
 $M_{o7}=0$ K-in., $L=18$ ft.

δ_{ox}	0.00216	0.216	0.432	0.864
---------------	---------	-------	-------	-------

P (K)	U (in)	U (in)	U (in)	U (in)
0	0.00216	0.216	0.432	0.864
0.5	0.002296	0.2296	0.4592	0.9184
1	0.00245	0.245	0.4901	0.9802
2	0.002831	0.2831	0.5662	1.1325
3	0.00336	0.3352	0.6704	1.3408
4	0.00406	0.4108	0.8216	1.6431
5	0.00526	0.5303	1.0607	2.1214
6	0.00746	0.7481	1.4961	2.9923
6.5	0.00946	0.9413	1.8826	3.7652
7	0.01266	1.2691	2.5382	5.0764
7.5	0.01946	1.9472	3.8944	7.7888
8	0.04186	4.1814	8.3629	16.7257
8.2	0.07726	7.7285	15.457	30.9141
8.4	0.50946	50.9449	101.8897	203.7794
8.453133	∞	∞	∞	∞

Table 50. IW660 uniaxial beam-column minor axis response.
 $M_{oy}=5.328$ K-in., $L=18$ ft.

δ_{ox}	0.00216	0.216	0.432	0.864
P (K)	U (in)	U (in)	U (in)	U (in)
0	0.00216	0.216	0.432	0.864
0.5	0.82186	1.0492	1.2788	1.738
1	0.87856	1.1211	1.3662	1.8563
2	1.01826	1.2986	1.5817	2.148
3	1.20956	1.5414	1.8767	2.5471
4	1.48726	1.894	2.3047	3.1263
5	1.92686	2.4519	2.9822	4.0429
6	2.72766	3.4682	4.2163	5.7124
6.5	3.43836	4.3703	5.3116	7.1942
7	4.64436	5.9008	7.1699	9.7081
7.5	7.13936	9.0671	11.0143	14.9087
8	15.36026	19.4999	23.6813	32.0441
8.2	28.41216	36.0634	43.7919	59.2289
8.4	187.432	237.8674	88.8122	390.7019
8.453133	∞	∞	∞	∞

Table 51. IW660 uniaxial beam-column minor axis response.
 $M_{oy}=10.656$ K-in., $L=18$ ft.

δ_{ox}	0.00216	0.216	0.432	0.864
P (K)	U (in)	U (in)	U (in)	U (in)
0	0.00216	0.216	0.432	0.864
0.5	1.64146	1.8688	2.0984	2.5576
1	1.75466	1.9972	2.2423	2.7324
2	2.03376	2.314	2.5972	3.1634
3	2.41586	2.7477	3.0829	3.7533
4	2.97046	3.3771	3.7879	4.6095
5	3.84836	4.3734	4.9038	5.9644
6	5.44776	6.1883	6.9364	8.4326
6.5	6.86736	7.7993	8.7406	10.6232
7	9.27606	10.5325	11.8016	14.3398
7.5	14.25926	16.187	18.1342	22.0286
8	30.67866	34.8183	38.9997	47.3626
8.2	56.74696	64.3982	72.1267	87.5837
8.4	374.3545	424.7899	475.7347	577.6244
8.453133	∞	∞	∞	∞

Table 52. IW660 uniaxial beam-column minor axis response.
 $M_{oy}=21.312$ K-in., $L=18$ ft.

δ_{ox}	0.00216	0.216	0.432	0.864
P (K)	U (in)	U (in)	U (in)	U (in)
0	0.00216	0.216	0.432	0.864
0.5	3.28066	3.508	3.7376	4.1968
1	3.50676	3.7494	3.9944	4.4845
2	4.06466	4.345	4.6281	5.1943
3	4.82826	5.1601	5.4954	6.1658
4	5.93686	6.3435	6.7543	7.5758
5	7.69146	8.2165	8.7468	9.8075
6	10.88806	11.6286	12.3767	13.8728
6.5	13.72536	14.6573	15.5986	17.4811
7	18.53946	19.7959	21.065	23.6032
7.5	28.49896	30.4267	32.3739	36.2683
8	61.31556	65.4552	69.6366	77.9895
8.2	113.4167	121.0679	128.7964	144.2534
8.4	748.1995	798.6349	849.5797	951.4694
8.453133	∞	∞	∞	∞

**Table 53. IW660 biaxial beam-column response . $M_{ox}=0$, $M_{oy}=0$,
L=6ft.**

δ_o (in)	0.00072		0.072		0.144		0.288	
-----------------	---------	--	-------	--	-------	--	-------	--

P (K)	U (in)	V (in)	U (in)	V (in)	U (in)	V (in)	U (in)	V (in)
0	0.00072	0.00072	0.072	0.072	0.144	0.144	0.288	0.288
7.6078	0.0008	0.000744	0.08	0.0744	0.16	0.1489	0.304	0.2929
15.216	0.0009	0.00077	0.09	0.077	0.1801	0.1541	0.3241	0.2981
22.823	0.00103	0.000798	0.1029	0.0798	0.2059	0.1597	0.3499	0.3037
30.431	0.0012	0.000829	0.1202	0.0829	0.2403	0.1657	0.3843	0.3097
38.039	0.00144	0.000861	0.1443	0.0861	0.2886	0.1722	0.4326	0.3162
45.647	0.00182	0.000896	0.1806	0.0896	0.3611	0.1792	0.5051	0.3232
53.255	0.00242	0.000934	0.2412	0.0934	0.4823	0.1868	0.6263	0.3308
60.862	0.00362	0.000976	0.363	0.0976	0.726	0.1951	0.87	0.3391
68.47	0.00732	0.001021	0.7336	0.1021	1.4672	0.2042	1.6112	0.3482
70.372	0.00982	0.001033	0.985	0.1033	1.97	0.2066	2.114	0.3506
72.274	0.01502	0.001045	1.4986	0.1045	2.9972	0.209	3.1412	0.353
74.176	0.03132	0.001058	3.1314	0.1058	6.2628	0.2115	6.4068	0.3555
75.317	0.09042	0.001065	9.0431	0.1065	18.0862	0.2131	18.2302	0.3571
76.078	∞		∞		∞		∞	

Table 54. IW660 biaxial beam-column response. $M_{ox}=16.304\text{K-in.}$, $M_{oy}=5.328\text{K-in.}$, $L=6\text{ft.}$

$\delta_o(\text{in})$	0.00072	0.072	0.144	0.288
-----------------------	---------	-------	-------	-------

P (K)	U (in)	V (in)	U (in)	V (in)	U (in)	V (in)	U (in)	V (in)
0	0.08712	0.08712	0.1584	0.1584	0.2304	0.2304	0.3744	0.3744
7.6078	0.09712	0.09012	0.1764	0.1638	0.2564	0.2383	0.4164	0.3872
15.216	0.10962	0.09342	0.1988	0.1697	0.2888	0.2467	0.4689	0.4008
22.823	0.12572	0.09692	0.2276	0.1759	0.3306	0.2558	0.5365	0.4155
30.431	0.14722	0.10062	0.2662	0.1827	0.3864	0.2655	0.6268	0.4312
38.039	0.17732	0.10462	0.3202	0.1899	0.4646	0.276	0.7532	0.4482
45.647	0.22262	0.10902	0.4014	0.1978	0.5821	0.2874	0.9434	0.4666
53.255	0.29832	0.11382	0.5373	0.2063	0.7786	0.2997	1.2613	0.4865
60.862	0.45082	0.11892	0.8106	0.2155	1.174	0.3131	1.9009	0.5083
68.47	0.91552	0.12462	1.6438	0.2257	2.3794	0.3278	3.8506	0.5321
70.372	1.23162	0.12612	2.2105	0.2284	3.1992	0.3318	5.1767	0.5384
72.274	1.87942	0.12772	3.3718	0.2312	4.8793	0.3358	7.8941	0.545
74.176	3.95702	0.12932	7.0963	0.2342	10.2673	0.3436	16.6093	0.552
75.317	11.718	0.13072	21.0097	0.2366				
76.078	∞		∞		∞		∞	

Table 55. IW660 biaxial beam-column response. $M_{ox}=32.608\text{K-in.}$, $M_{oy}=10.656\text{K-in.}$, $L=6\text{ft.}$

$\delta_o(\text{in})$	0.00072		0.072		0.144		0.288	
-----------------------	---------	--	-------	--	-------	--	-------	--

P (K)	U (in)	V (in)	U (in)	V (in)	U (in)	V (in)	U (in)	V (in)
0	0.17382	0.17352	0.2451	0.2448	0.3171	0.3168	0.4611	0.4608
7.6078	0.19372	0.17962	0.2729	0.2533	0.353	0.3277	0.513	0.4766
15.216	0.21862	0.18602	0.3078	0.2623	0.3979	0.3394	0.578	0.4935
22.823	0.25072	0.19302	0.3527	0.272	0.4557	0.3519	0.6618	0.5116
30.431	0.29372	0.20042	0.4127	0.2825	0.533	0.3654	0.7736	0.5311
38.039	0.35392	0.20852	0.4969	0.2938	0.6414	0.3799	0.9304	0.5521
45.647	0.44452	0.21722	0.6236	0.306	0.8045	0.3956	1.1663	0.5748
53.255	0.59622	0.22672	0.8357	0.3192	1.0776	0.4127	1.5613	0.5996
60.862	0.90222	0.23702	1.2634	0.3337	1.6282	0.4313	2.3578	0.6265
68.47	1.84092	0.24852	2.5753	0.3497	3.317	0.4519	4.8006	0.6563
70.372	2.48432	0.25162	3.4744	0.354	4.4746	0.4575	6.4749	0.6644
72.274	3.81542	0.25492	5.3349	0.3586	6.8696	0.4634	9.9391	0.673
74.176	8.20352	0.25882	11.4675	0.3642	14.7645	0.4706	21.3584	0.6834
75.317	26.3843	0.26432	36.8764	0.3718	47.4745	0.4804	68.6706	0.6975
76.078	∞		∞		∞		∞	

Table 56. IW660 biaxial beam-column response. $M_{ox}=65.216\text{K-in.}$, $M_{oy}=21.262\text{K-in.}$, $L=6\text{ft.}$

$\delta_o(\text{in})$	0.00072	0.072	0.144	0.288
-----------------------	---------	-------	-------	-------

P (K)	U (in)	V (in)	U (in)	V (in)	U (in)	V (in)	U (in)	V (in)
0	0.34832	0.34652	0.4196	0.4178	0.4916	0.4898	0.5356	0.6338
7.6078	0.38852	0.35862	0.4678	0.4323	0.5478	0.5068	0.708	0.6556
15.216	0.43872	0.37152	0.528	0.4479	0.6182	0.5249	0.7985	0.679
22.823	0.50362	0.38542	0.6057	0.4645	0.7089	0.5444	0.9153	0.7041
30.431	0.59032	0.40042	0.7097	0.4825	0.8303	0.5654	1.0715	0.7311
38.039	0.71222	0.41652	0.8559	0.5019	1.0009	0.588	1.291	0.7603
45.647	0.89632	0.43412	1.0765	0.5229	1.2584	0.6126	1.6224	0.7919
53.255	1.20602	0.45322	1.4477	0.5458	1.6917	0.6393	2.1799	0.8264
60.862	1.83662	0.47422	2.2034	0.571	2.5739	0.6688	3.3148	0.8643
68.47	3.82122	0.49822	4.5817	0.5998	5.3499	0.7024	6.8864	0.9077
70.372	5.22722	0.50522	6.2667	0.6083	7.3166	0.7123	9.4166	0.9204
72.274	8.26162	0.51372	9.9031	0.6184	11.5612	0.7242	14.8773	0.9357
74.176	19.6461	0.52892	23.5461	0.6367	27.4855	0.7455	35.3643	0.9631
75.317	112.651	0.60622	135.0021	0.7292	157.5779	0.8535	202.7326	1.1021
76.078	∞		∞		∞		∞	

**Table 57. IW660 biaxial beam-column response. $M_{ox}=0$, $M_{oy}=0$,
L=12ft.**

δ_o (in)	0.00144	0.144	0.288	0.576
-----------------	---------	-------	-------	-------

P (K)	U (in)	V (in)	U (in)	V (in)	U (in)	V (in)	U (in)	V (in)
0	0.00144	0.00144	0.144	0.144	0.288	0.288	0.576	0.576
1.902	0.0016	0.001489	0.16	0.1489	0.3201	0.2978	0.6401	0.5955
3.804	0.001801	0.001541	0.1801	0.1541	0.3602	0.3082	0.7204	0.6164
5.706	0.002059	0.001597	0.2059	0.1597	0.4118	0.3194	0.8236	0.6388
7.608	0.002403	0.001657	0.2403	0.1657	0.4807	0.3314	0.9613	0.6628
9.51	0.00284	0.001722	0.2886	0.1722	0.5772	0.3444	1.1544	0.6888
11.412	0.00364	0.001792	0.3611	0.1792	0.7222	0.3584	1.4445	0.7168
13.314	0.00484	0.001868	0.4823	0.1868	0.9646	0.3736	1.9293	0.7473
15.216	0.00724	0.001951	0.726	0.1951	1.452	0.3902	2.9039	0.7805
17.118	0.01464	0.002042	1.4672	0.2042	2.9344	0.4083	5.8687	0.8167
17.5935	0.01974	0.002066	1.97	0.2066	3.94	0.4131	7.8801	0.8263
18.069	0.02994	0.00209	2.9972	0.209	5.9945	0.4181	11.989	0.8361
18.5445	0.06264	0.002115	6.2628	0.2115	12.5257	0.4231	25.0514	0.8462
18.8298	0.18084	0.002131	18.0862	0.2131	36.1724	0.4262	72.3447	0.8523
19.02	∞		∞		∞		∞	

Table 58. IW660 biaxial beam-column response. $M_{ox}=16.304\text{K-in.}$, $M_{oy}=5.328\text{K-in.}$, $L=12\text{ft.}$

$\delta_o(\text{in})$	0.00144	0.144	0.288	0.576				
P (K)	U (in)	V (in)	U (in)	V (in)	U (in)	V (in)	U (in)	V (in)
0	0.34794	0.34714	0.4905	0.4897	0.6345	0.6337	0.9225	0.9217
1.901955	0.38794	0.35924	0.5464	0.5066	0.7065	0.6555	1.0267	0.9533
3.80391	0.43794	0.37214	0.6164	0.5247	0.7966	0.6788	1.157	0.9871
5.705865	0.50244	0.38604	0.7065	0.5442	0.9126	0.7039	1.3249	1.0233
7.60782	0.58854	0.40104	0.8269	0.5651	1.0677	0.7308	1.5493	1.0623
9.509775	0.70954	0.41714	0.996	0.5877	1.2854	0.7599	1.8642	1.1044
11.41173	0.89184	0.43464	1.2507	0.6121	1.6133	0.7914	2.3384	1.15
13.31369	1.19744	0.45364	1.6779	0.6387	2.1632	0.8257	3.1337	1.1996
15.21564	1.81594	0.47444	2.5421	0.6679	3.2756	0.8632	4.7426	1.2539
17.1176	3.72934	0.49774	5.2156	0.7004	6.7169	0.9051	9.7194	1.3146
17.5935	5.05534	0.50424	7.0683	0.7095	9.1016	0.9168	13.1683	1.3315
18.069	7.83694	0.51144	10.9549	0.7196	14.1044	0.9299	20.4032	1.3504
18.5445	17.38754	0.52164	24.2993	0.7338	31.2808	0.9482	45.2438	1.3769
18.8298	64.43694	0.54484	90.0377	0.7662	115.8971	0.9899	167.6158	1.4372
19.01955	∞		∞		∞		∞	

Table 59. IW660 biaxial beam-column response. $M_{ox}=32.608\text{K-in.}$, $M_{oy}=10.656\text{K-in.}$, $L=12\text{ft.}$

$\delta_o(\text{in})$	0.00144	0.144	0.288	0.576				
P (K)	U (in)	V (in)	U (in)	V (in)	U (in)	V (in)	U (in)	V (in)
0	0.70094	0.69354	0.8435	0.8361	0.9875	0.9801	1.2755	1.2681
1.901955	0.78224	0.71774	0.9409	0.8652	1.1011	1.0141	1.4216	1.3119
3.80391	0.88424	0.74374	1.0631	0.8964	1.2437	1.0505	1.605	1.3588
5.705865	1.01594	0.77164	1.2209	0.9299	1.4279	1.0896	1.8419	1.4092
7.60782	1.19274	0.80174	1.4326	0.966	1.6749	1.1318	2.1595	1.4635
9.509775	1.44224	0.83434	1.7314	1.005	2.0235	1.1774	2.6077	1.5223
11.41173	1.82064	0.86974	2.1846	1.0475	2.5523	1.2271	3.2876	1.5862
13.31369	2.46294	0.90864	2.9538	1.095	3.4496	1.2815	4.4411	1.6564
15.21564	3.79184	0.95204	4.545	1.1463	5.3059	1.3424	6.8275	1.7348
17.1176	8.16924	1.00494	9.7867	1.2096	11.4204	1.4165	14.695	1.8301
17.5935	11.46294	1.02274	13.7305	1.2311	16.021	1.4415	20.6021	1.8623
18.069	19.18304	1.04904	22.9747	1.2625	26.8046	1.4781	34.4645	1.9094
18.5445	58.53034	1.13304	70.0895	1.3632	81.7653	1.5956	105.1171	2.0605
19.01955	∞		∞		∞		∞	

Table 60. IW660 biaxial beam-column response. $M_{ox}=65.216\text{K-in.}$, $M_{oy}=21.312\text{K-in.}$, $L=12\text{ft.}$

$\delta_o(\text{in})$	0.00144	0.144	0.288	0.576				
P (K)	U (in)	V (in)	U (in)	V (in)	U (in)	V (in)	U (in)	V (in)
0	1.48284	1.39444	1.6254	1.537	1.7694	1.681	2.0574	1.969
1.901955	1.66584	1.44434	1.8256	1.5919	1.9869	1.7409	2.3095	2.0389
3.80391	1.89884	1.49814	2.0803	1.651	2.2636	1.8054	2.6303	2.1142
5.705865	2.20534	1.55644	2.4155	1.7151	2.6278	1.8753	3.0523	2.1958
7.60782	2.62654	1.62014	2.8761	1.785	3.1281	1.9516	3.6322	2.2848
9.509775	3.24164	1.69034	3.5486	1.8622	3.8586	2.0358	4.4787	2.383
11.41173	4.22354	1.76954	4.6222	1.9492	5.0248	2.1307	5.8301	2.4937
13.31369	6.03904	1.86304	6.6071	2.0519	7.1808	2.2426	8.3283	2.6241
15.21564	10.52864	1.99004	11.51513	2.1912	12.5121	2.3944	14.5055	2.8007
17.1176	40.04344	2.37524	43.7826	2.6129	47.5596	2.8529	55.1136	3.3329
17.5935	132.1068	3.32104	144.4313	3.647	156.8803	3.9763	181.7762	4.6348
19.01955								

**Table 61. IW660 biaxial beam-column response. $M_{ox}=0$, $M_{oy}=0$,
L=18ft.**

δ_o (in)	0.00216		0.216		0.432		0.864	
-----------------	---------	--	-------	--	-------	--	-------	--

P (K)	U (in)	V (in)	U (in)	V (in)	U (in)	V (in)	U (in)	V (in)
0	0.00216	0.00216	0.216	0.216	0.432	0.432	0.864	0.864
0.8453	0.002401	0.002233	0.2401	0.2233	0.4801	0.4466	0.9602	0.8933
1.6906	0.002701	0.002311	0.2701	0.2311	0.5403	0.4623	1.0806	0.9246
2.5359	0.003088	0.002395	0.3088	0.2395	0.6177	0.4791	1.2354	0.9581
3.3812	0.00356	0.002486	0.3605	0.2486	0.721	0.4971	1.442	0.9942
4.2265	0.00436	0.002583	0.4329	0.2583	0.8658	0.5166	1.7316	1.0332
5.0718	0.00546	0.002688	0.5417	0.2688	1.0833	0.5376	2.1667	1.0753
5.9171	0.00726	0.002802	0.7235	0.2802	1.447	0.5605	2.8939	1.1209
6.7624	0.01086	0.002927	1.089	0.2927	2.1779	0.5853	4.3559	1.1707
7.6077	0.02196	0.003063	2.2008	0.3063	4.4016	0.6125	8.8031	1.225
7.819025	0.02956	0.003099	2.955	0.3099	5.9101	0.6197	11.8201	1.2394
8.03035	0.04496	0.003135	4.4959	0.3135	8.9917	0.6271	17.9834	1.2542
8.241675	0.09396	0.00316	9.3943	0.3173	18.7885	0.6346	37.577	1.2692
8.36847	0.27126	0.00316	27.1293	0.3196	54.2585	0.6392	108.5171	1.2785
8.453	∞		∞		∞		∞	

Table 62. IW660 biaxial beam-column response. $M_{ox}=16.304K$ -in., $M_{oy}=5.328K$ -in., $L=18ft$.

δ_o (in)	0.00216	0.216	0.432	0.864				
P (K)	U (in)	V (in)	U (in)	V (in)	U (in)	V (in)	U (in)	V (in)
0	0.77426	0.77916	0.9881	0.993	1.2041	1.209	1.6361	1.641
0.8453	0.86256	0.80626	1.1002	1.0273	1.3402	1.2506	1.8202	1.6973
1.6906	0.97306	0.83526	1.2404	1.0641	1.5104	1.2952	2.0504	1.7575
2.5359	1.11526	0.86636	1.4207	1.1035	1.7293	1.343	2.3465	1.822
3.3812	1.30486	0.89986	1.6612	1.1459	2.0212	1.3944	2.7412	1.8914
4.2265	1.57036	0.93586	1.998	1.1915	2.4299	1.4498	3.2938	1.9663
5.0718	1.96856	0.97486	2.503	1.2409	3.0429	1.5097	4.1226	2.047
5.9171	2.63216	1.01706	3.3445	1.2944	4.0641	1.5746	5.5033	2.1348
6.7624	3.95816	1.06296	5.026	1.3525	6.1046	1.645	8.1719	2.2299
7.6077	7.92536	1.11246	10.0566	1.4152	12.2093	1.721	16.5147	2.3326
7.819025	10.56086	1.12516	13.3983	1.4313	16.2645	1.7406	21.9968	2.359
8.03035	15.80916	1.13766	20.0532	1.4471	24.3402	1.7596	32.914	2.3847
8.241675	31.37526	1.14786	39.791	1.46	48.2917	1.7753	65.2932	2.406
8.36847	76.51946	1.14556	97.0337	1.457	117.7552	1.7717	159.1982	2.401
8.453	∞		∞		∞		∞	

**Table 63. IW660 biaxial beam-column response. $M_{ox}=32.608K$ -
in., $M_{oy}=10.656K$ -in., $L=18ft$.**

δ_o (in)	0.00216	0.216	0.432	0.864				
P (K)	U (in)	V (in)	U (in)	V (in)	U (in)	V (in)	U (in)	V (in)
0	1.55436	1.55706	1.7682	1.7709	1.9842	1.9869	2.4162	2.4189
0.8453	1.73546	1.61166	1.9735	1.8327	2.2139	2.0561	2.6948	2.5028
1.6906	1.96286	1.67016	2.2313	1.899	2.5024	2.1303	3.0447	2.5927
2.5359	2.25726	1.73306	2.5649	1.9704	2.8757	2.2101	3.4973	2.6895
3.3812	2.65286	1.80096	3.0133	2.0474	3.3774	2.2962	4.1056	2.7939
4.2265	3.21296	1.87466	3.648	2.1308	4.0874	2.3896	4.9663	2.9071
5.0718	4.06616	1.95516	4.6148	2.222	5.169	2.4916	6.2774	3.0308
5.9171	5.52426	2.04406	6.2669	2.3228	7.017	2.6043	8.5174	3.1674
6.7624	8.58126	2.14536	9.7306	2.4374	10.8914	2.73277	13.2132	3.323
7.6077	19.05306	2.27766	21.5948	2.5874	24.1622	2.9003	29.2969	3.5261
7.819025	27.36386	2.32936	31.0106	2.646	34.6942	2.9659	42.0613	3.6056
8.03035	48.46536	2.42036	54.9177	2.7492	61.4351	3.0813	74.4701	3.7454
8.241675	210.4509	2.93776	238.4397	3.3353	266.7113	3.7369	323.2544	4.54
8.453	∞		∞		∞		∞	

Table 64. IW660 biaxial beam-column response. $M_{ox}=65.216\text{K-in.}$, $M_{oy}=21.312\text{K-in.}$, $L=18\text{ft.}$

$\delta_o(\text{in})$	0.00216	0.216	0.432	0.864
-----------------------	---------	-------	-------	-------

P (K)	U (in)	V (in)	U (in)	V (in)	U (in)	V (in)	U (in)	V (in)
0	5.62576	3.38096	5.8396	3.5948	6.0556	3.8108	6.4876	4.2428
0.8453	6.99426	3.57216	7.2542	3.7954	7.5168	4.021	8.042	4.4721
1.6906	9.20796	3.82326	9.5421	4.0582	9.8796	4.2955	10.5547	4.7702
2.5359	13.38986	4.20456	13.8636	4.4557	14.3421	4.7094	15.2992	5.2168
3.3812	24.22946	5.00726	25.0639	5.2889	25.9068	5.5734	27.5927	6.1423
4.2265	118.6182	10.98926	122.588	11.4736	126.5979	11.9629	134.6178	12.9414
8.453	∞	∞	∞	∞	∞	∞	∞	∞

Table 65. IW660-Load-Interaction L/500. Major axis

$P_u/\Phi \cdot P_n$	P_u (K)	V (in.)	$P_u V$ (K-in.)	$P_u V/\Phi_b M_n$	$M_u/\Phi_b M_n$
0	0	0.144	0	0	1.000
0.1	12.06007	0.242348	2.9227394	0.0168364	0.883
0.2	24.12014	0.25655	6.1880214	0.0356459	0.764
0.3	36.18021	0.277243	10.030706	0.0577816	0.642
0.4	48.24028	0.29039	14.008494	0.0806956	0.519
0.5	60.30035	0.310877	18.74599	0.1079858	0.392
0.6	72.36041	0.334646	24.215123	0.1394906	0.261
0.7	84.42048	0.362307	30.586132	0.1761907	0.124
0.8	96.48055	0.394734	38.084154	0.2193828	-0.019
0.9	108.5406	0.43324	47.024139	0.2708814	-0.171
1.0	120.6007	0.479835	57.868432	0.3333497	-0.333

Table 66. IW660-Load-Interaction L/100000. Major axis

$P_u/\Phi_c P_n$	P_u	V (in.)	$P_u V$ (K-in.)	$P_u V/\Phi_b M_n$	$M_u/\Phi_b M_n$
0	0	0.144	0	0	1.0000
0.1	13.8	0.09189	1.266908	0.007297993	0.8927
0.2	27.6	0.09827	2.709574	0.015608433	0.7844
0.3	41.4	0.11017	4.556643	0.026248431	0.6738
0.4	55.1	0.11394	6.283822	0.036197802	0.5638
0.5	68.9	0.12368	8.525861	0.049113014	0.4509
0.6	82.7	0.13546	11.20582	0.064550864	0.3354
0.7	96.5	0.14949	14.42731	0.083108195	0.2169
0.8	110	0.16648	18.36262	0.10577741	0.0942
0.9	124	0.18843	23.38126	0.134687169	-0.0347
1.0	138	0.21629	29.8207	0.171781392	-0.1718

Table 67. IW880 column major axis response. L=6ft.

P (K)	K_P/K_0
0	1
50	0.8921
100	0.7913
150	0.6973
200	0.6096
250	0.5281
300	0.4524
350	0.3822
400	0.3173
450	0.2574
500	0.2022
550	0.1515
600	0.1051
650	0.0628
700	0.0243
750	-0.0107

Table 68. IW880 column major axis response. L=12ft.

P (K)	K _P /K ₀
1	0
0.8308	20
0.6792	40
0.5439	60
0.4237	80
0.3173	100
0.2237	120
0.1419	140
0.0709	160
0.0099	180
-0.0422	200

Table 69. IW880 column major axis response. L=18ft.

P (K)	K _P /K ₀
0	1
10	0.8109
20	0.6439
30	0.4971
40	0.3688
50	0.2574
60	0.1613
70	0.0793
80	0.009
90	-0.0481
100	-0.0957

Table 70. IW880 column minor axis response. L=6ft.

P (K)	K_P/K_0
0	1
20	0.8689
40	0.7483
60	0.6376
80	0.5362
100	0.4436
120	0.3592
140	0.2826
160	0.2132
180	0.1507
200	0.0946
220	0.0444
240	-0.0002
260	-0.0396

Table 71. IW880 column minor axis response. L=12ft

P (K)	K_P/K_0
0	1
10	0.7483
20	0.5362
30	0.3592
40	0.2132
50	0.0946
60	-0.0002
70	-0.0741

Table 72. IW880 column minor axis response. L=18ft

P (K)	K_P/K_0
0	1
3	0.8256
6	0.6699
9	0.5314
12	0.4089
15	0.3011
18	0.2067
21	0.1247
24	0.054
27	-0.0064
30	-0.0574

APPENDIX

FIGURES

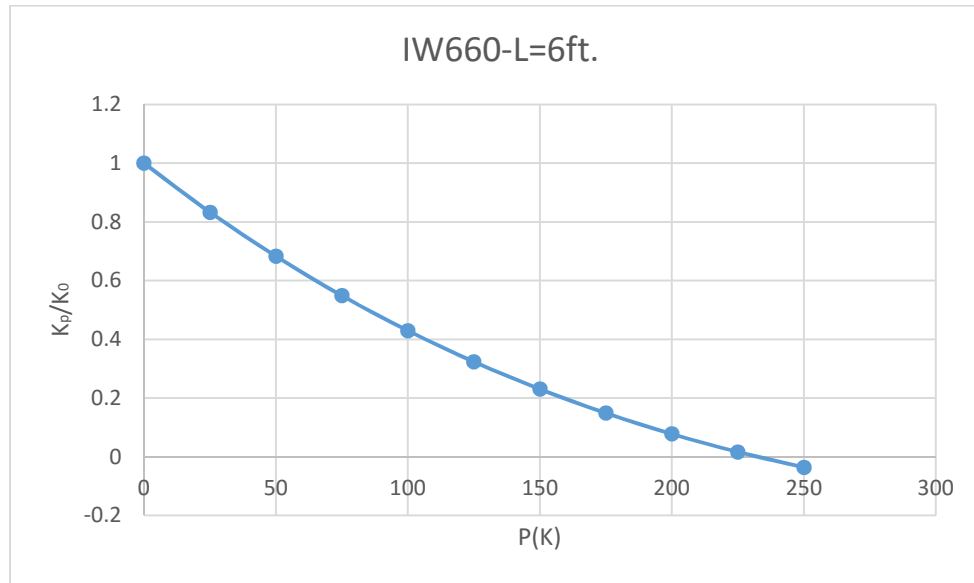


Fig. 1. Stiffness degradation for column major axis response.

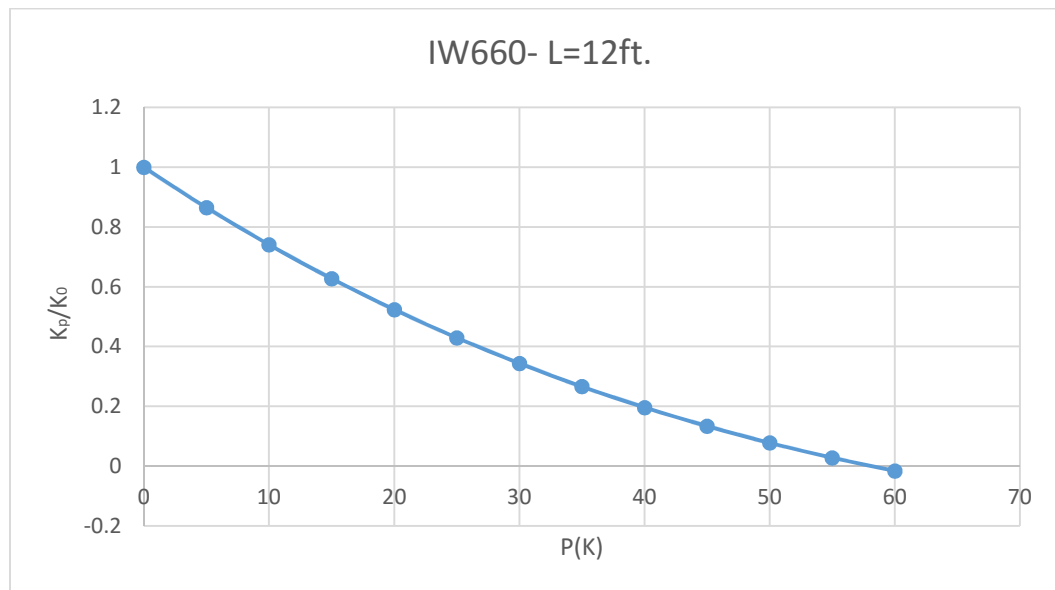


Fig. 2. Stiffness degrading for column major axis response.

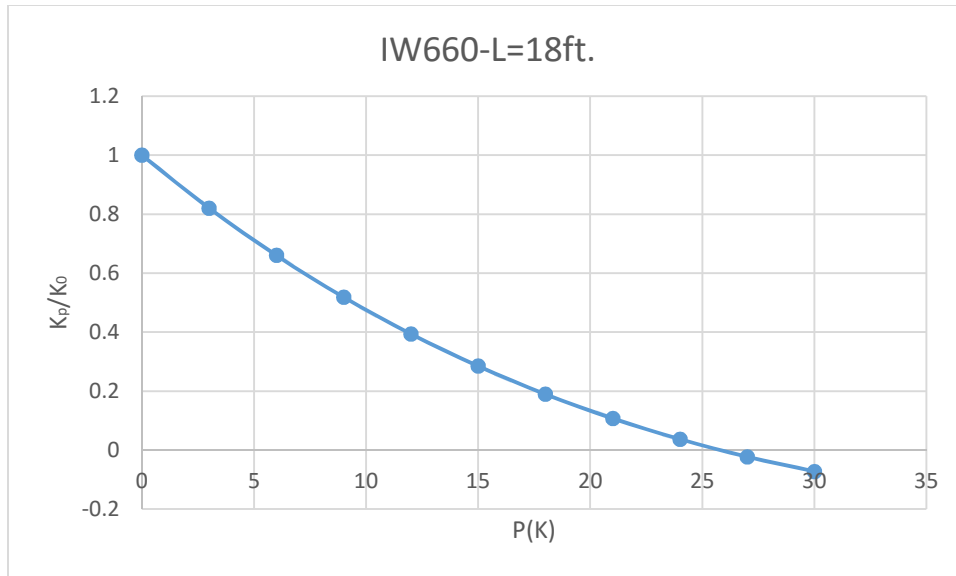


Fig. 3. Stiffness degrading for column major axis response.

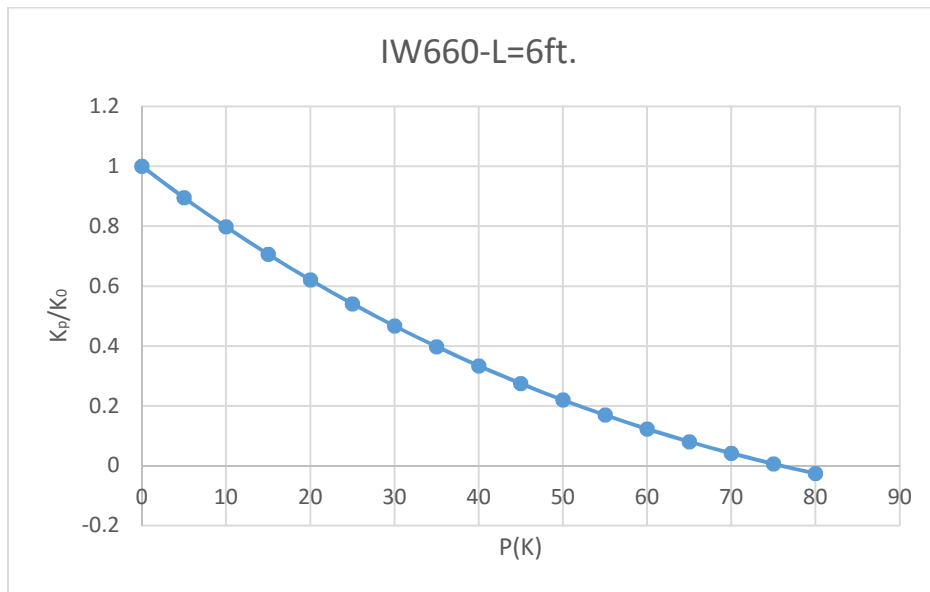


Fig. 4. Stiffness degrading for column minor axis response

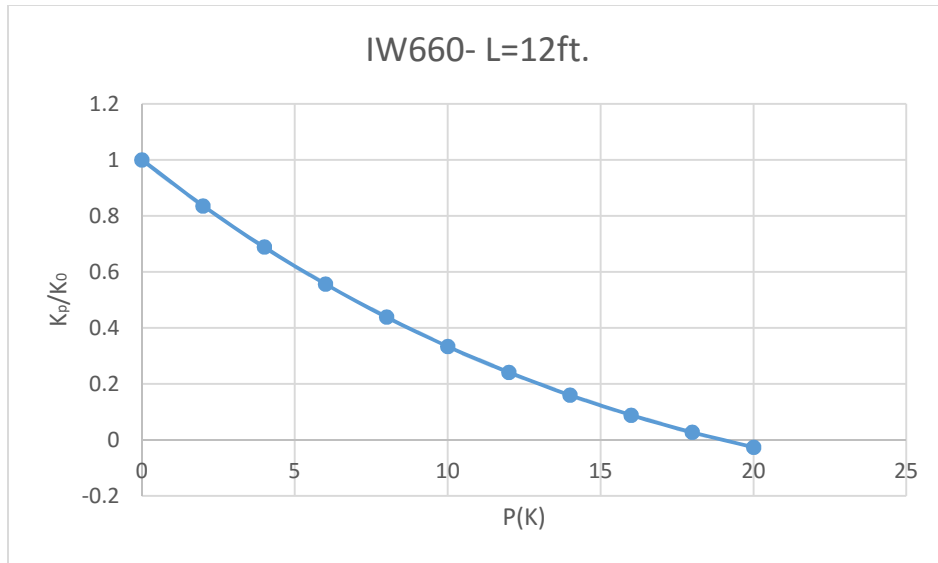


Fig. 5. Stiffness degrading for column minor axis response

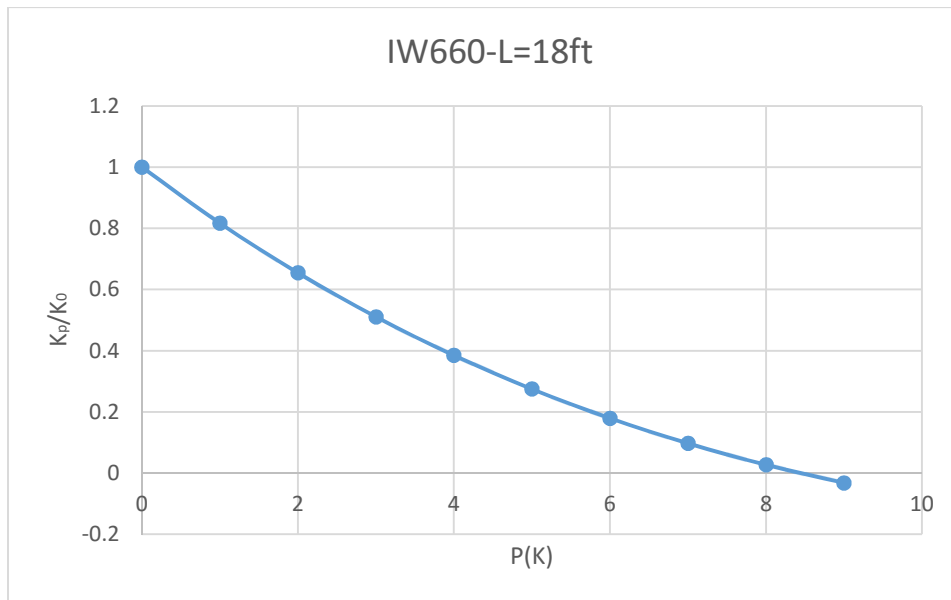


Fig. 6. Stiffness degrading for column minor axis response

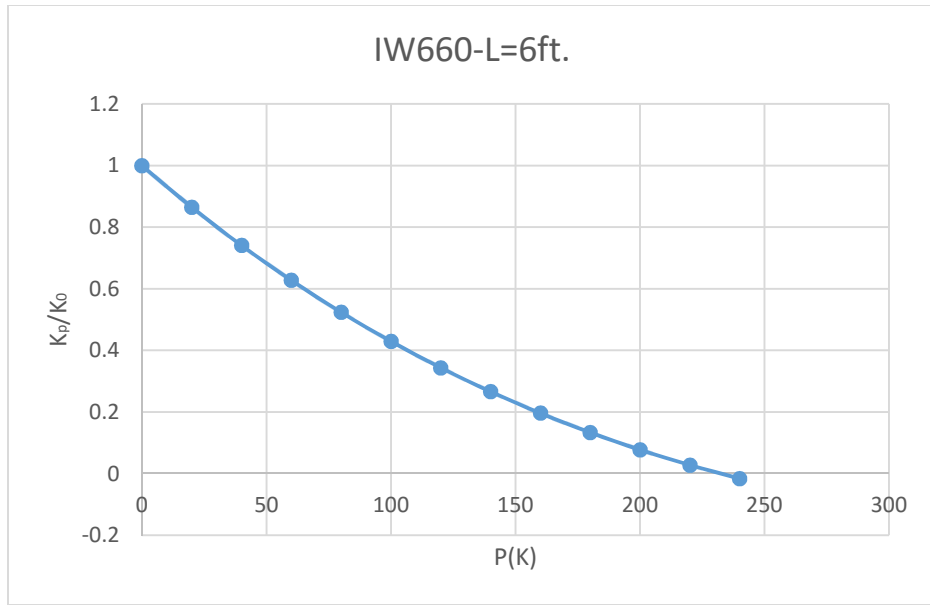


Fig. 7. Stiffness degrading for uniaxial beam-column major axis response

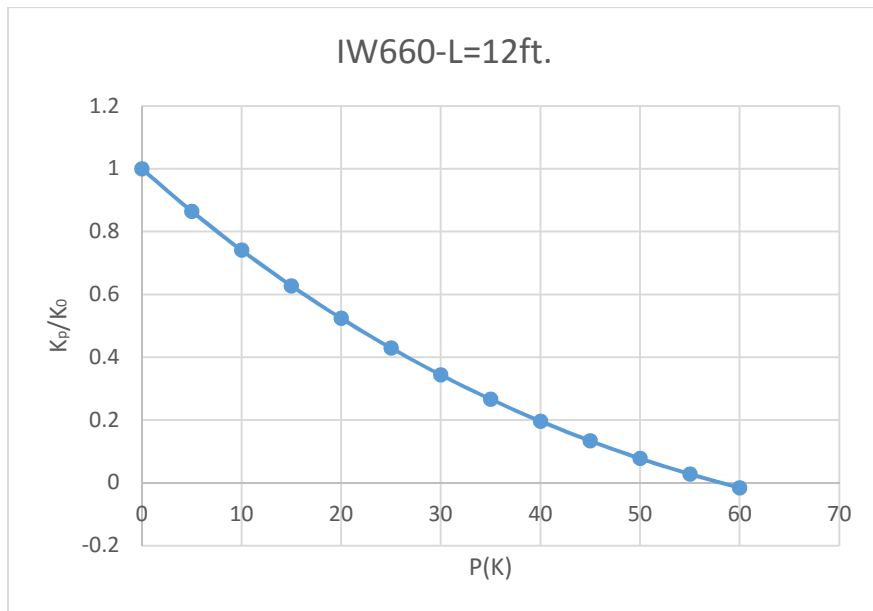


Fig. 8. Stiffness degrading for uniaxial beam-column major axis response

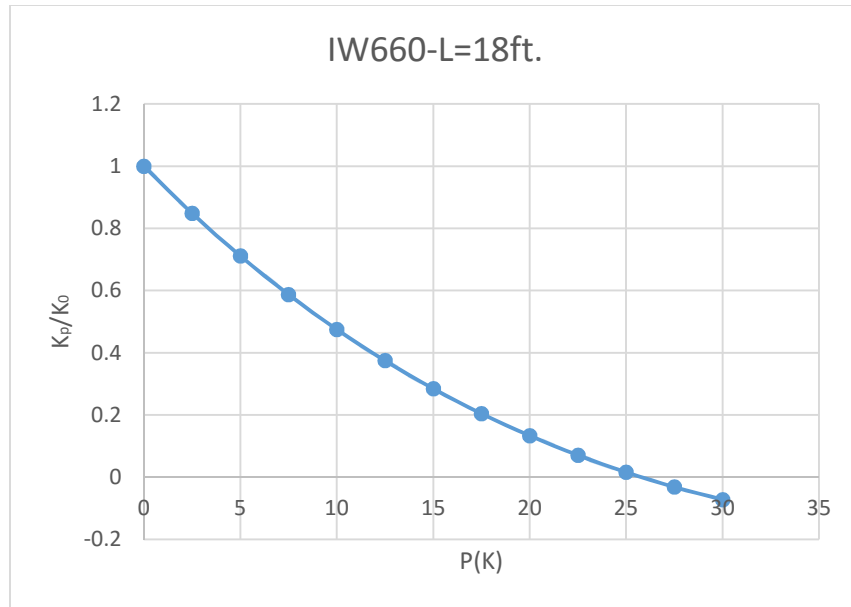


Fig. 9. Stiffness degrading for uniaxial beam-column major axis response

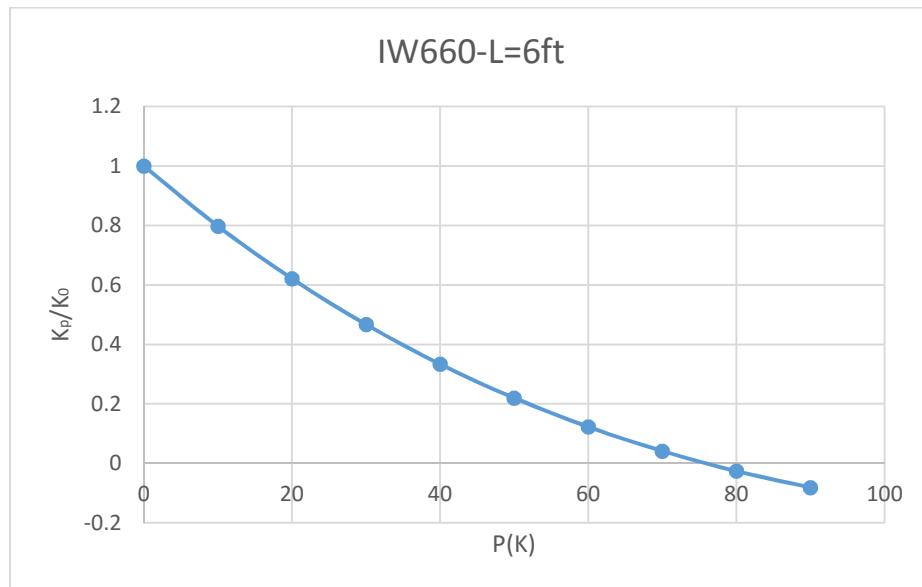


Fig. 10. Stiffness degrading for uniaxial beam-column minor axis response

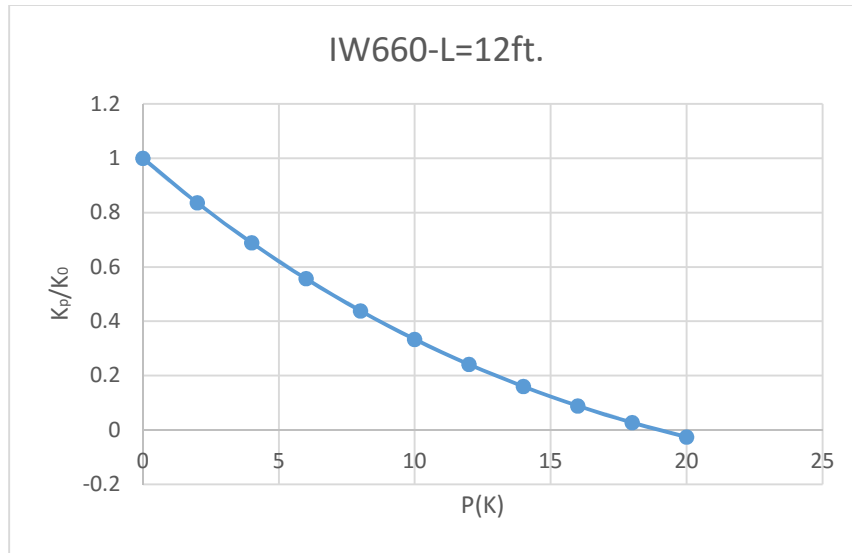


Fig11. Stiffness degrading for uniaxial beam-column minor axis response

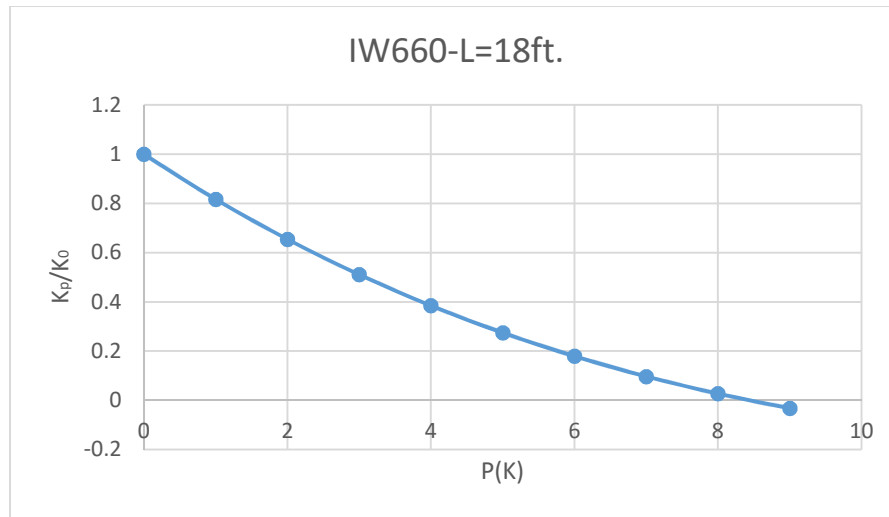


Fig. 12. Stiffness degrading for uniaxial beam-column minor axis response

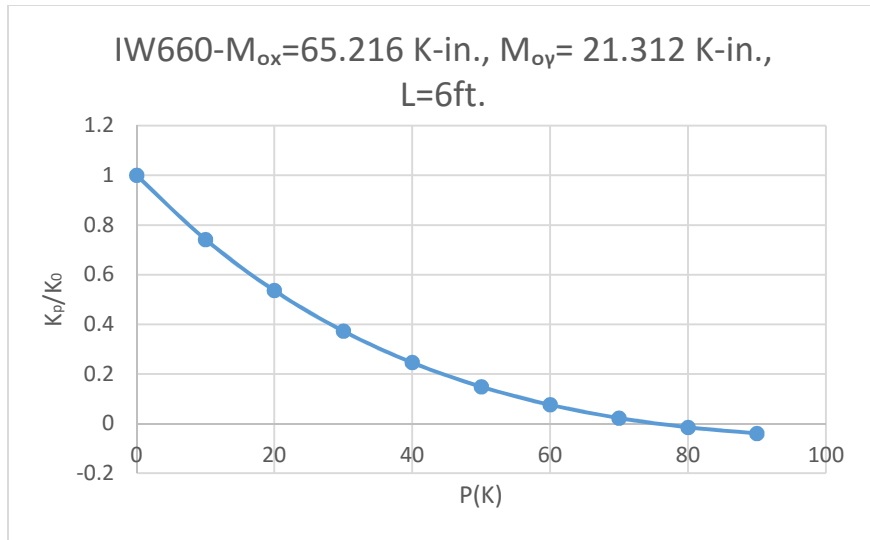


Fig. 13 Stiffness Degradation for biaxial beam-column response

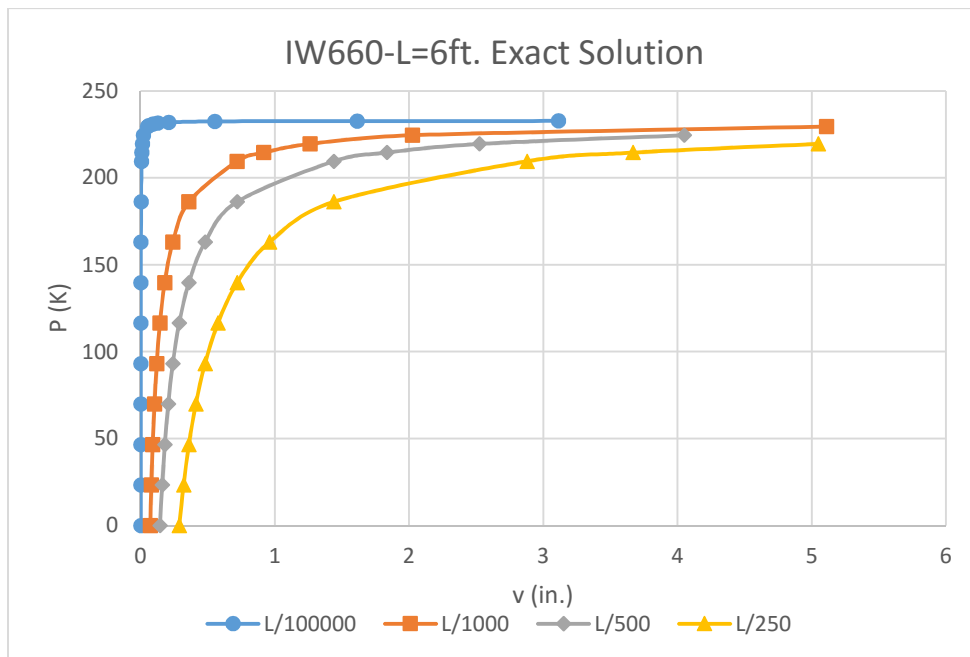


Fig. 14 Load vs. Deflection for column major axis response

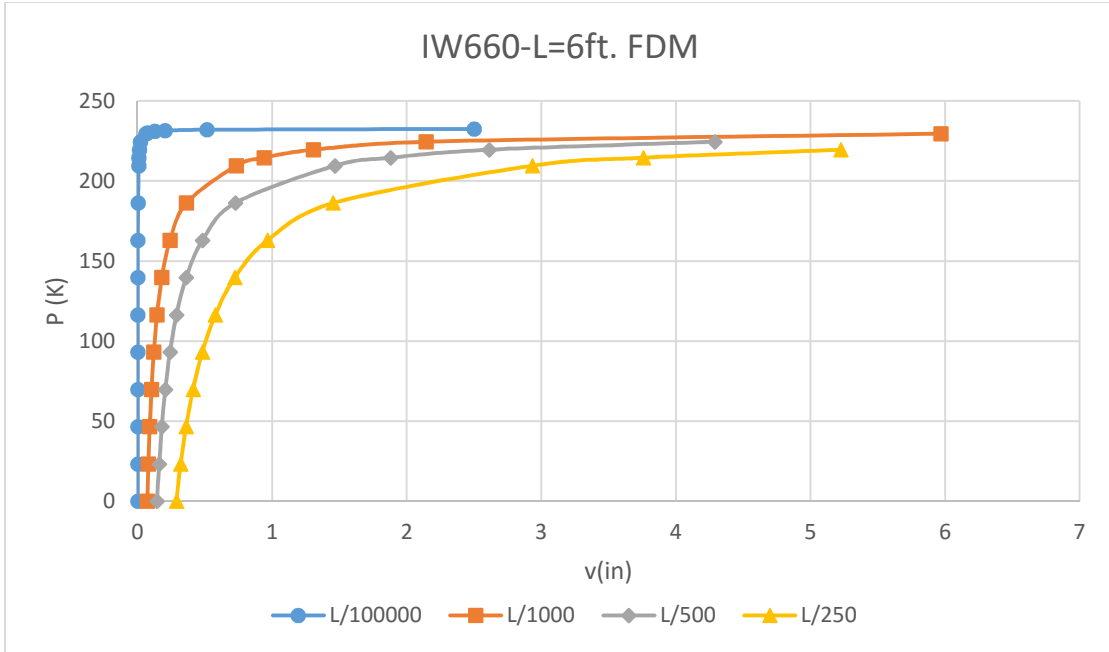


Fig.15 Load vs. Deflection for column major axis response

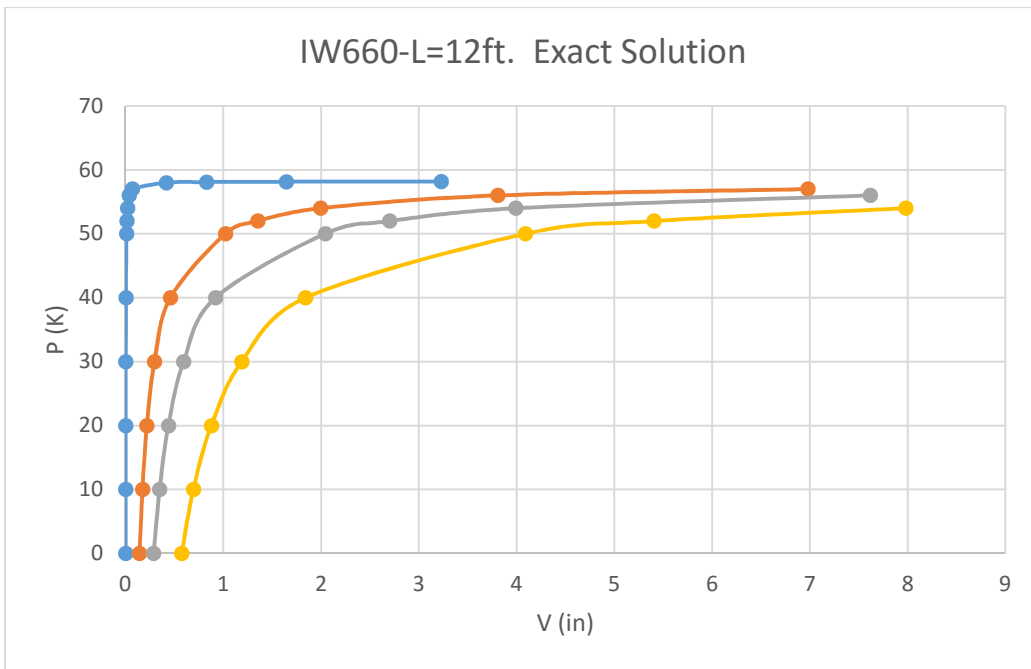


Fig. 16 Load vs. Deflection for column major axis response

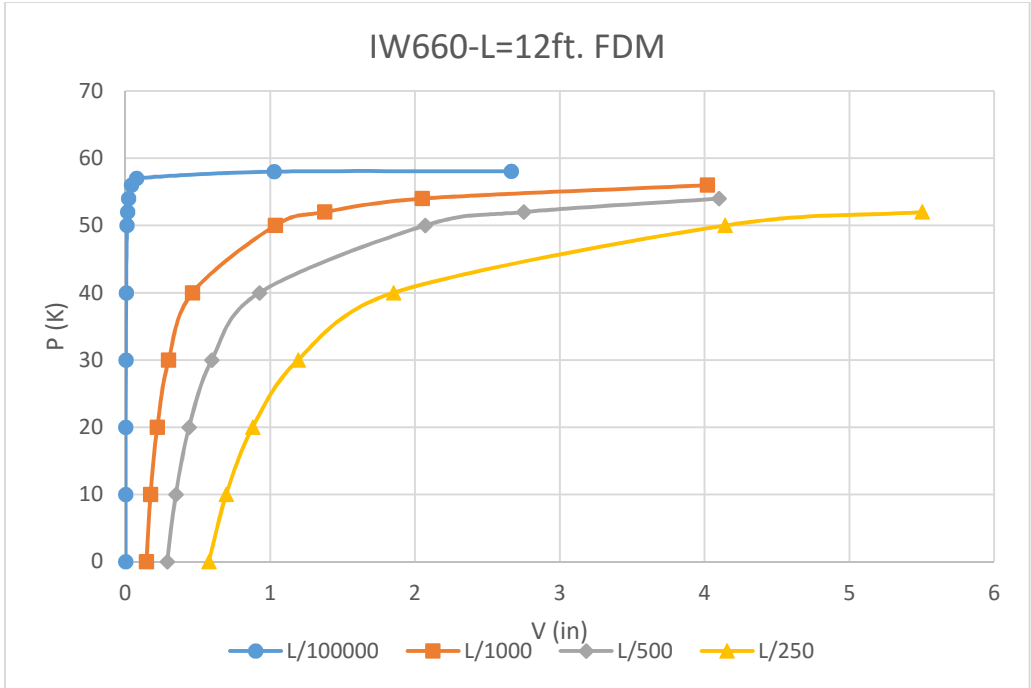


Fig. 17 Load vs. Deflection for column major axis response

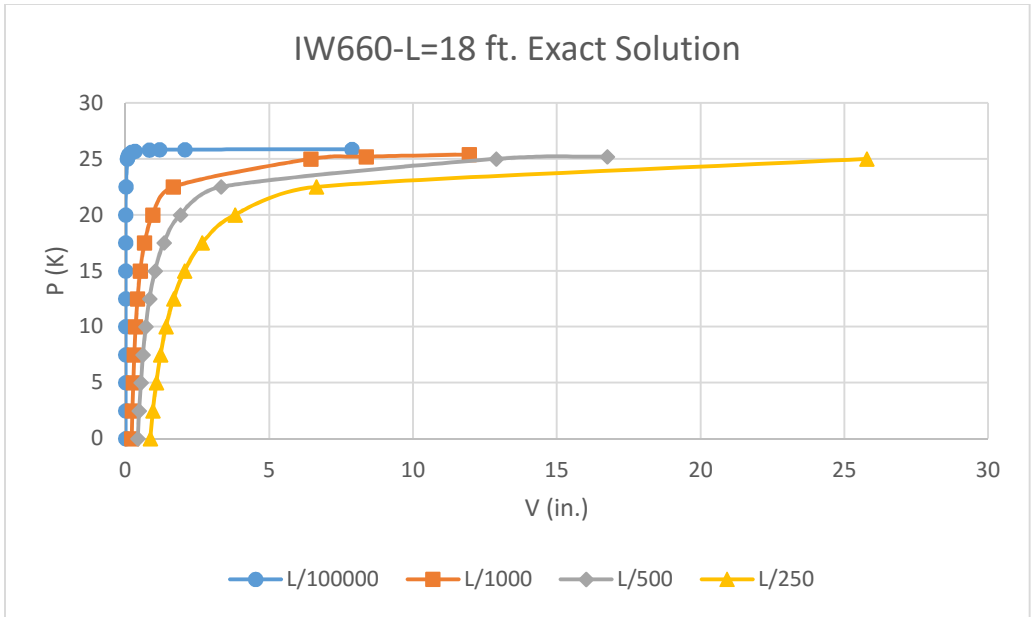


Fig. 18 Load vs. Deflection for column major axis response

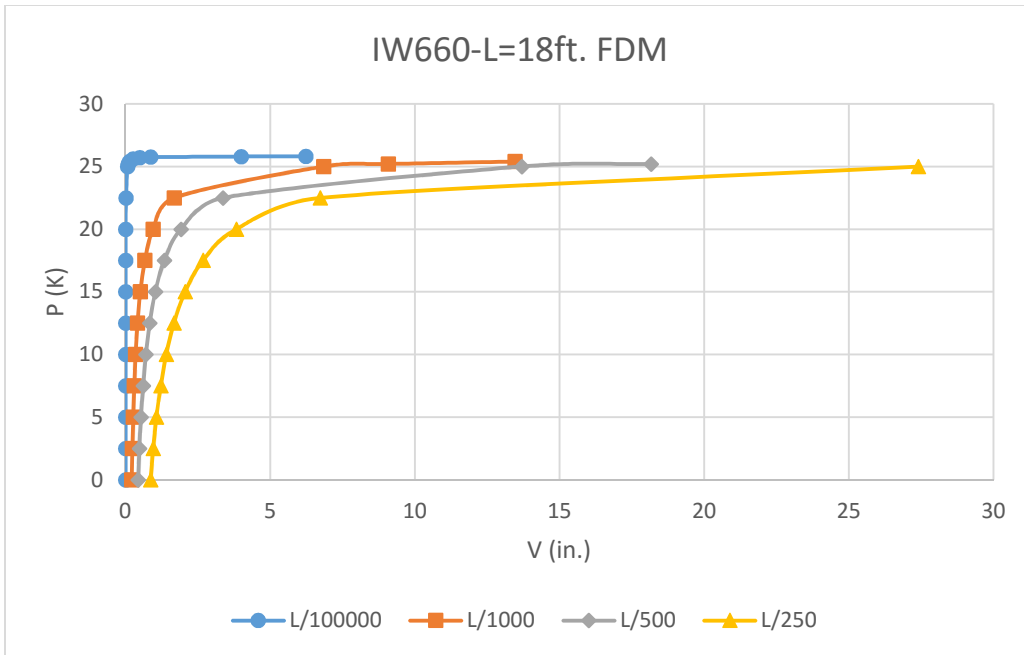


Fig. 19 Load vs. Deflection for column major axis response

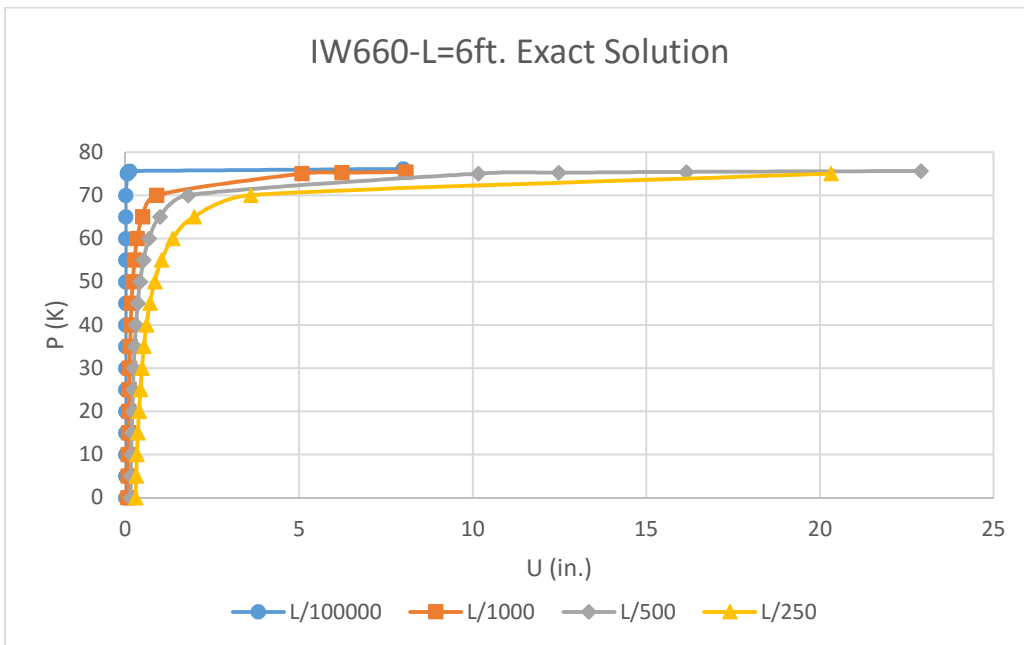


Fig. 20 Load vs. Deflection for column minor axis response

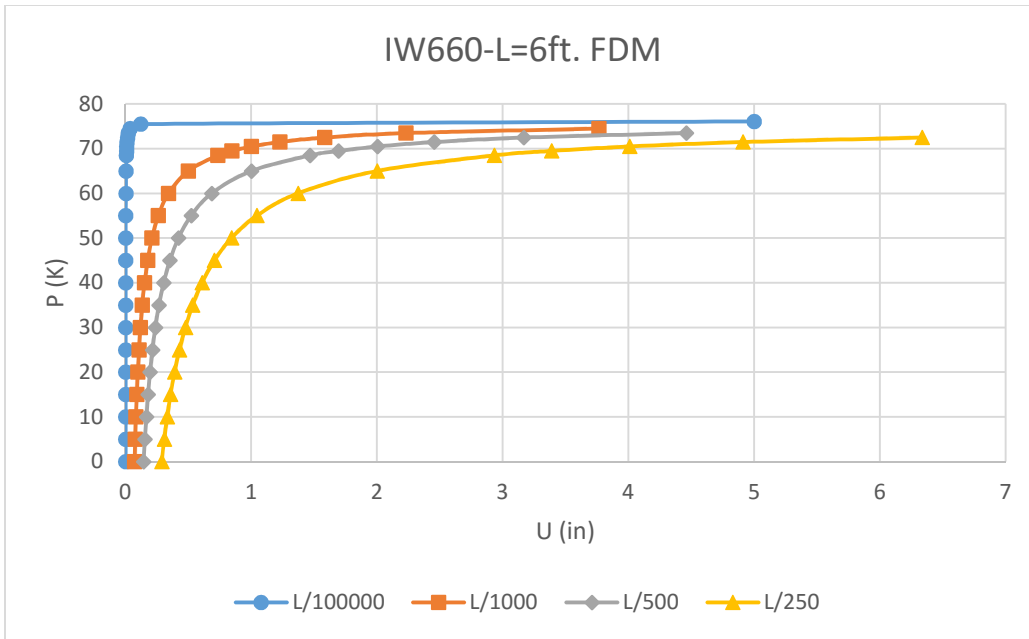


Fig. 21 Load vs. Deflection for column minor axis response

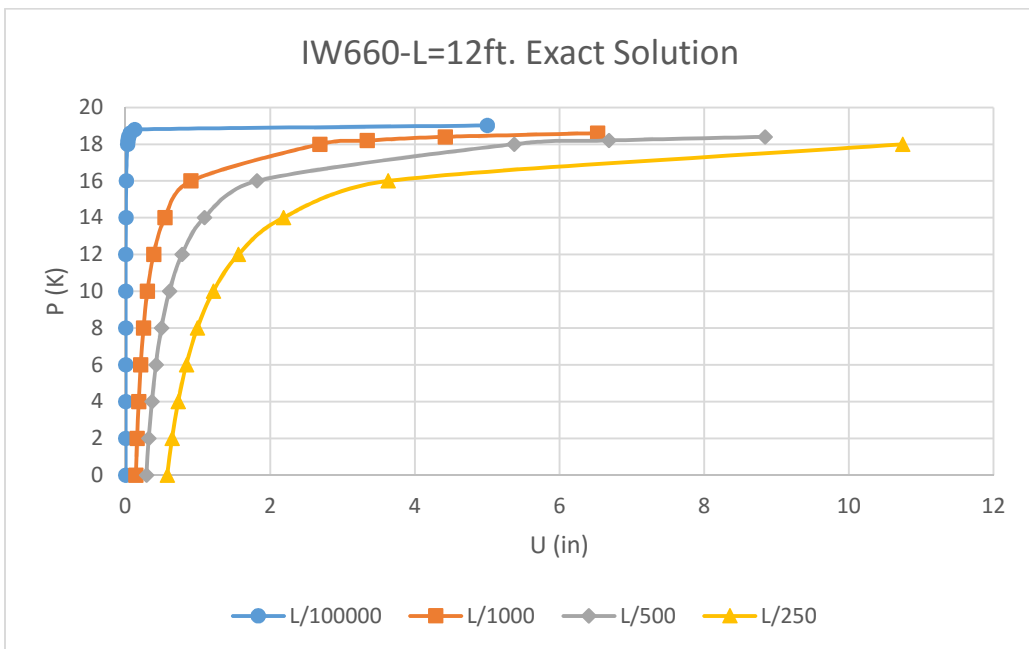


Fig. 22 Load vs. Deflection for column minor axis response

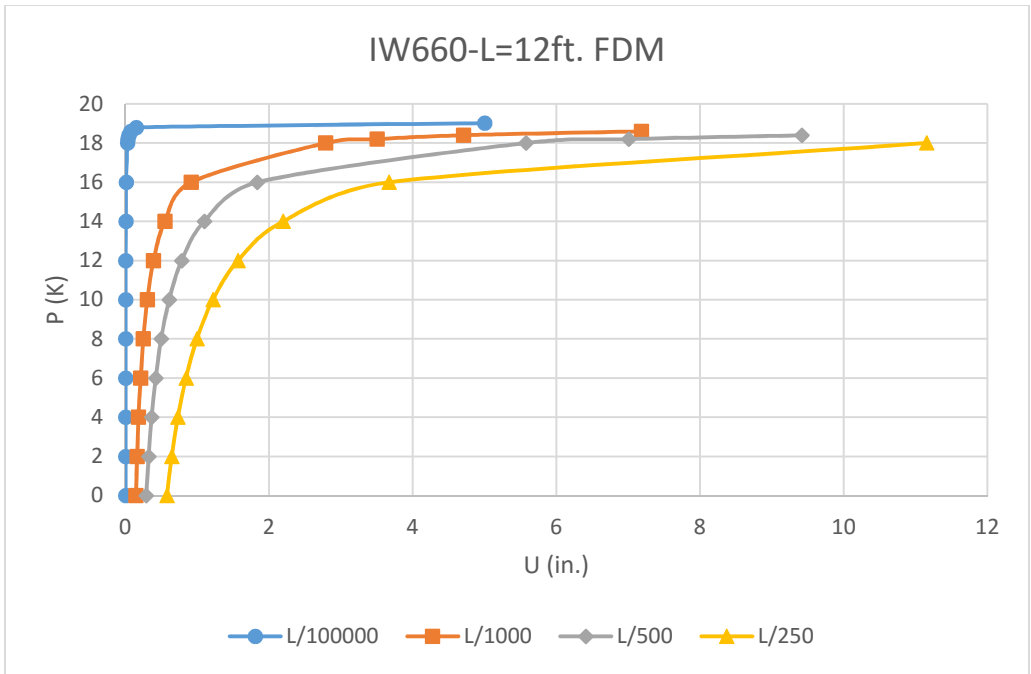


Fig. 23 Load vs. Deflection for column minor axis response

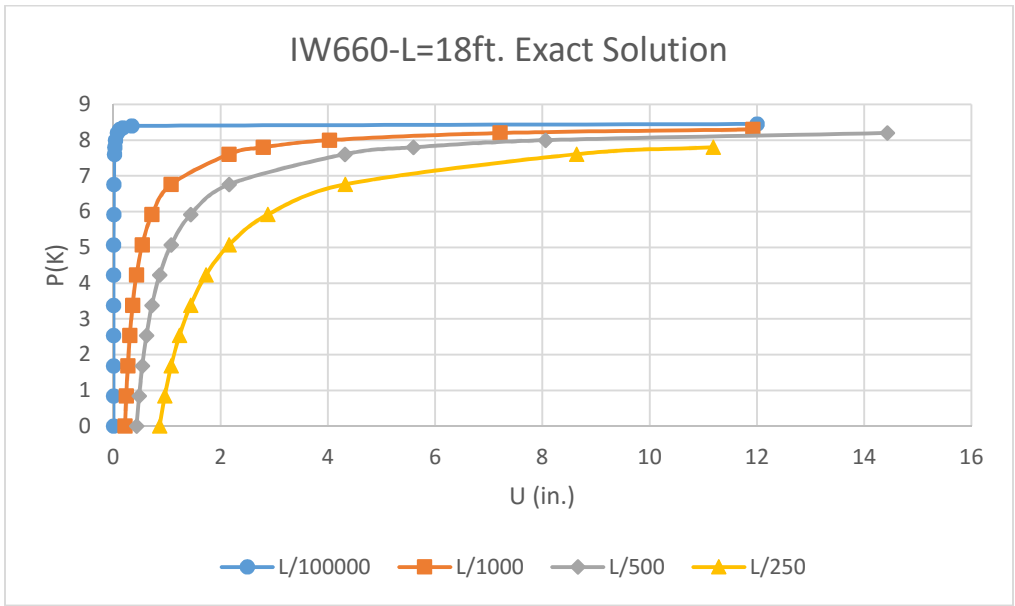


Fig. 24 Load vs. Deflection for column minor axis response

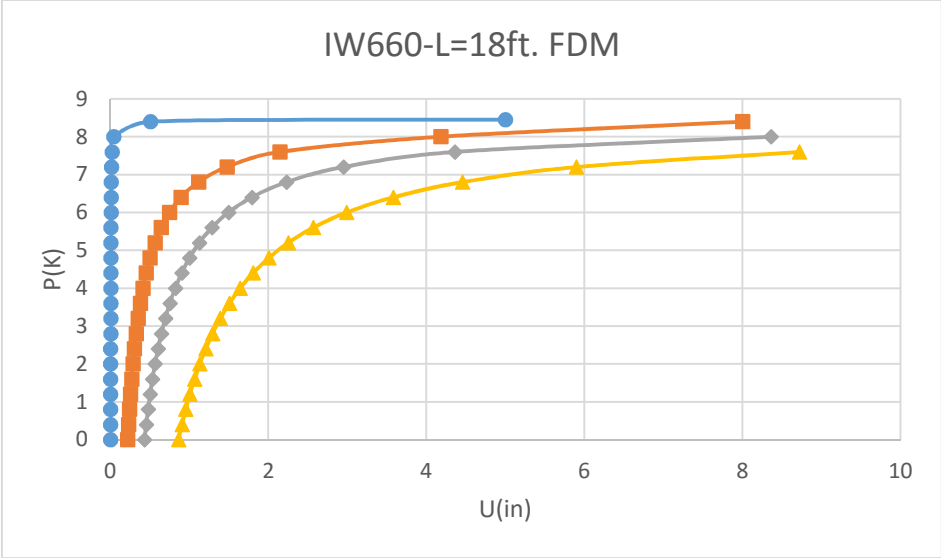


Fig. 25 Load vs. Deflection for column minor axis response

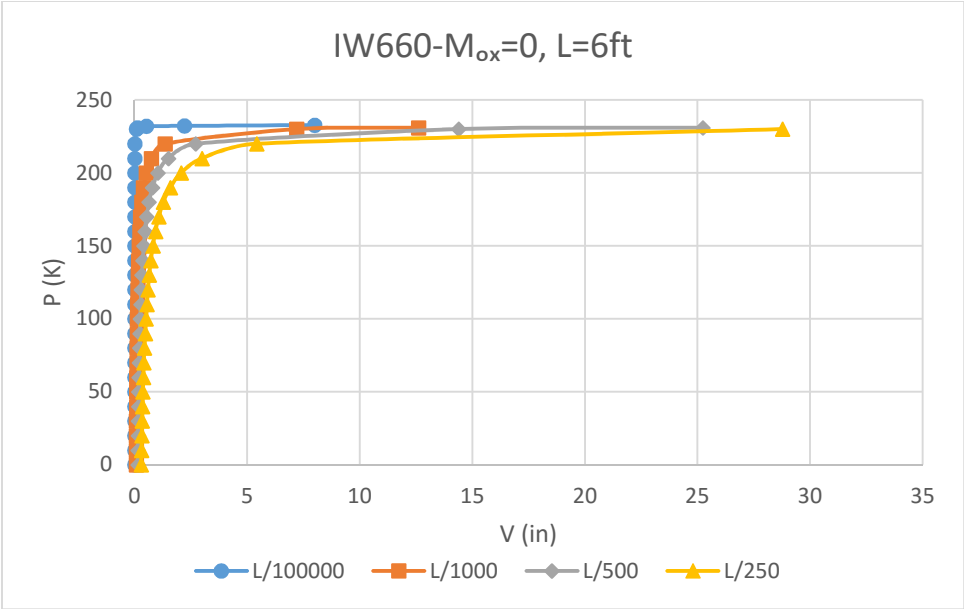


Fig. 26 Load vs. Deflection for uniaxial beam-column major axis response

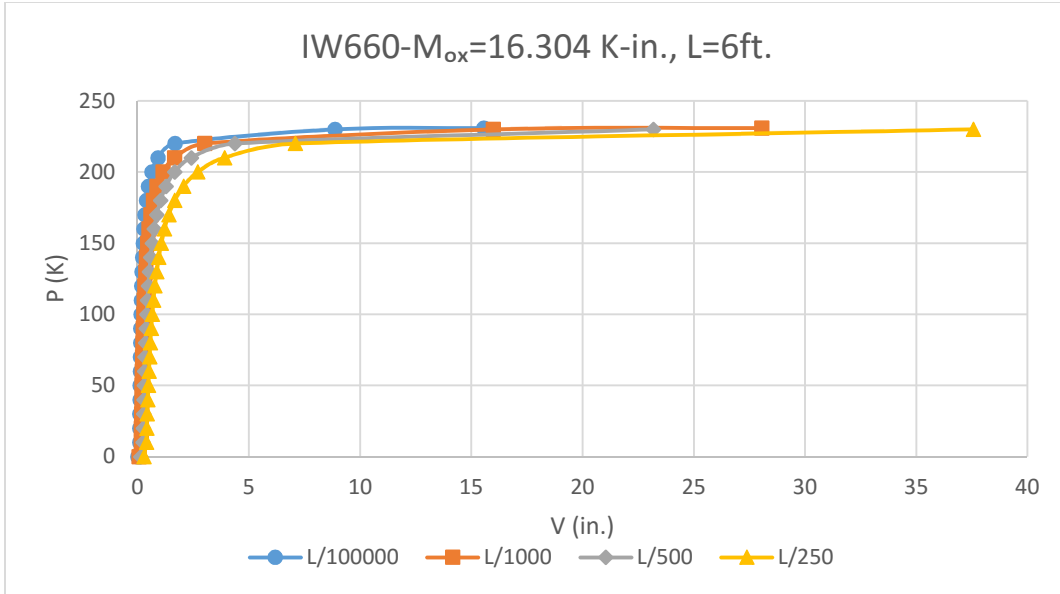


Fig. 27 Load vs. Deflection for uniaxial beam-column major axis response

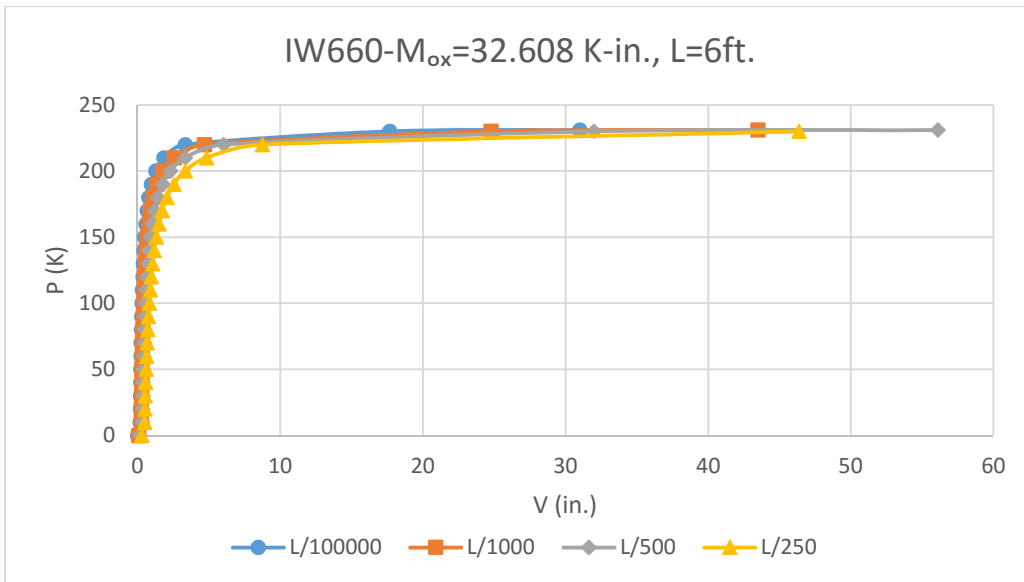


Fig. 28 Load vs. Deflection for uniaxial beam-column major axis response

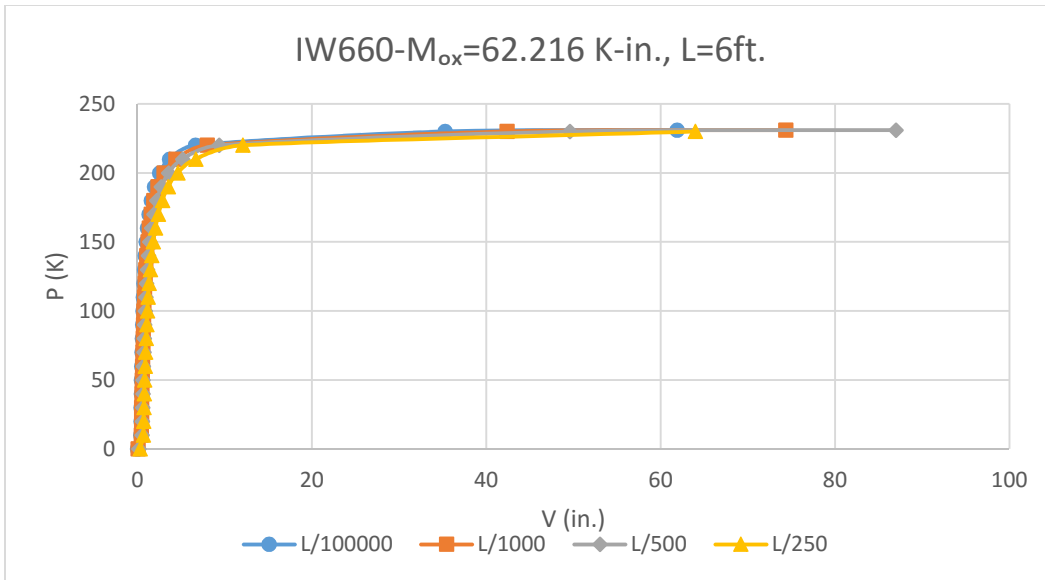


Fig. 29 Load vs. Deflection for uniaxial beam-column major axis response

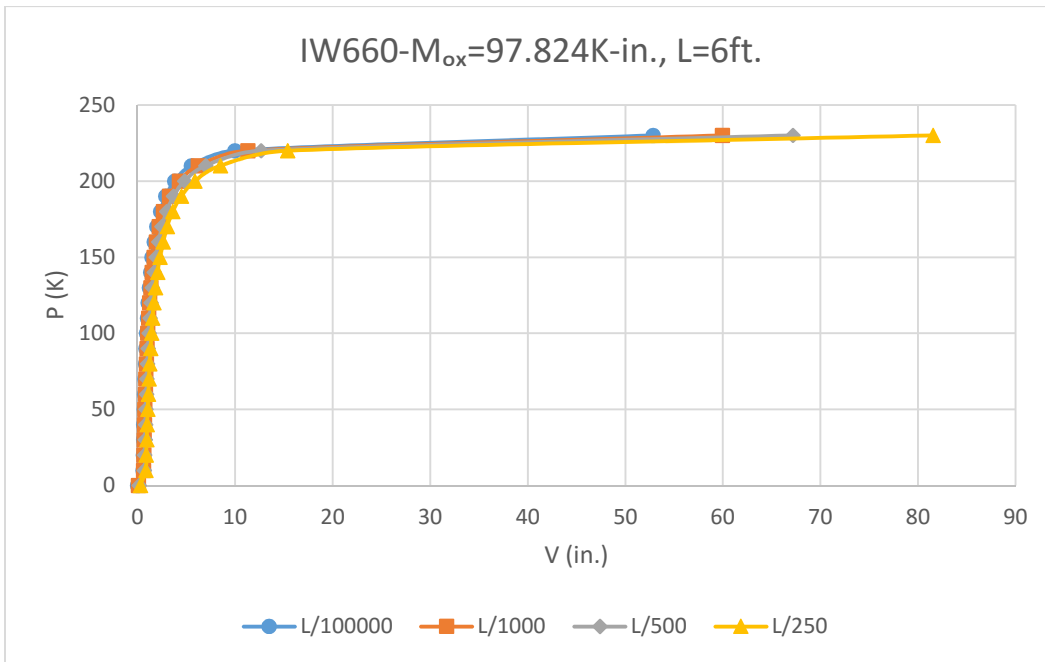


Fig. 30 Load vs. Deflection for uniaxial beam-column major axis response

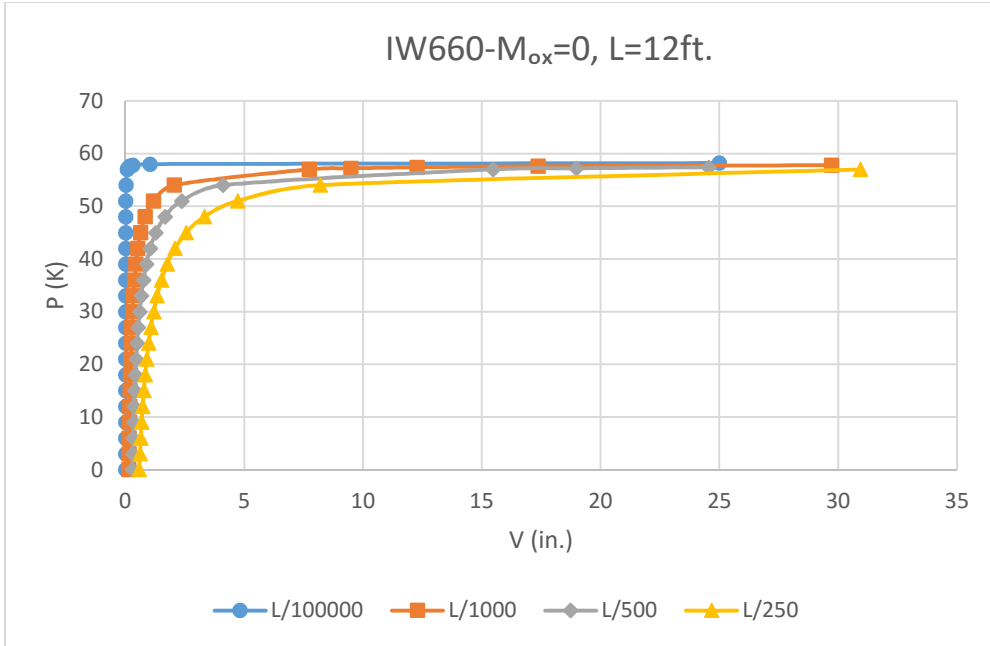


Fig. 31 Load vs. Deflection for uniaxial beam-column major axis response

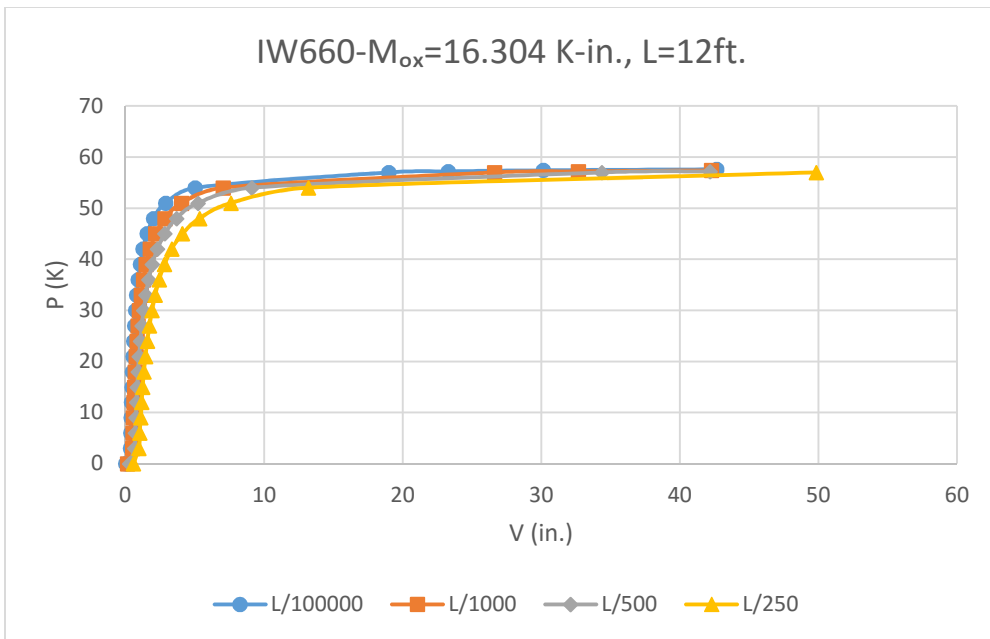


Fig. 32 Load vs. Deflection for uniaxial beam-column major axis response

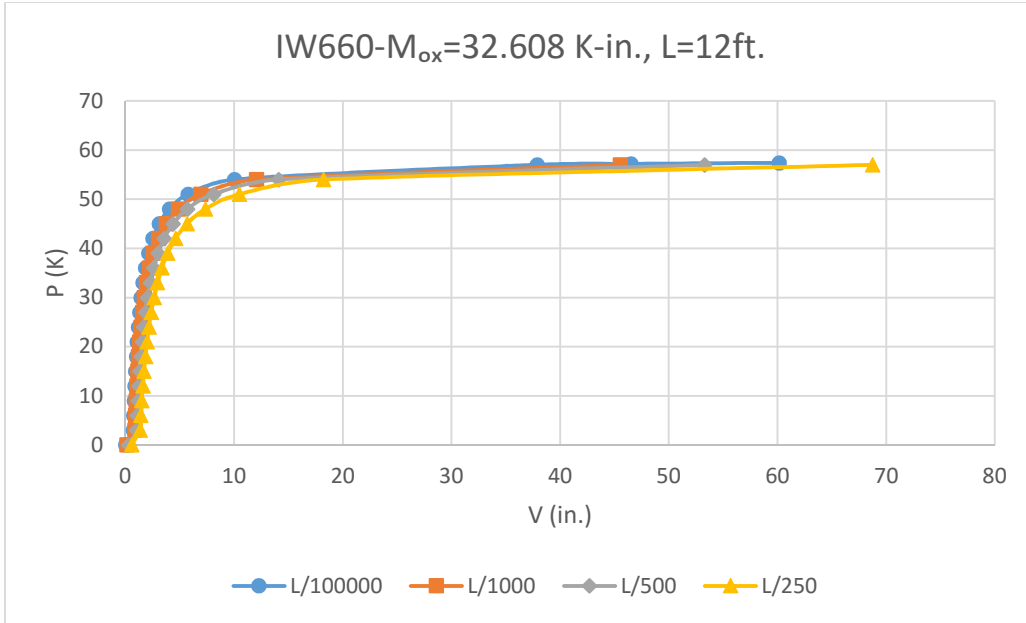


Fig.33 Load vs. Deflection for uniaxial beam-column major axis response.

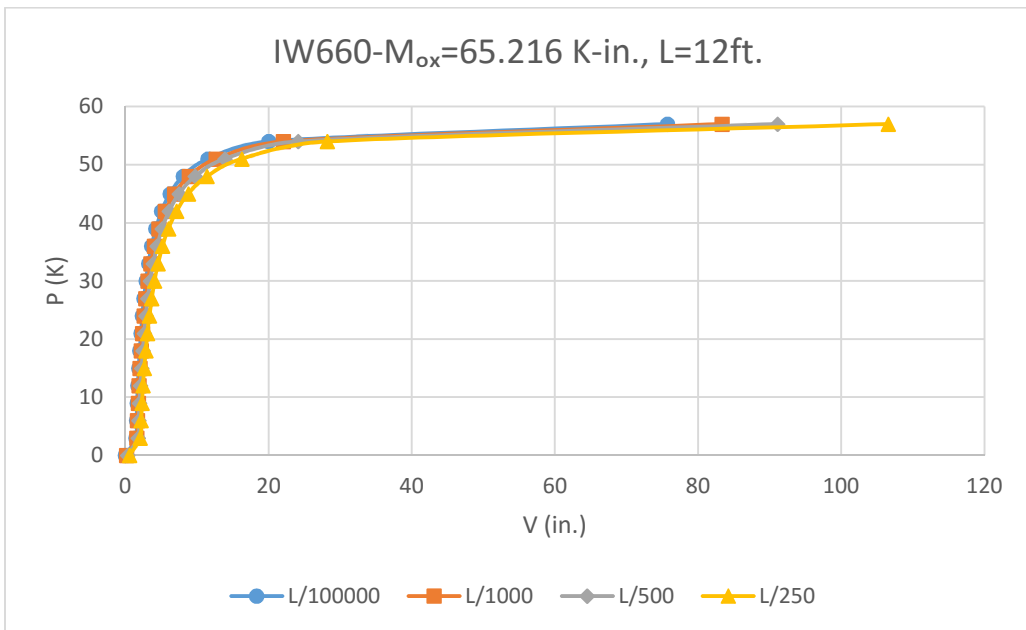


Fig.34 Load vs. Deflection for uniaxial beam-column major axis response

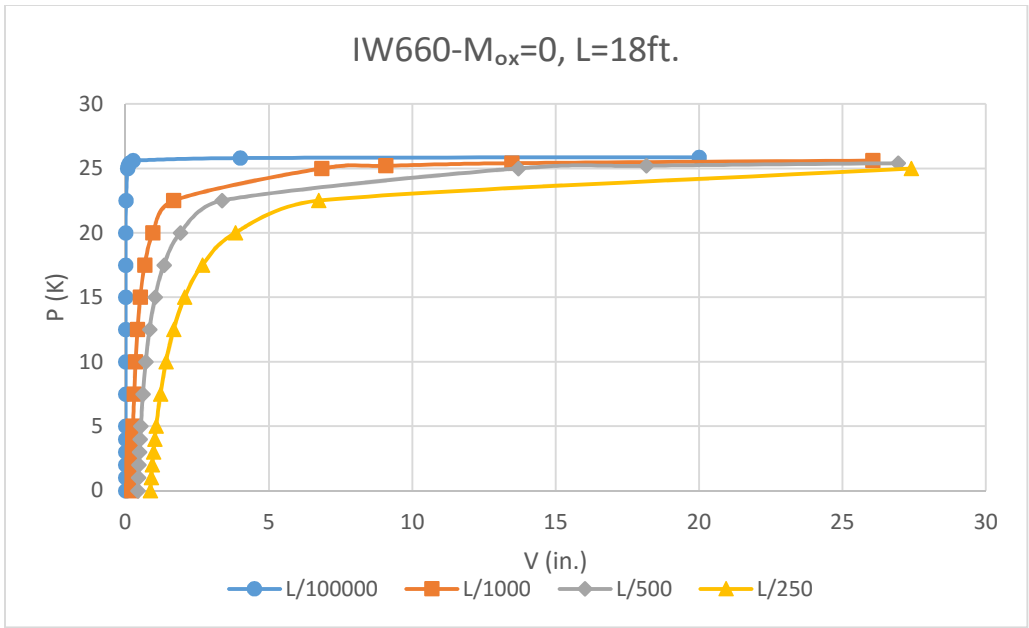


Fig.35 Load vs. Deflection for uniaxial beam-column major axis response

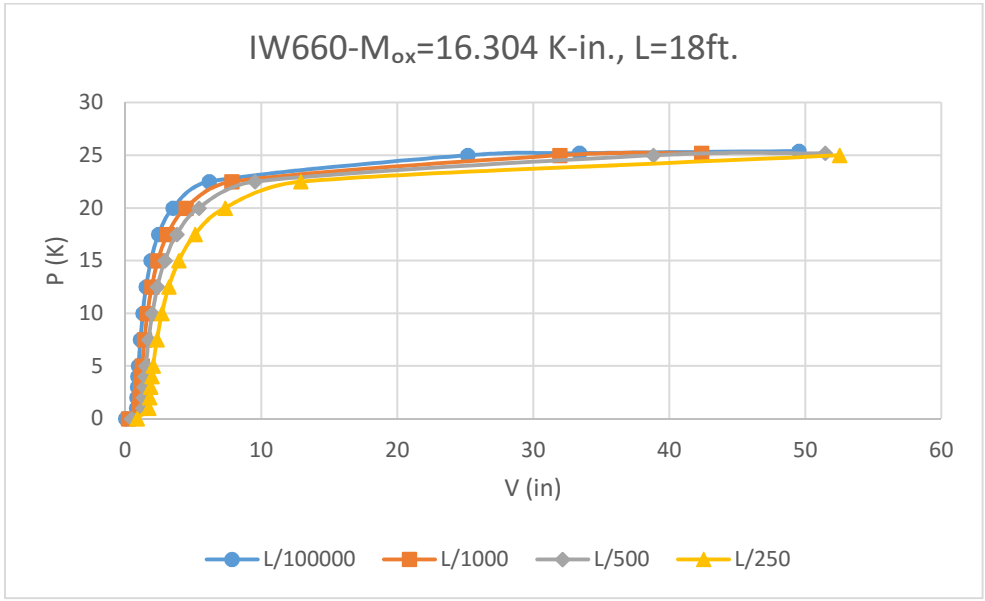


Fig.36 Load vs. Deflection for uniaxial beam-column major axis response

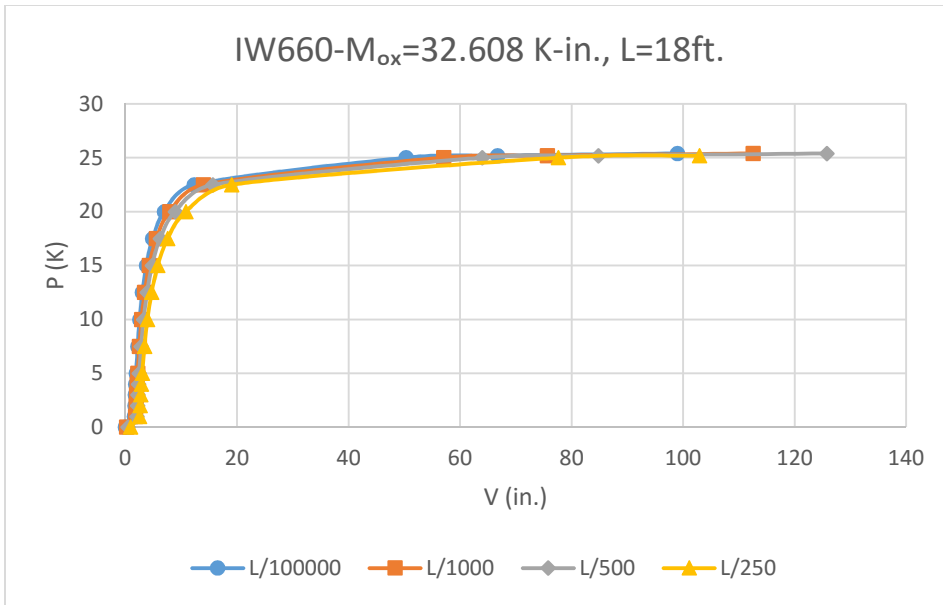


Fig.37 Load vs. Deflection for uniaxial beam-column major axis response

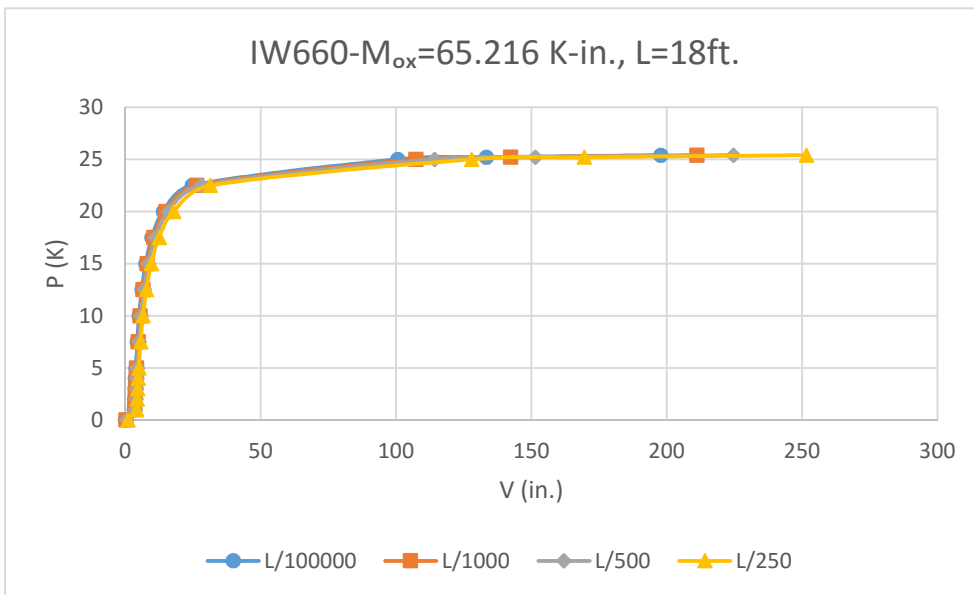


Fig.38 Load vs. Deflection for uniaxial beam-column major axis response

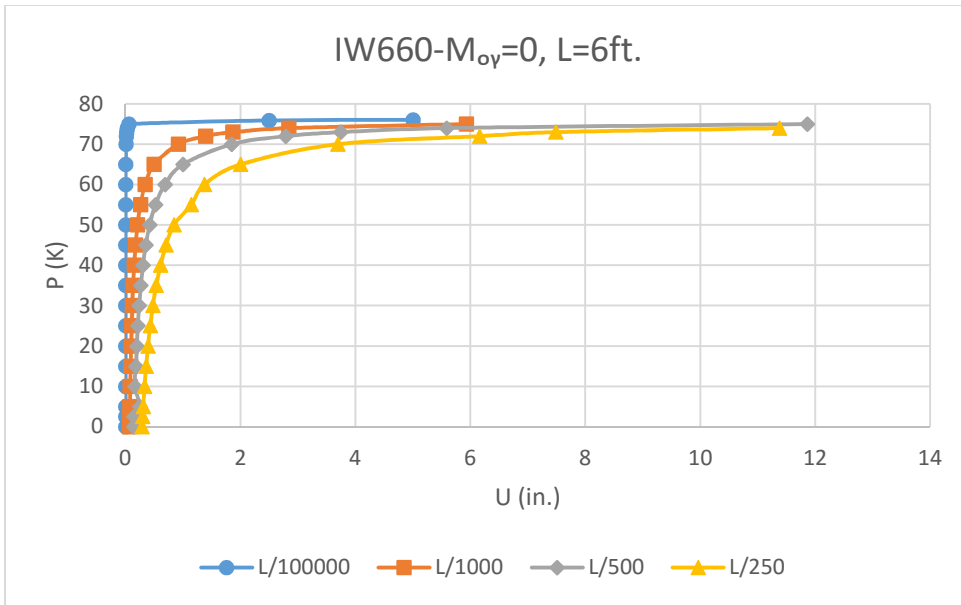


Fig.39 Load vs. Deflection for uniaxial beam-column minor axis response

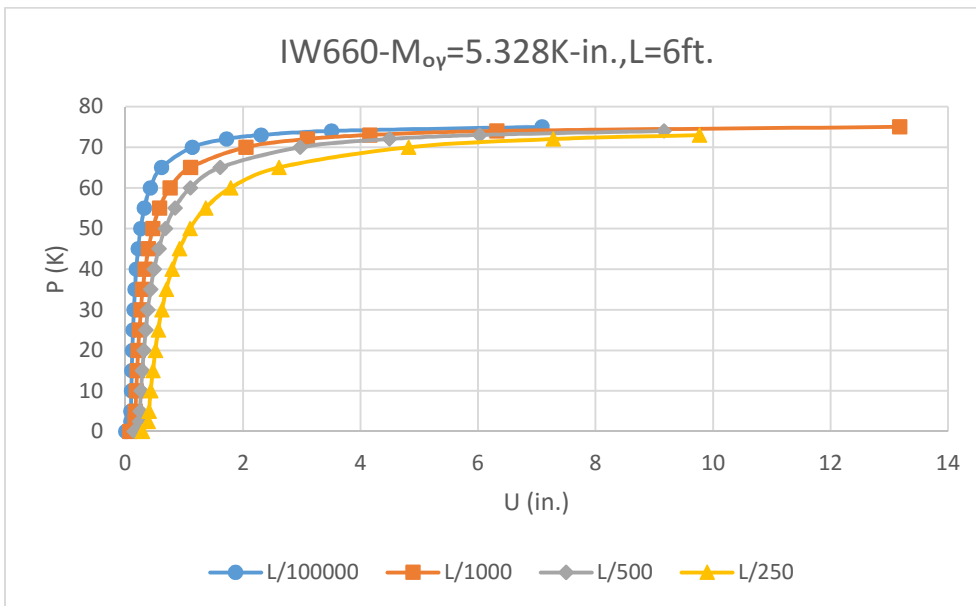


Fig.40 Load vs. Deflection for uniaxial beam-column minor axis response

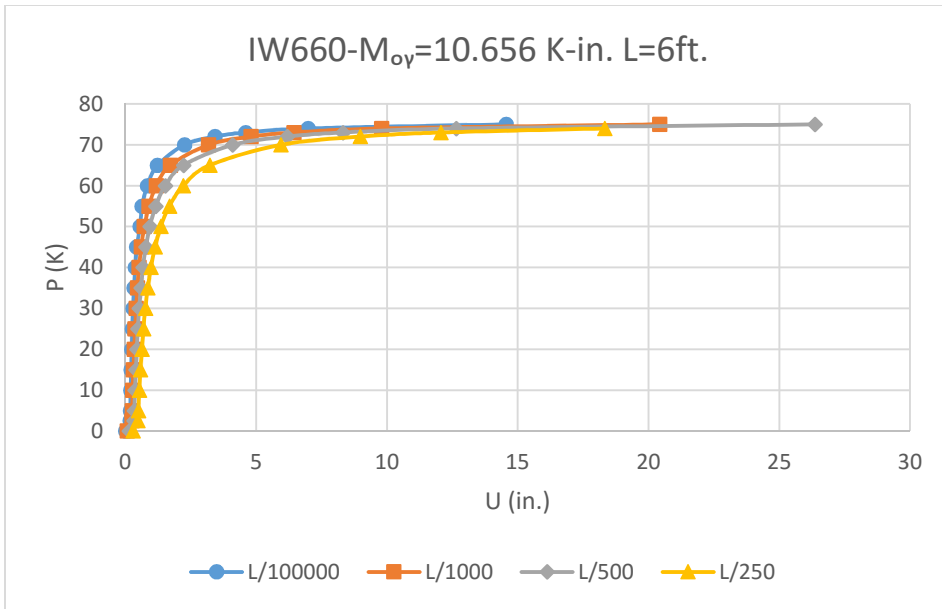


Fig.41 Load vs. Deflection for uniaxial beam-column minor axis response

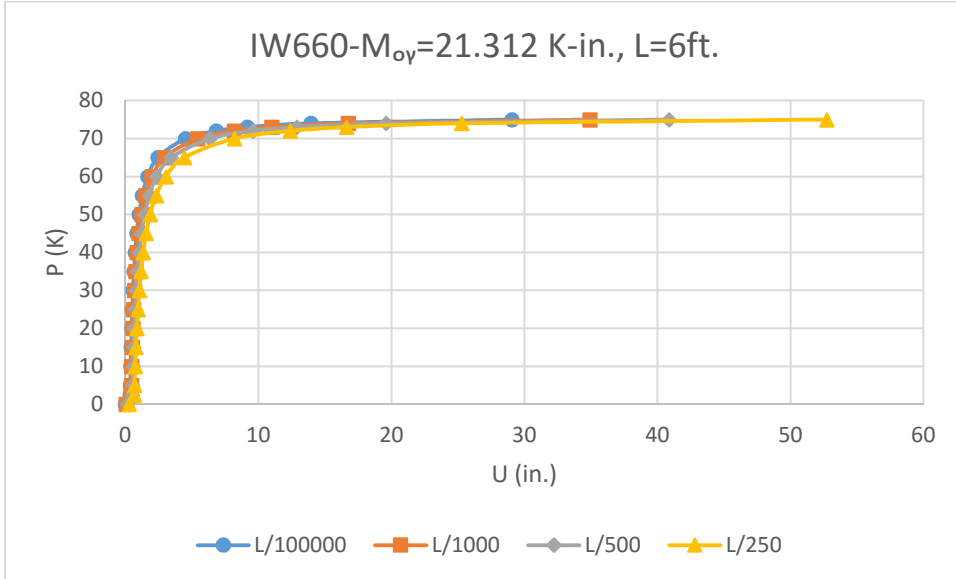


Fig.42 Load vs. Deflection for uniaxial beam-column minor axis response

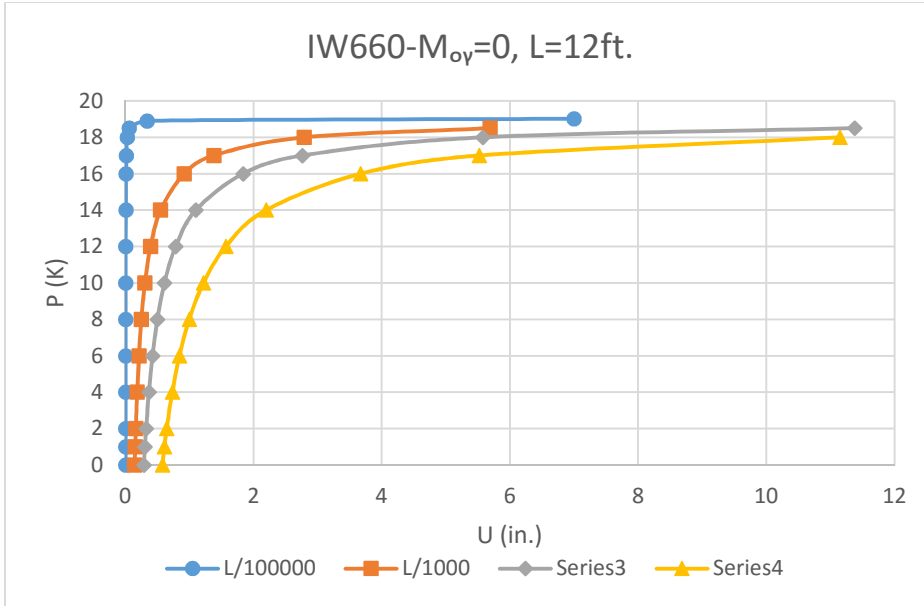


Fig.43 Load vs. Deflection for uniaxial beam-column minor axis response

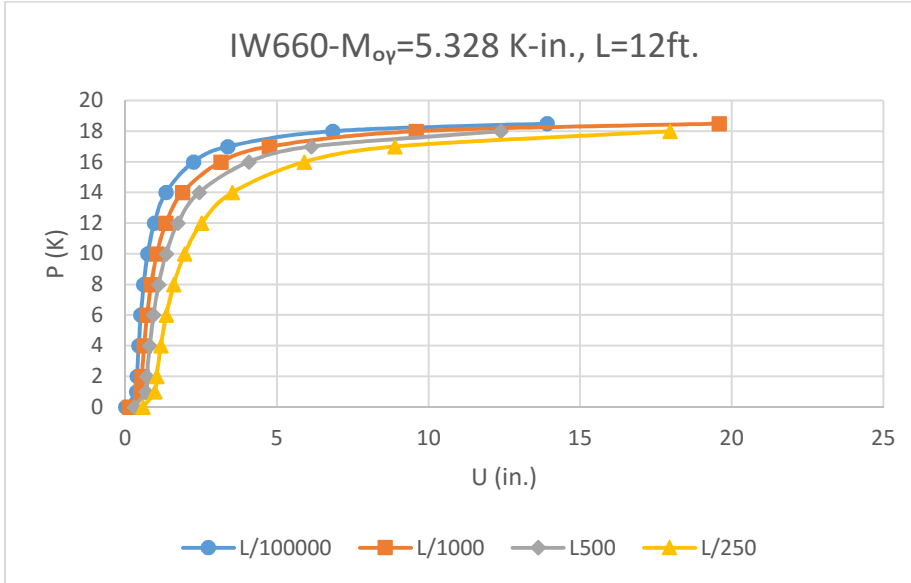


Fig.44 Load vs. Deflection for uniaxial beam-column minor axis response

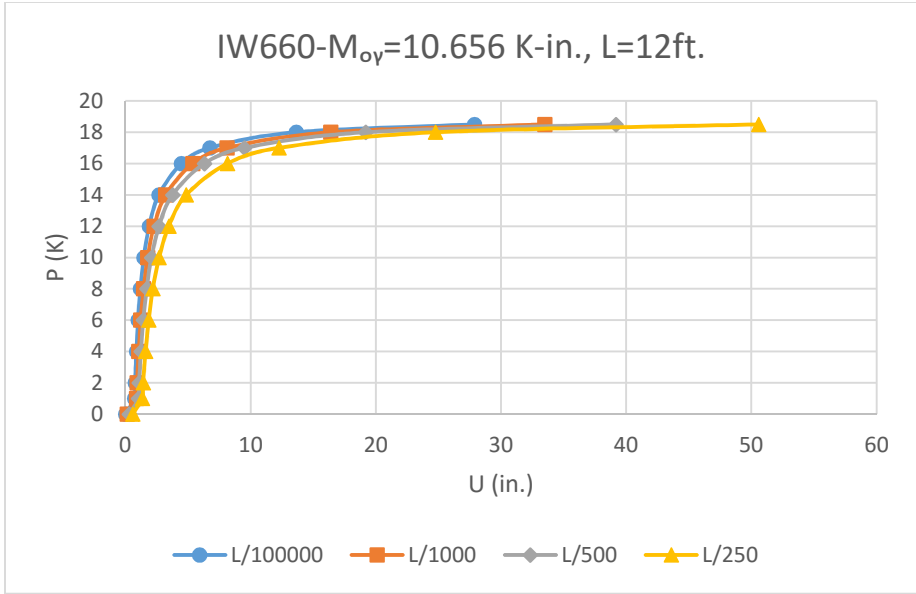


Fig.45 Load vs. Deflection for uniaxial beam-column minor axis response

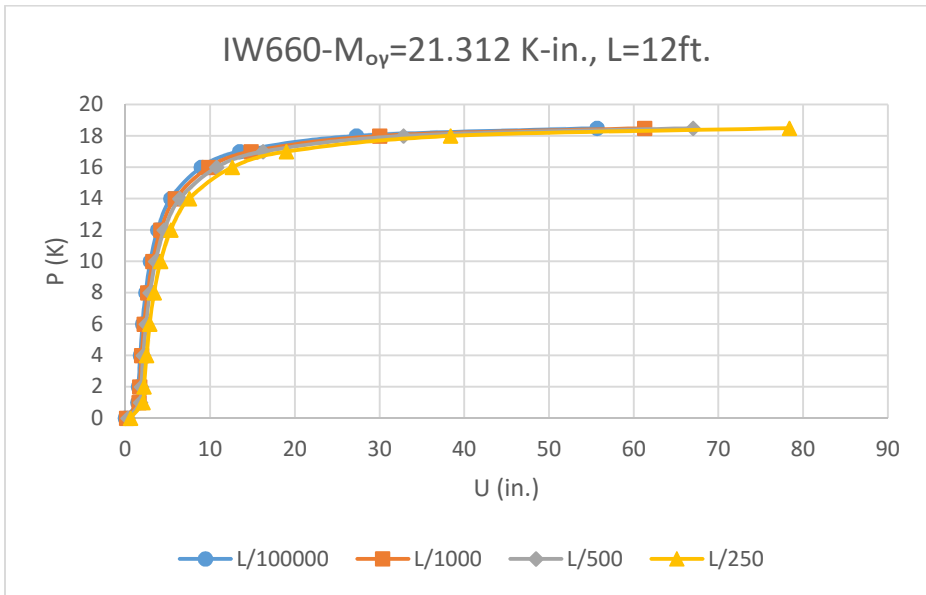


Fig.46 Load vs. Deflection for uniaxial beam-column minor axis response

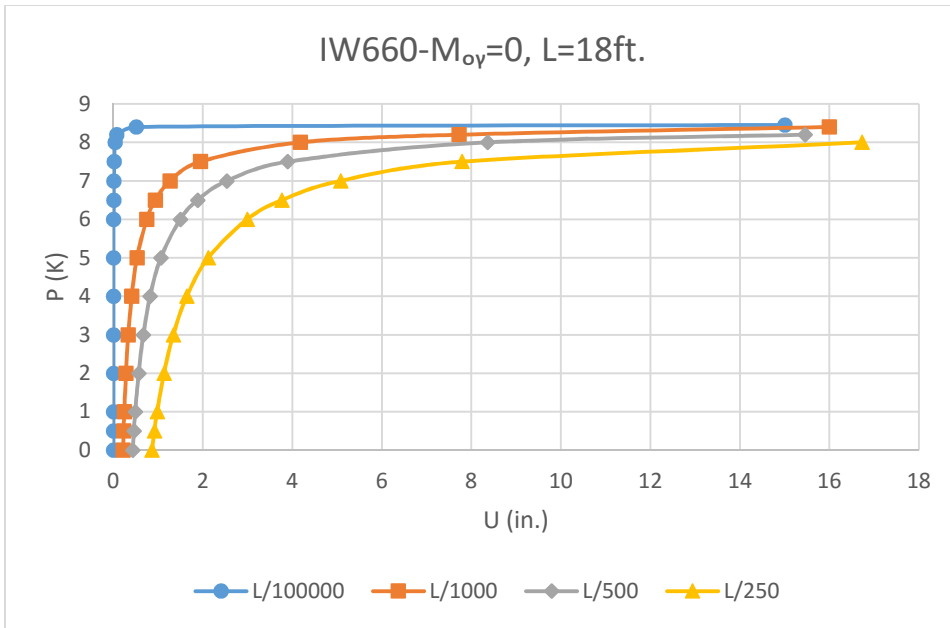


Fig.47 Load vs. Deflection for uniaxial beam-column minor axis response

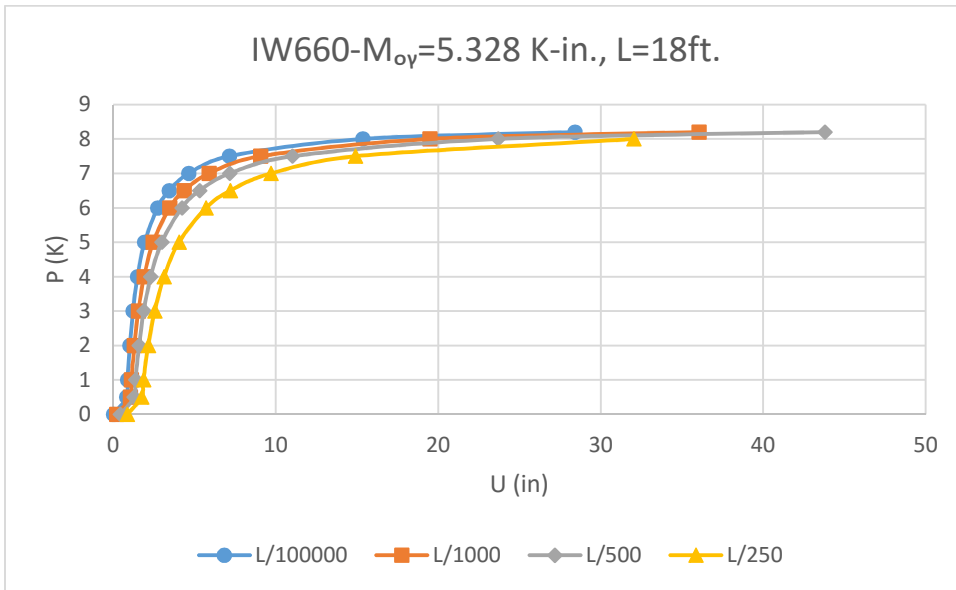


Fig.48 Load vs. Deflection for uniaxial beam-column minor axis response

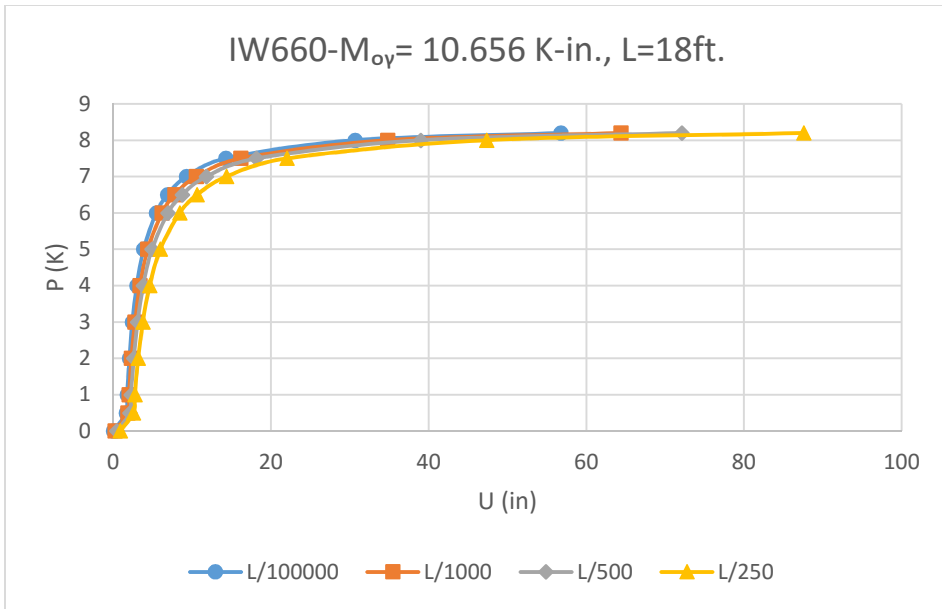


Fig.49 Load vs. Deflection for uniaxial beam-column minor axis response

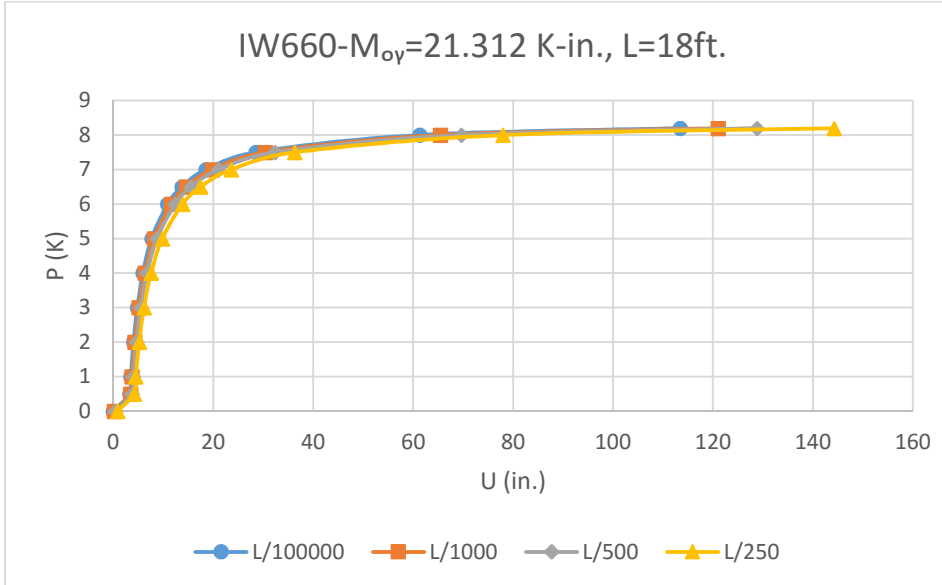


Fig.50 Load vs. Deflection for uniaxial beam-column minor axis response

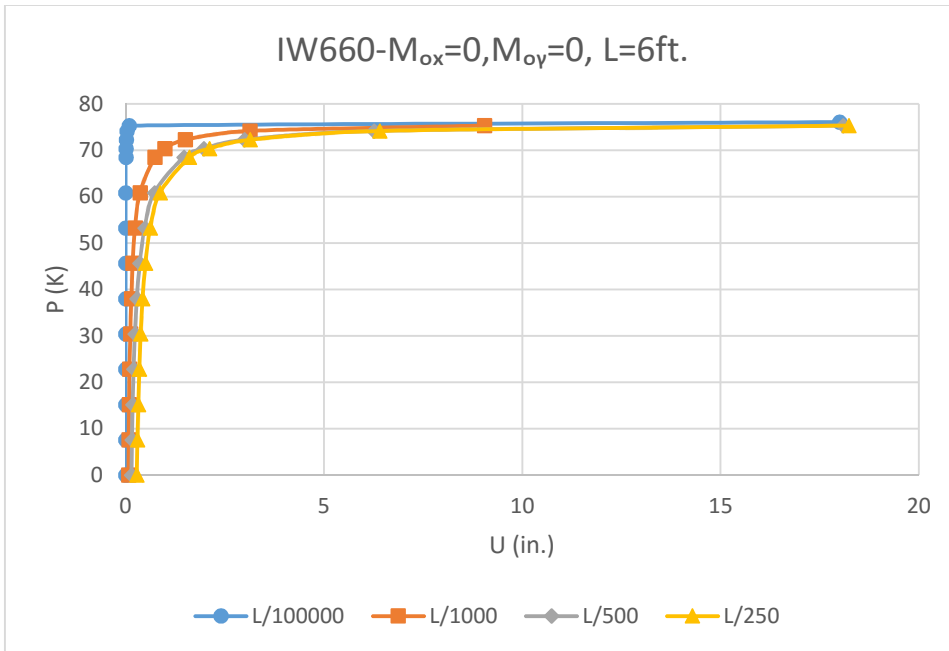


Fig.51 Load vs. Deflection for biaxial beam-column response

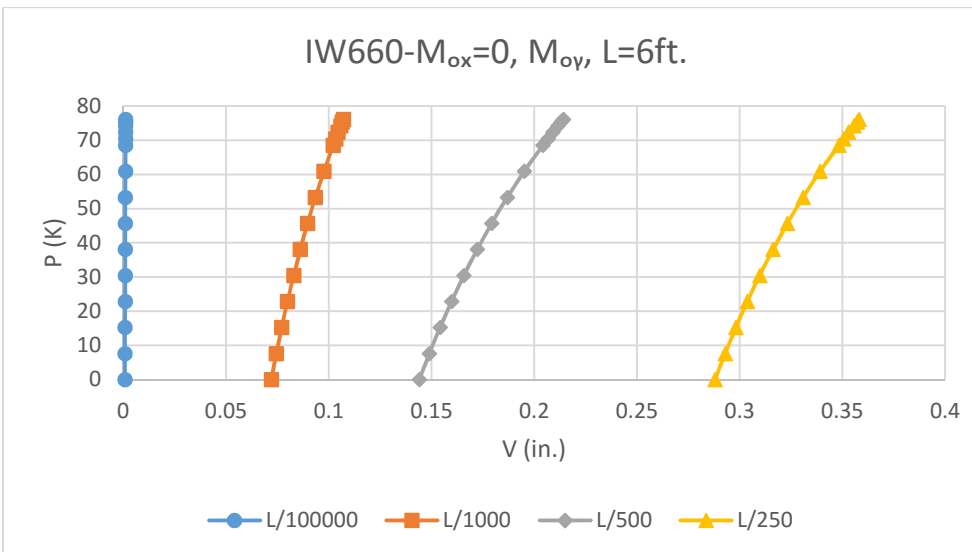


Fig.52 Load vs. Deflection for biaxial beam-column response

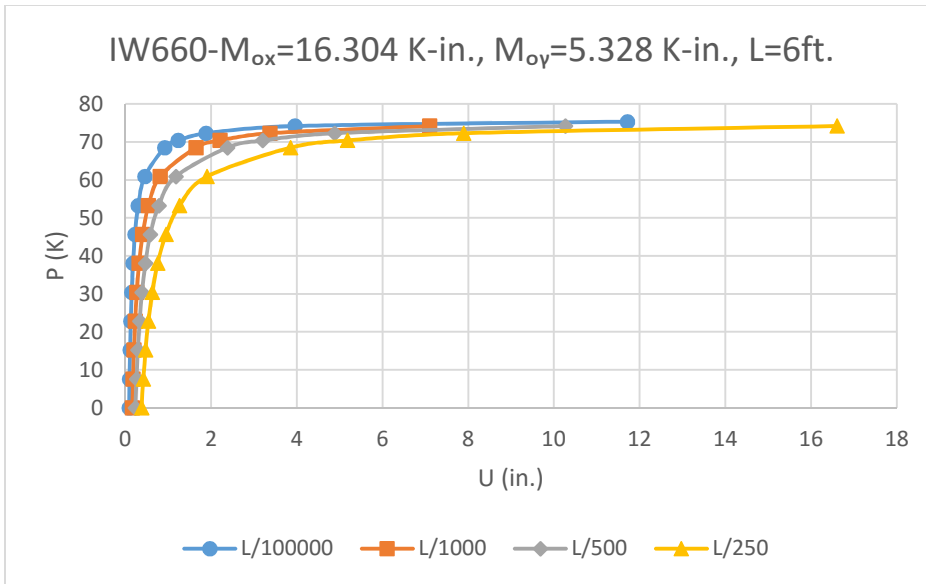


Fig.53 Load vs. Deflection for biaxial beam-column response

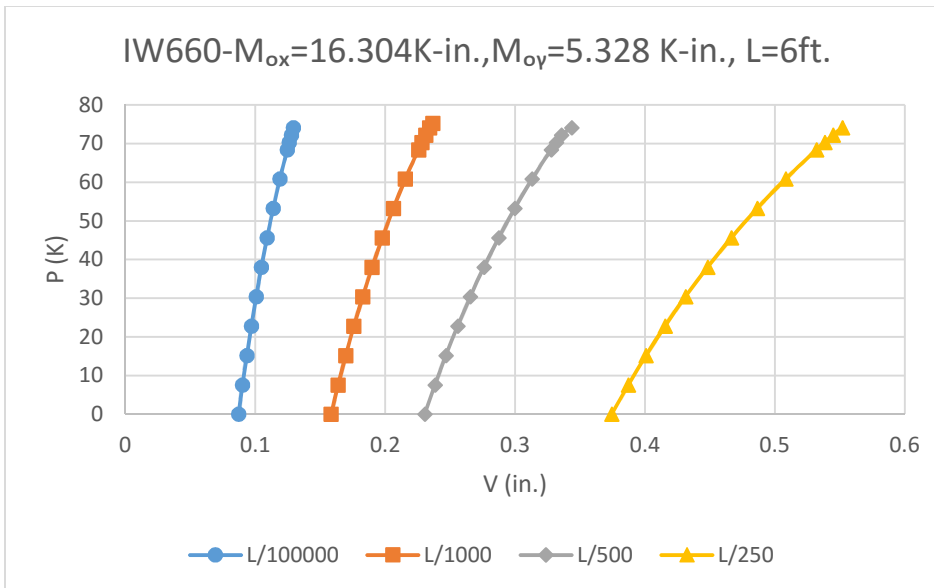


Fig.54 Load vs. Deflection for biaxial beam-column response

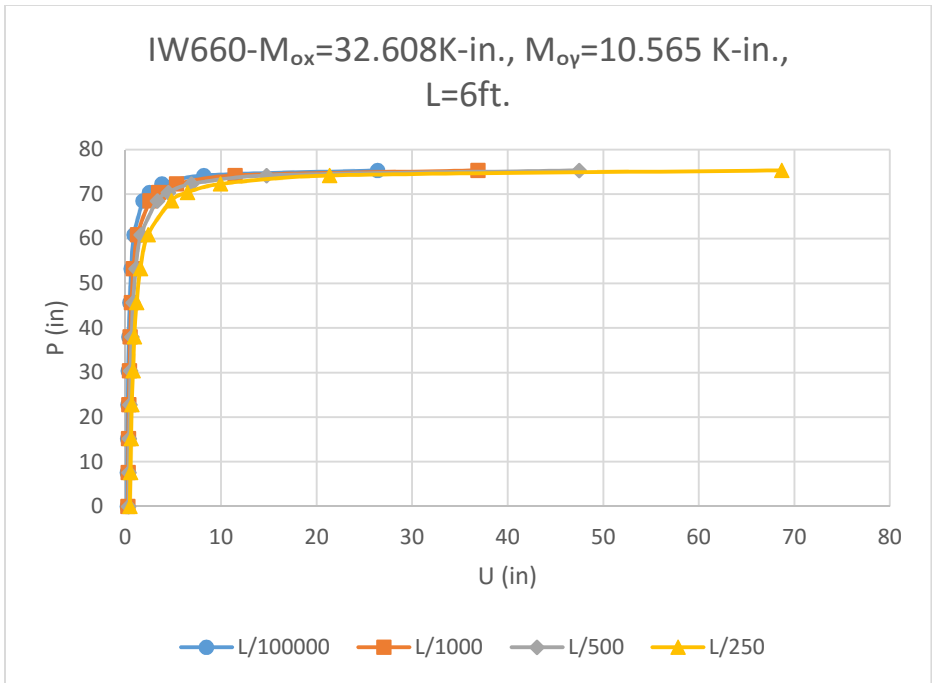


Fig.55 Load vs. Deflection for biaxial beam-column response

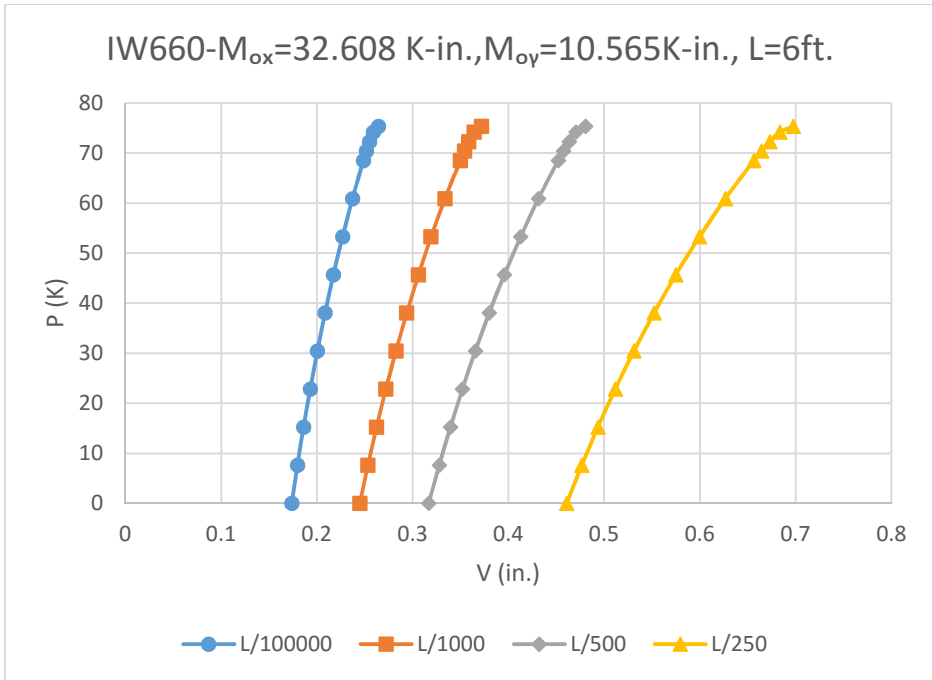


Fig.56 Load vs. Deflection for biaxial beam-column response

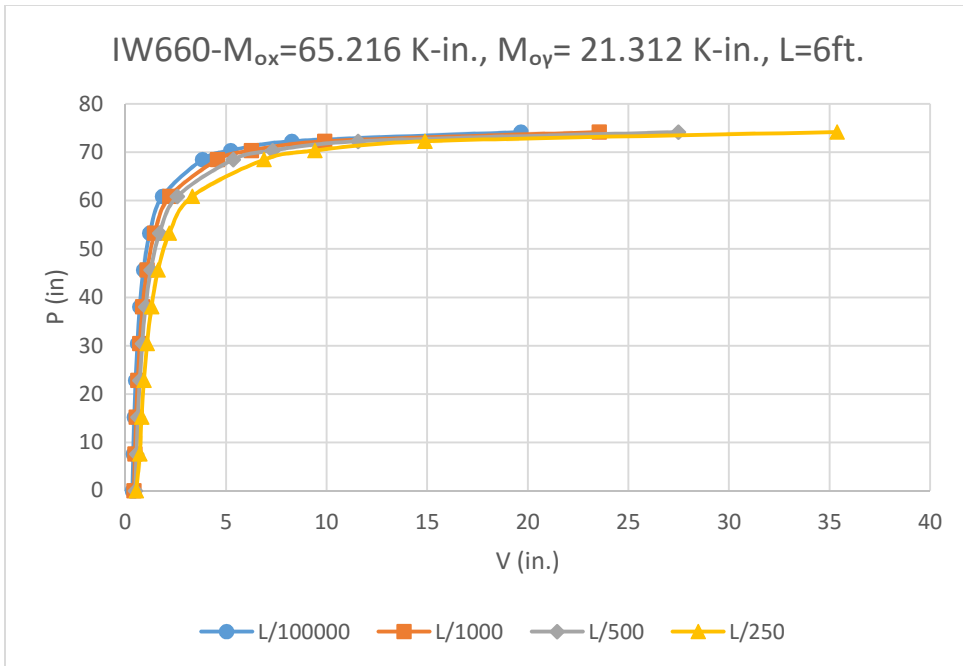


Fig.57 Load vs. Deflection for biaxial beam-column response

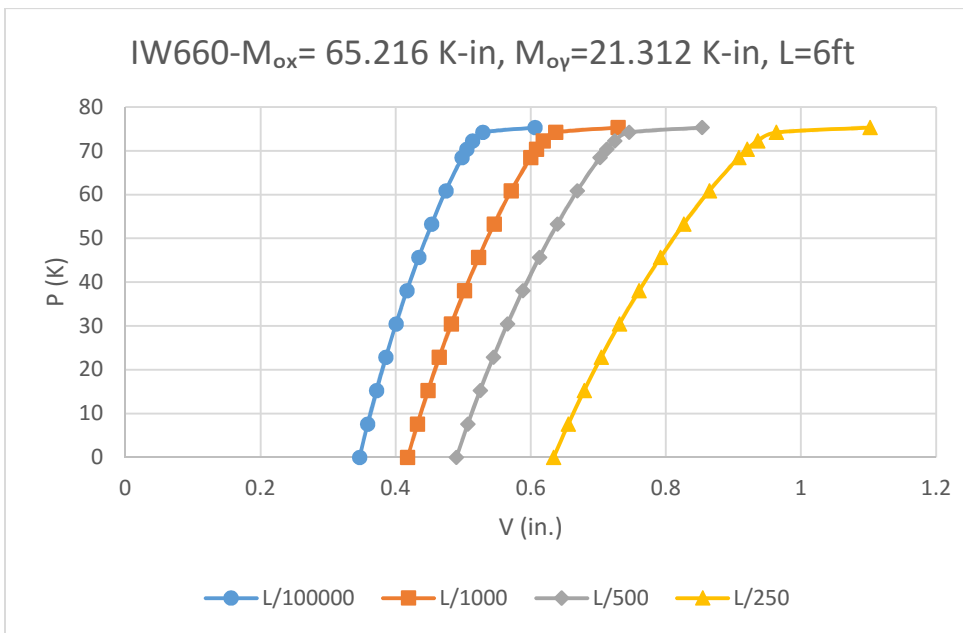


Fig.58 Load vs. Deflection for biaxial beam-column response

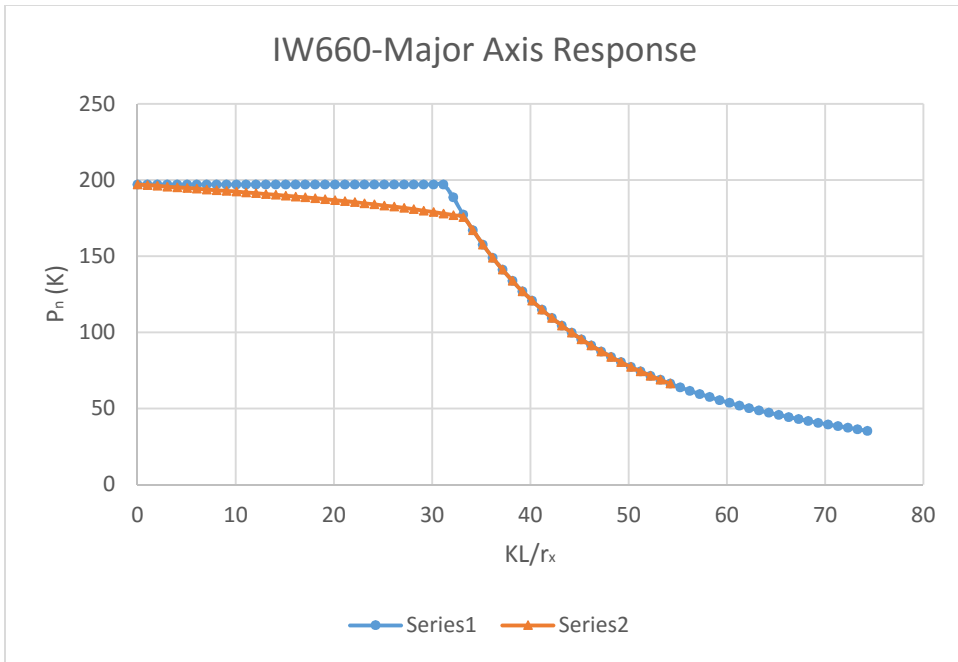


Fig.59 Load vs. slenderness ratio for major axis L/500 vs. L/100000

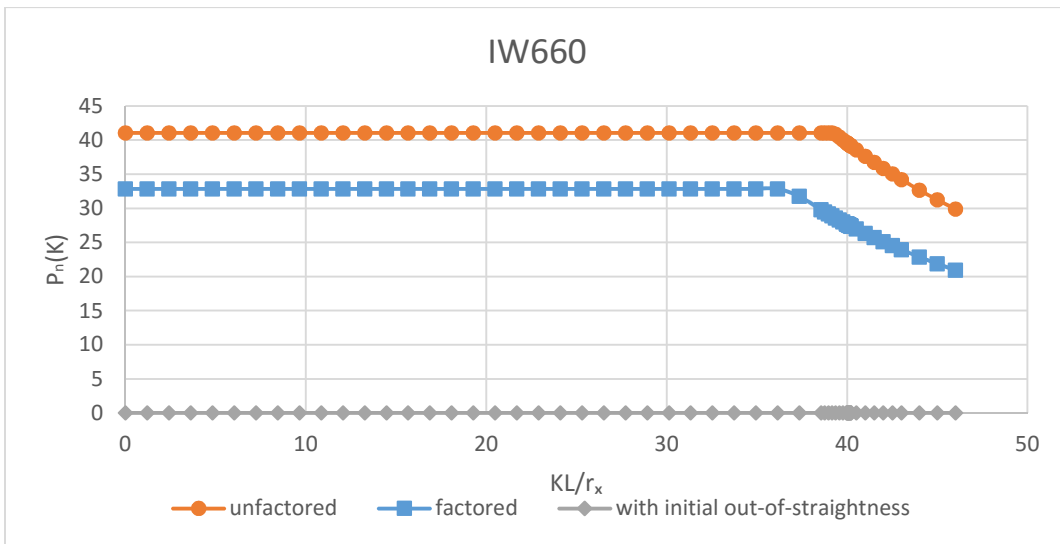


Fig.60 Load vs. slenderness ratio for major axis-ASCE Pre-Standard L/500

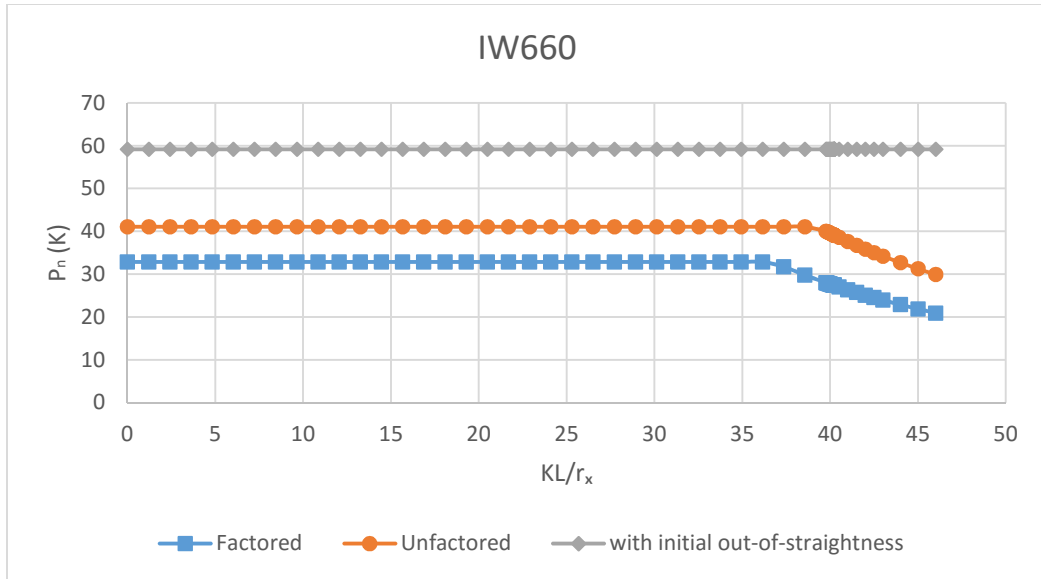


Fig. 61 Load vs. slenderness ratio for major axis-ASCE Pre-Standard

L/100000

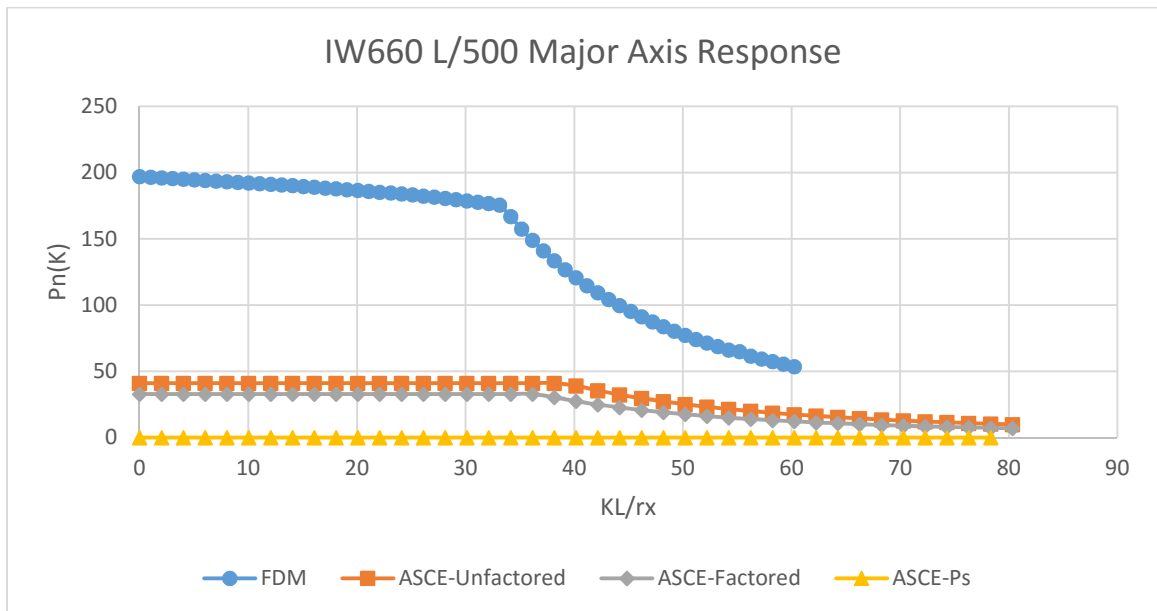


Fig. 62 Load vs. slenderness ratio for major axis. ASCE Pre-Standard

vs. FDM-L/500

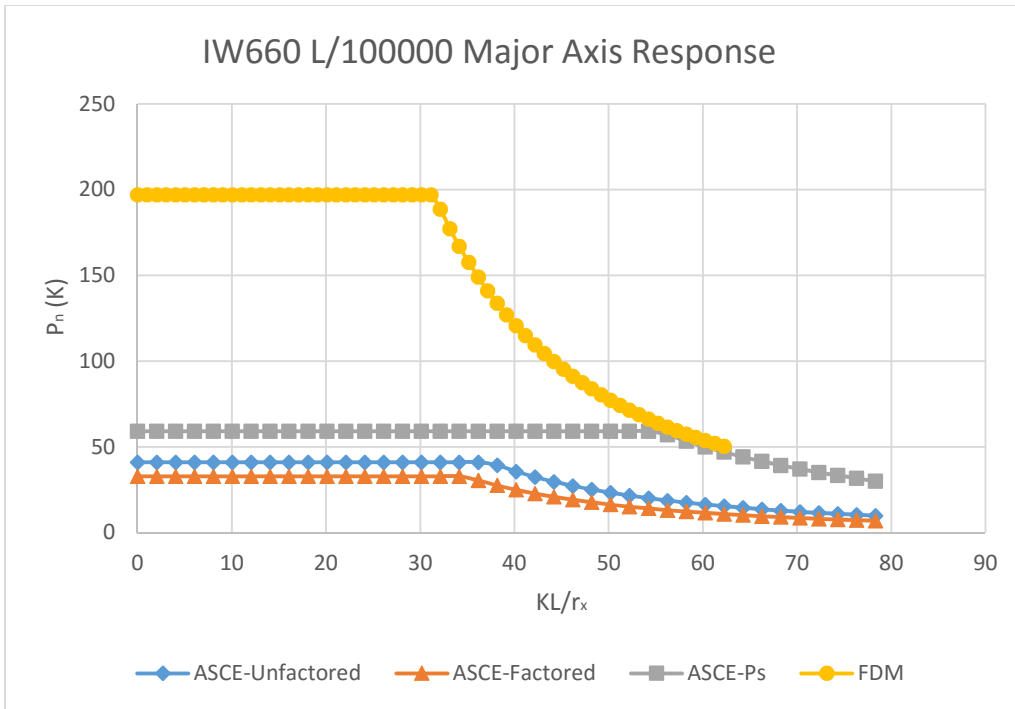


Fig. 63 Load vs. slenderness ratio for major axis response. ASCE Pre-Standard vs. FDM-L/100000

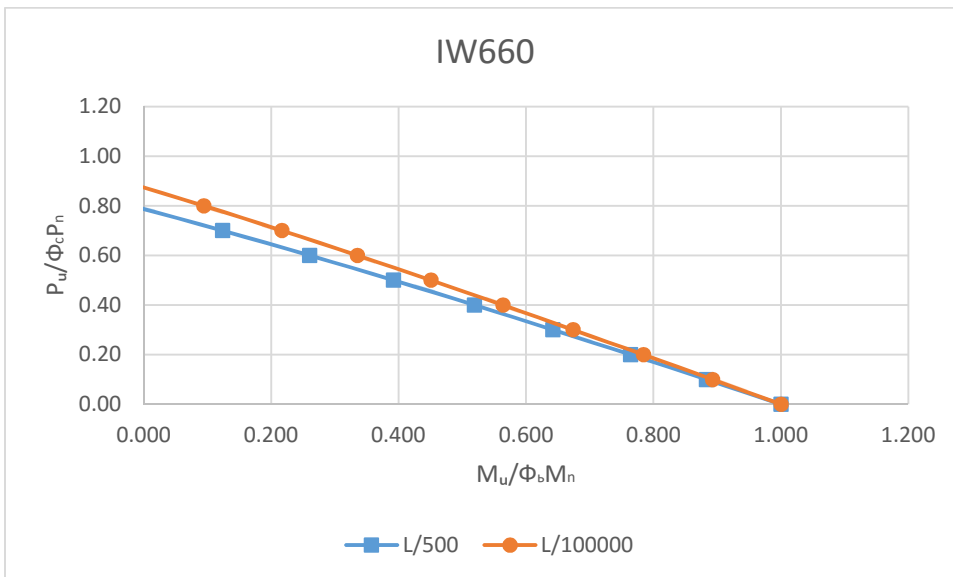
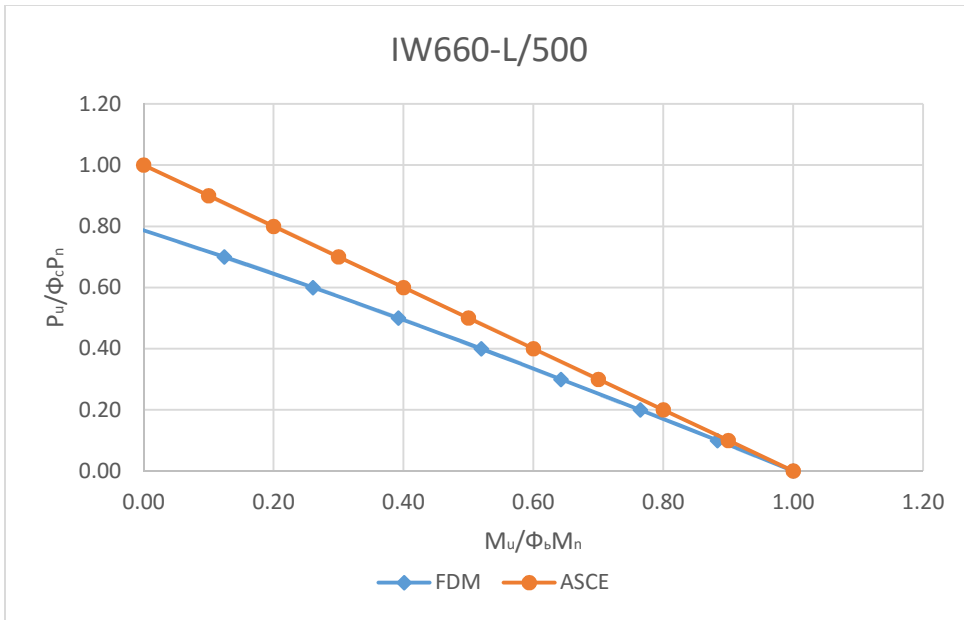
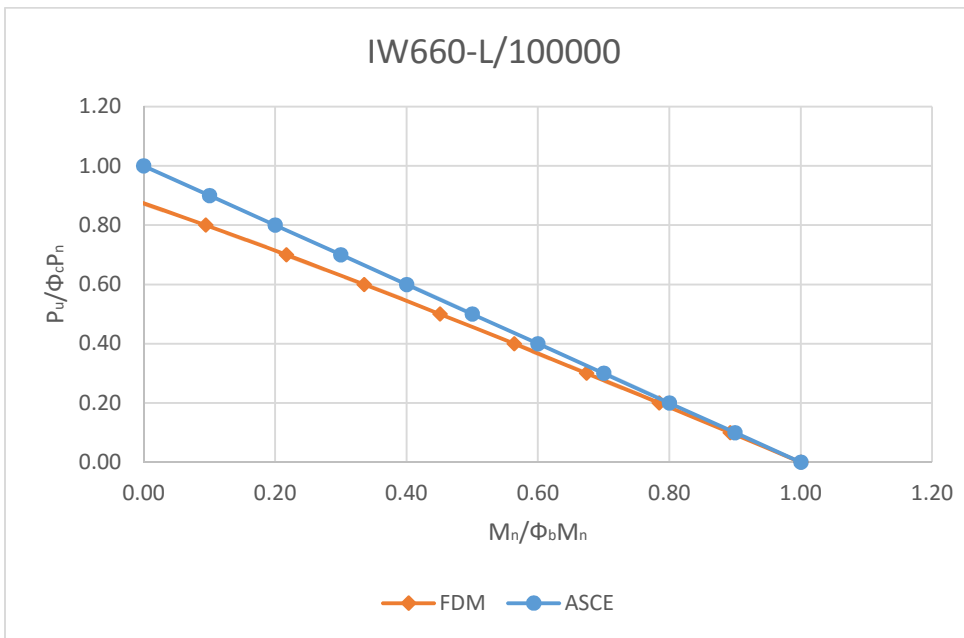


Fig. 64 Load-Moment Interaction for major axis. L/500 vs. L/100000



**Fig. 65 Load-Moment Interaction for major axis for FDM vs. ASCE
Pre-Standard**



**Fig. 66 Load-Moment Interaction for major axis for FDM vs. ASCE
Pre-Standard**

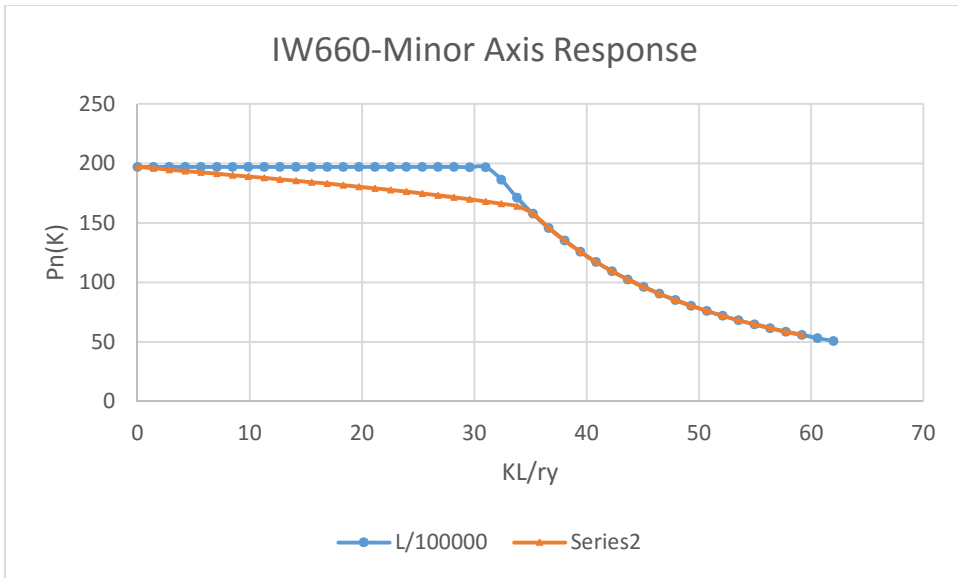


Fig. 67 Load vs. slenderness ratio for minor axis response. L/500 vs. L/100000-FDM

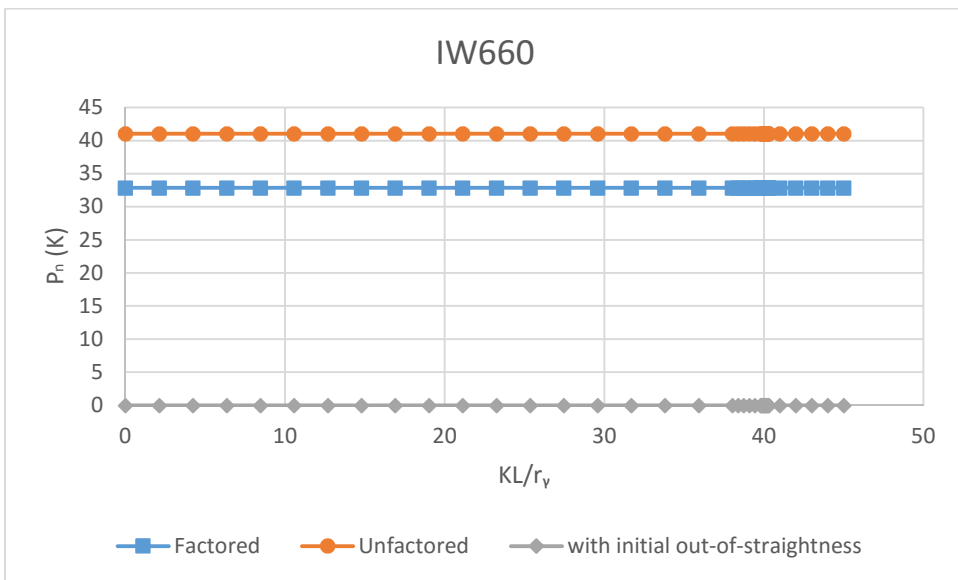


Fig. 68 Load vs. slenderness ratio for minor axis-ASCE LRFD Pre-Standard-L/500

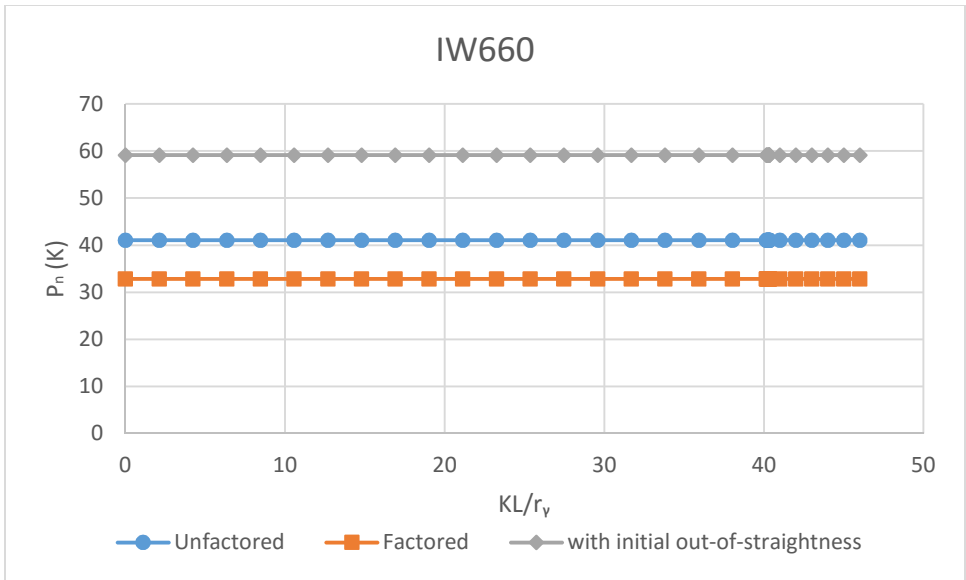


Fig. 69 Load vs. slenderness ratio for minor axis-ASCE LRFD Pre-Standard-L/100000

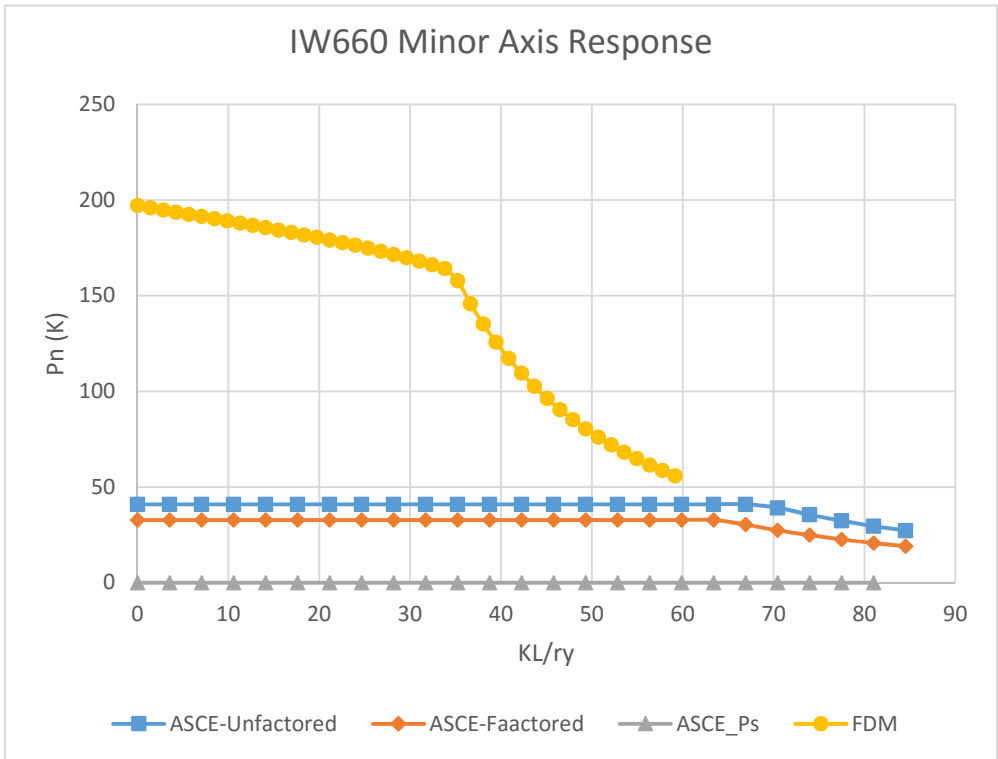


Fig. 70 Load vs. slenderness ratio for minor axis for ASCE LRFD Pre-Standard vs. FDM.L/500



Fig. 71 Load vs. slenderness ratio for minor axis for ASCE LRFD Pre-Standard vs. FDM. L/100000

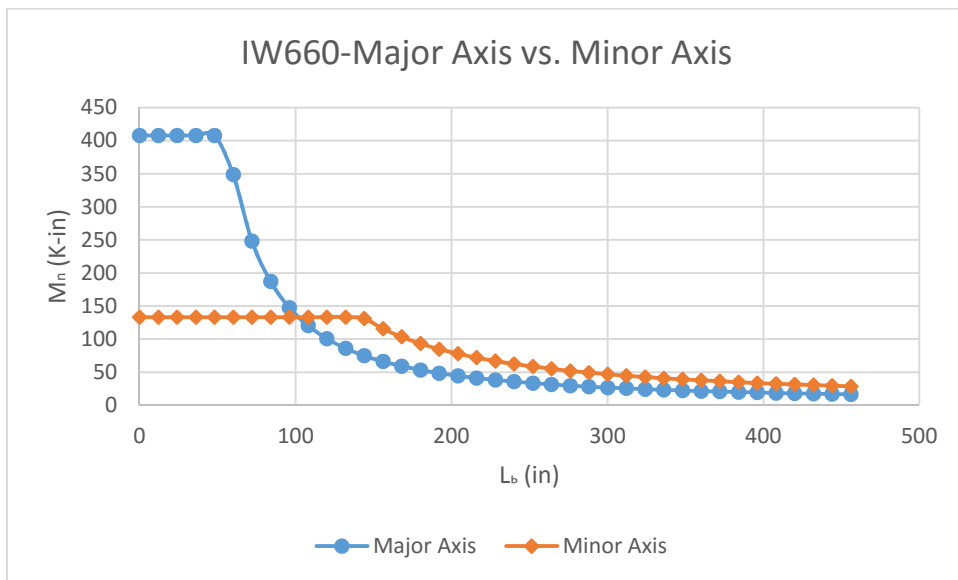


Fig. 72 Moment vs. Length for major axis vs. minor axis

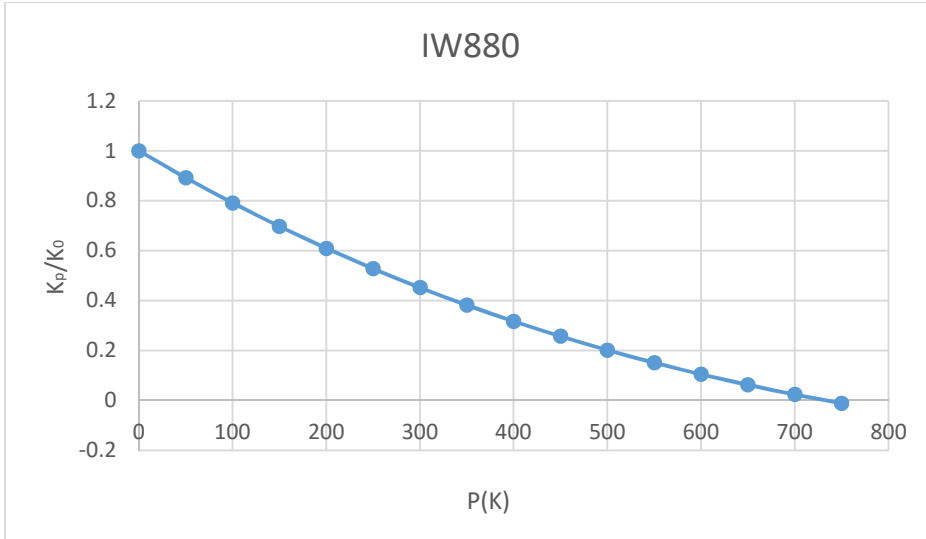


Fig. 73 Stiffness degrading for column major axis effect L=6ft.

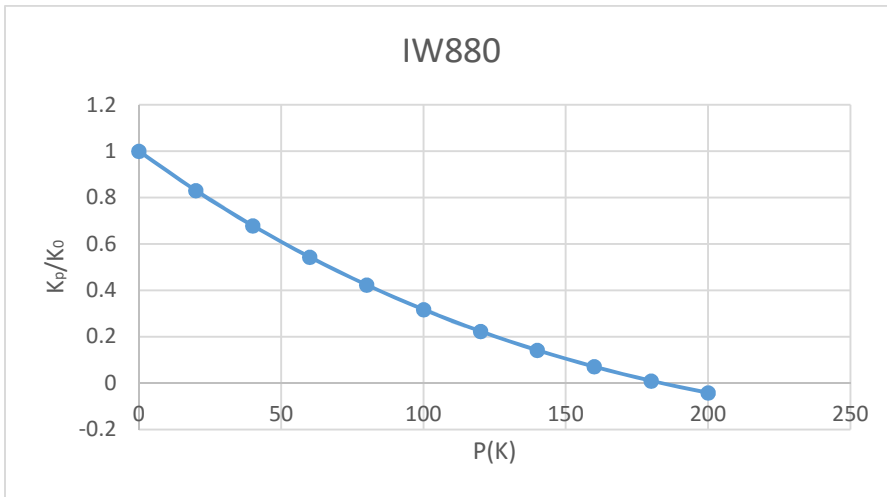


Fig. 74 Stiffness degrading for column major axis effect. L=12ft.

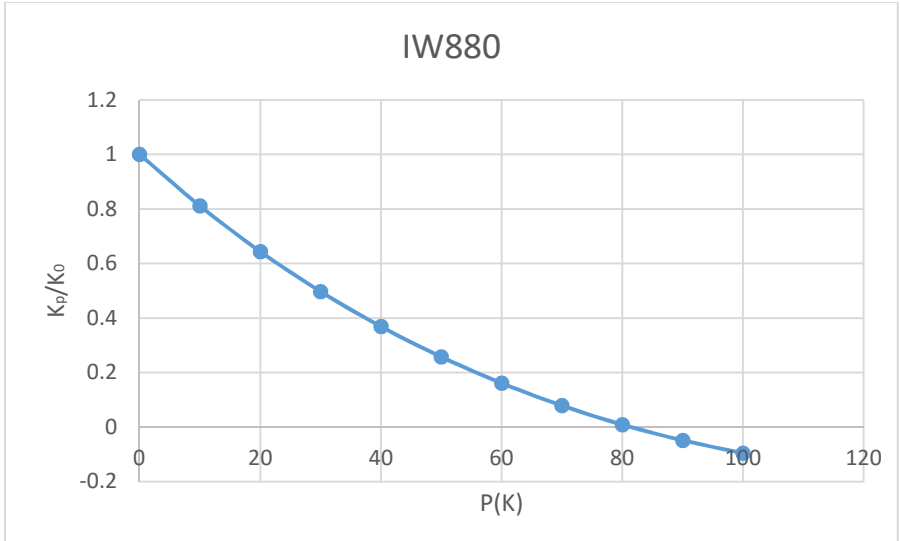


Fig. 75 Stiffness degrading for column major axis effect. L=18ft.

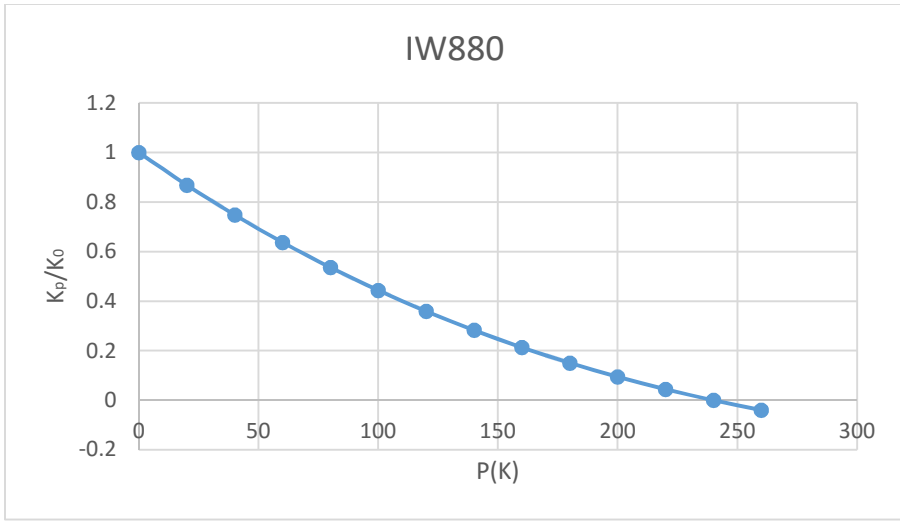


Fig. 76 Stiffness degrading for column minor axis effect. L=6ft.

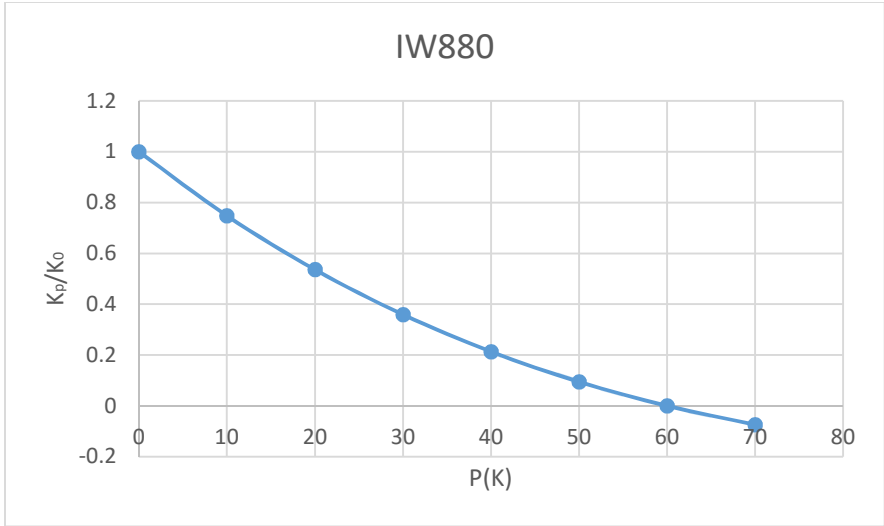


Fig. 77 Stiffness degrading for column minor axis effect. L=12ft.

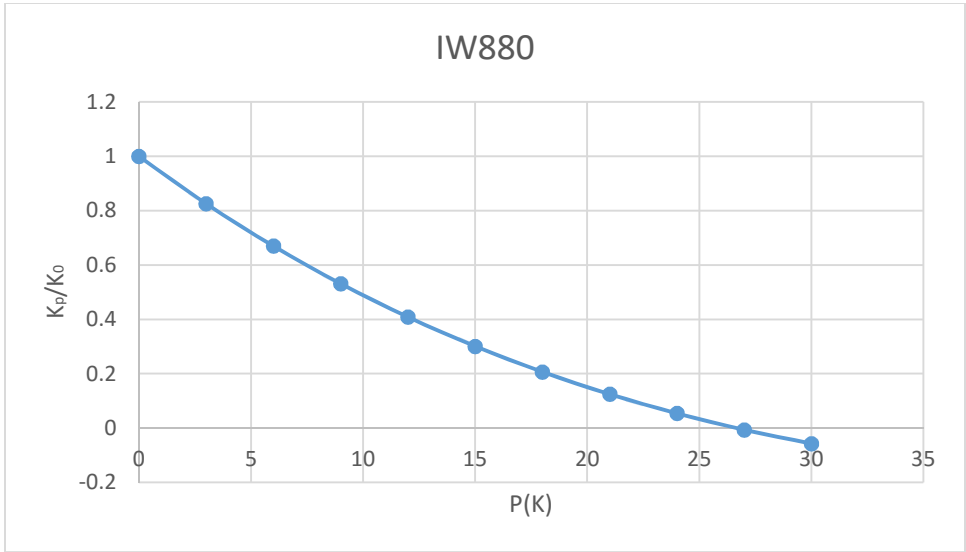


Fig. 78 Stiffness degrading for column minor axis effect. L=18ft.

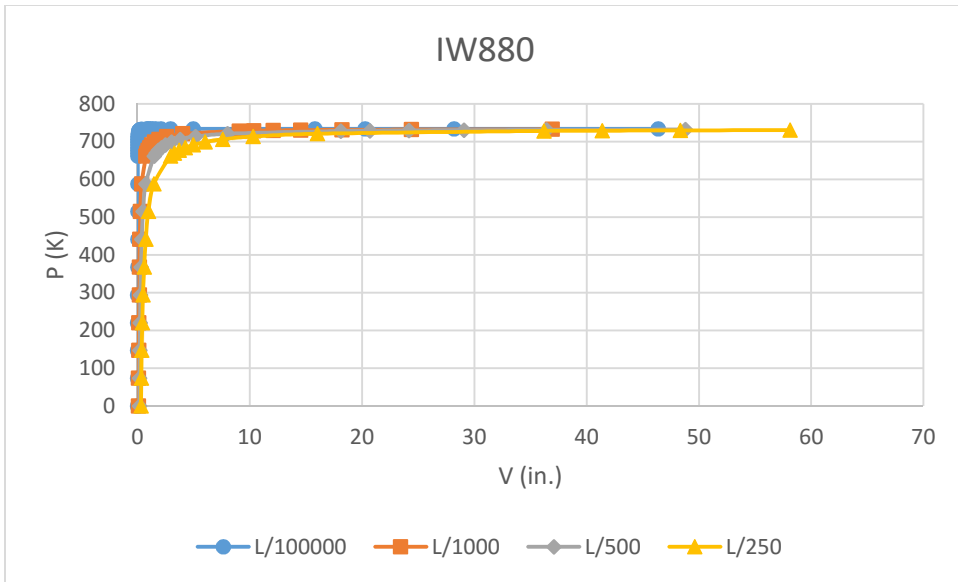


Fig. 79 Load vs. Deflection for column major axis response L=6ft.

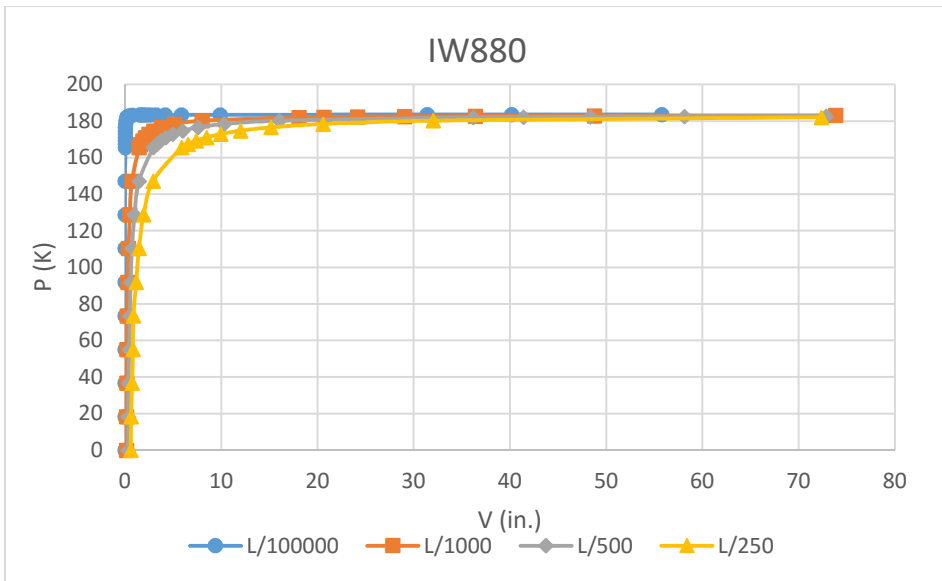


Fig. 80 Load vs. Deflection for column major axis response L=12ft.

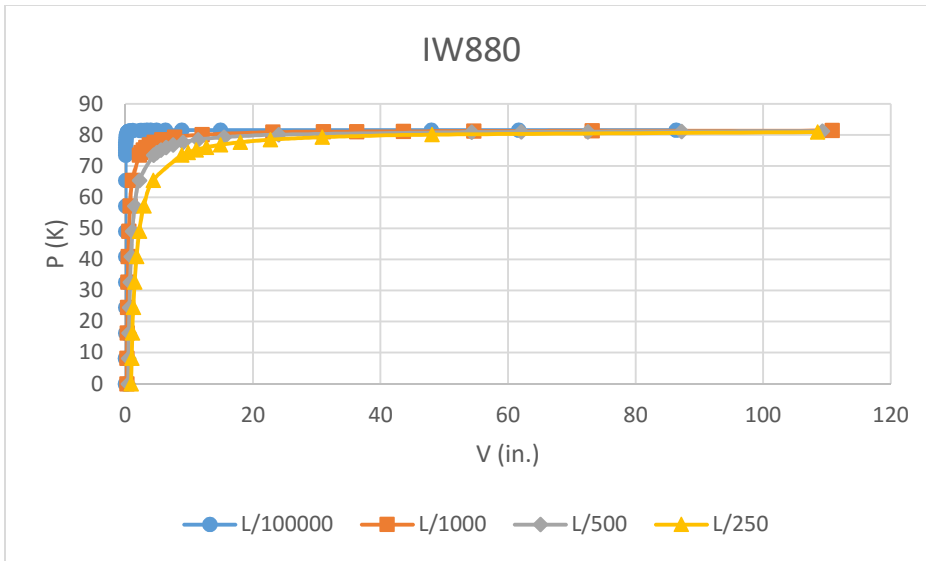


Fig. 81 Load vs. Deflection for column major axis response $L=18$ ft.

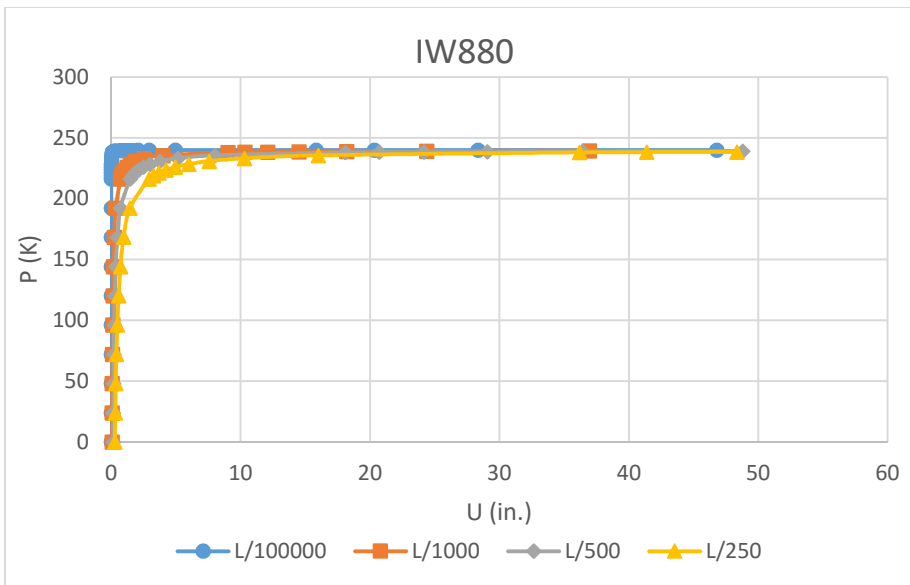


Fig. 82 Load vs. Deflection for column minor axis response $L=6$ ft.

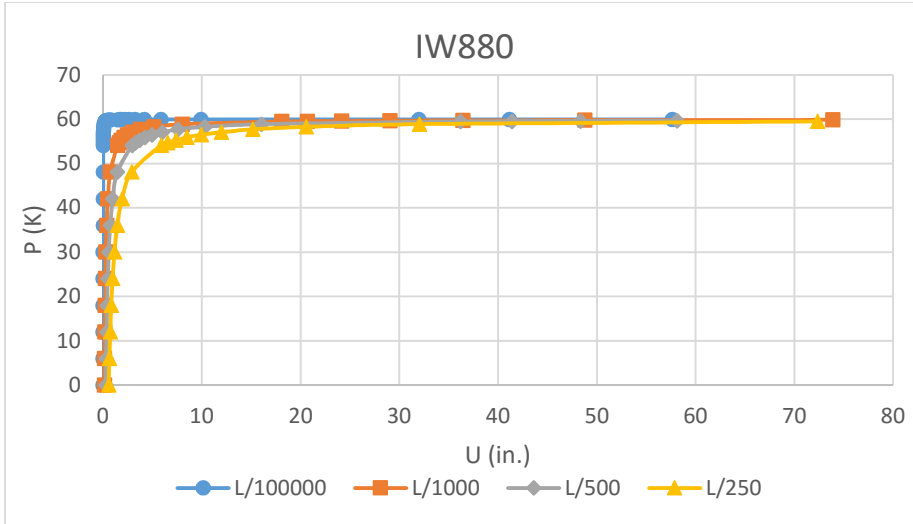


Fig. 83 Load vs. Deflection for column minor axis response L=12ft.

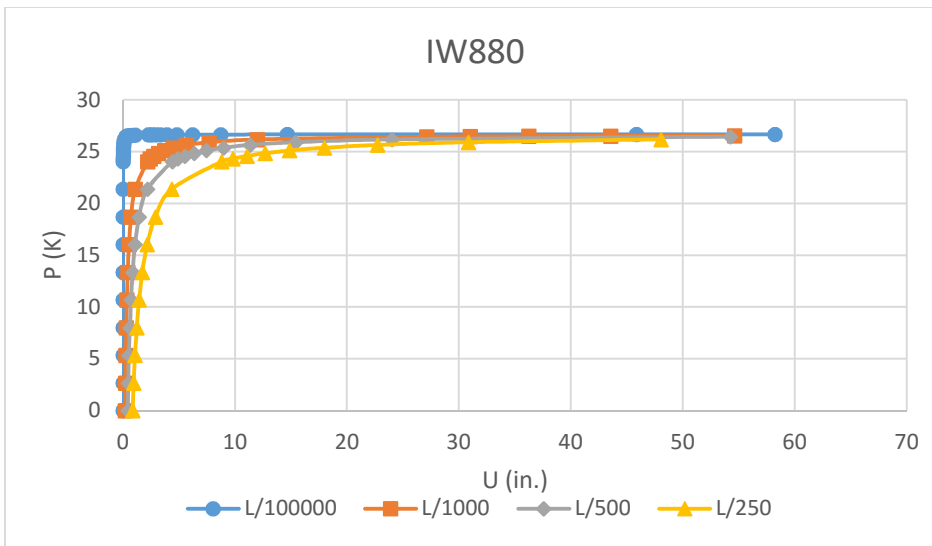


Fig. 84 Load vs. Deflection for column minor axis response L=18ft.

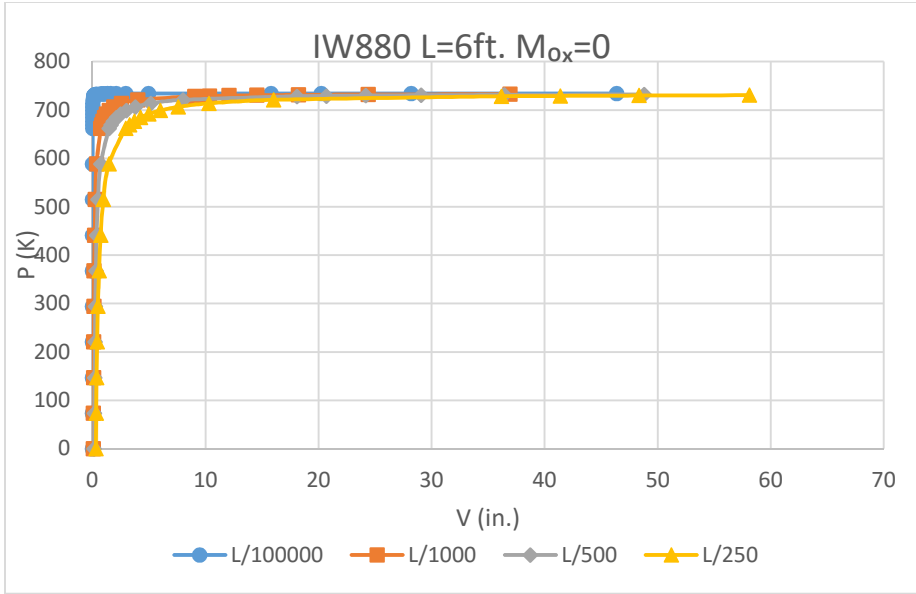


Fig. 85 Load vs. Deflection for uniaxial beam-column major axis response.

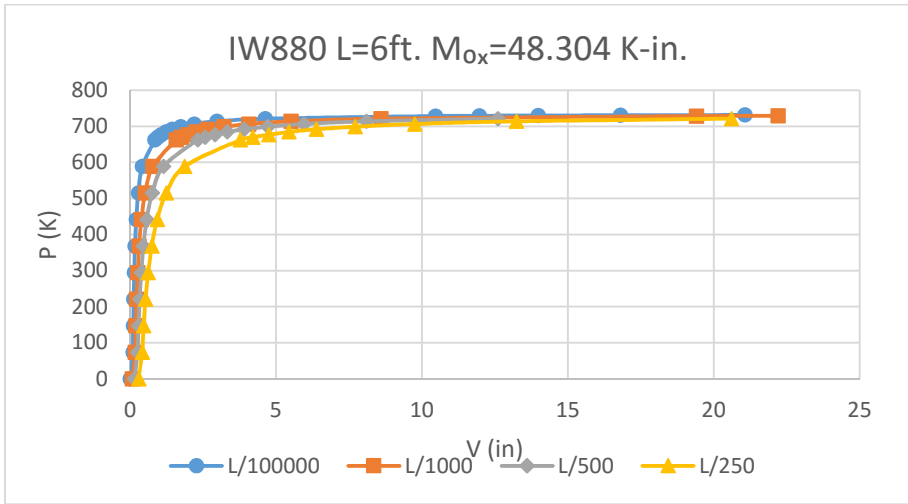


Fig. 86 Load vs. Deflection for uniaxial beam-column major axis response

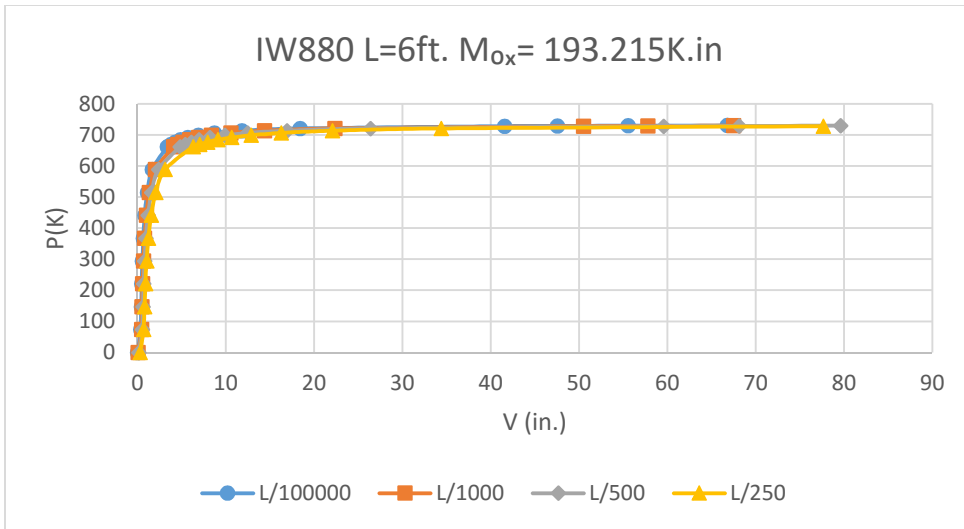


Fig. 87 Load vs. Deflection for uniaxial beam-column major axis response

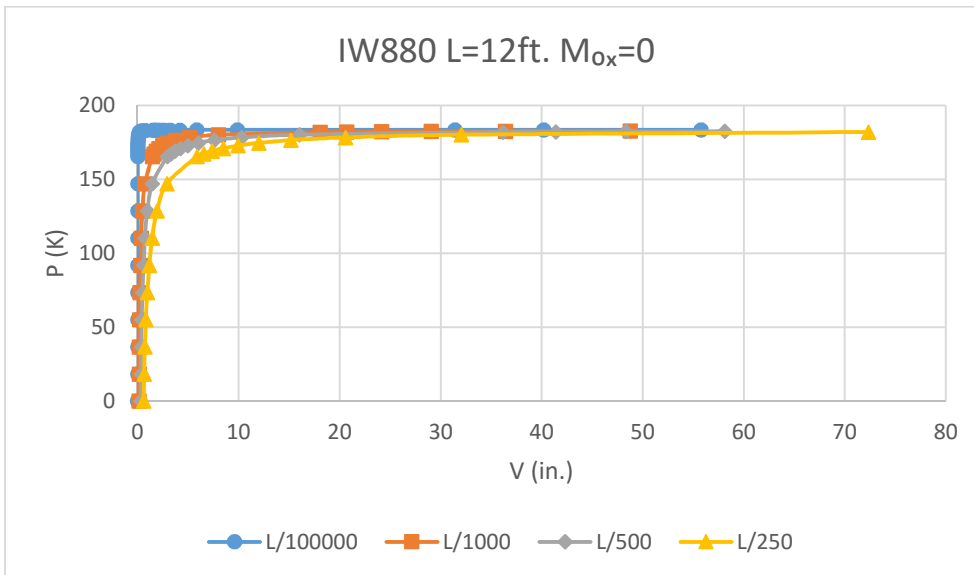


Fig. 88 Load vs. Deflection for uniaxial beam-column major axis response

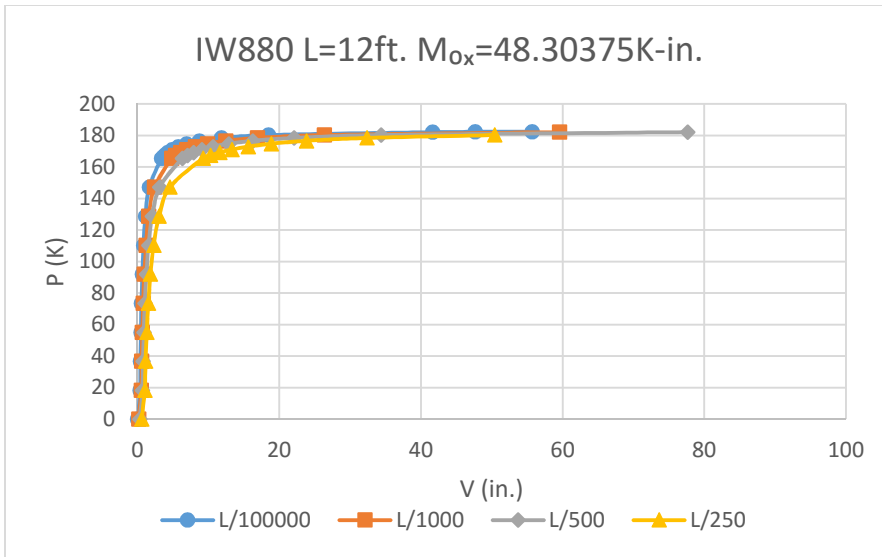


Fig. 89 Load vs. Deflection for uniaxial beam-column major axis response

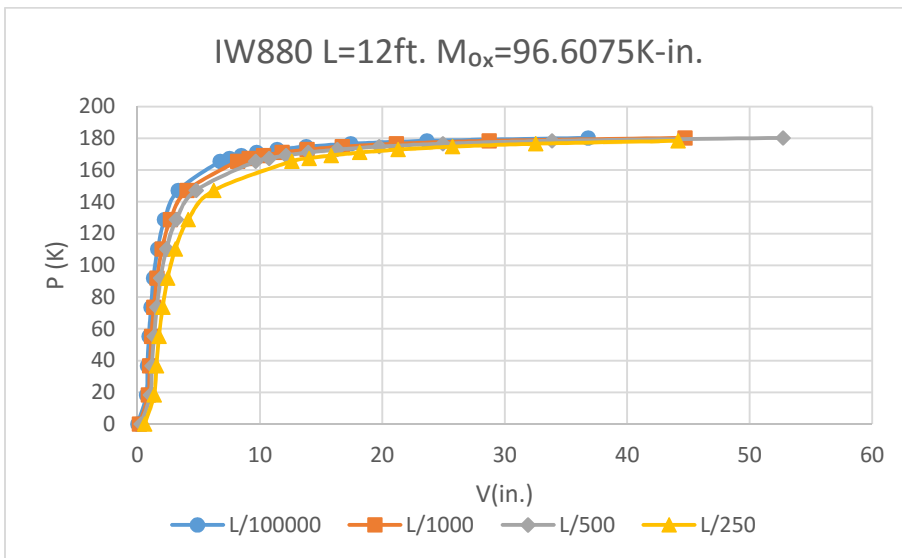


Fig. 90 Load vs. Deflection for uniaxial beam-column major axis response

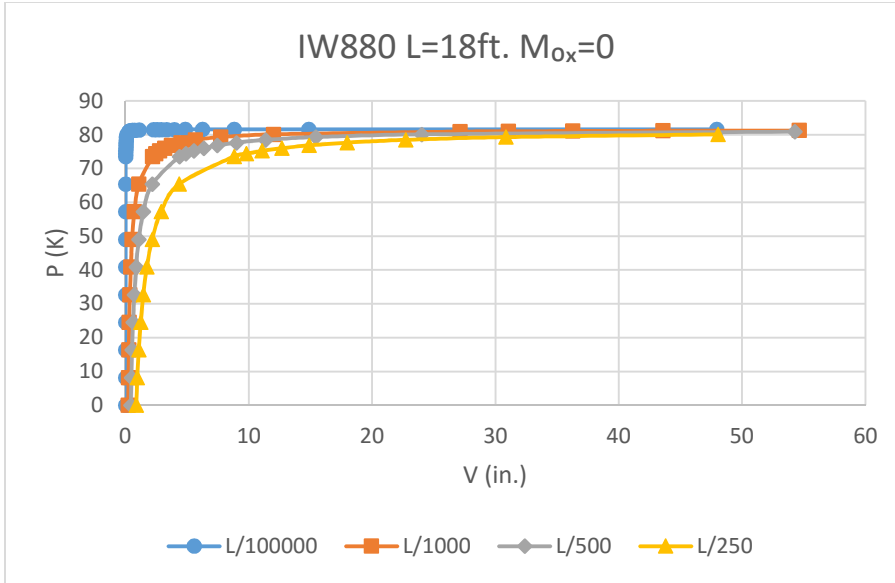


Fig. 91 Load vs. Deflection for uniaxial beam-column major axis response

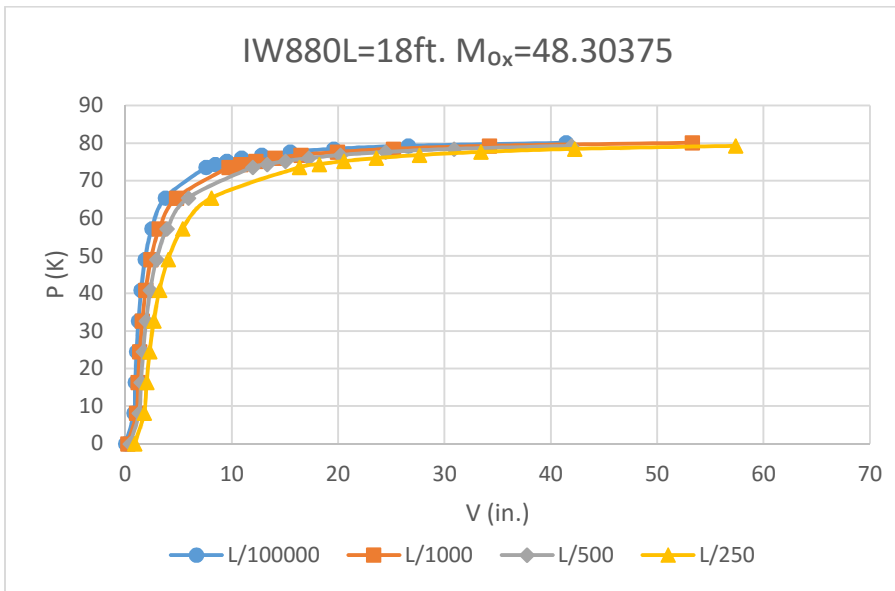


Fig. 92 Load vs. Deflection for uniaxial beam-column major axis response

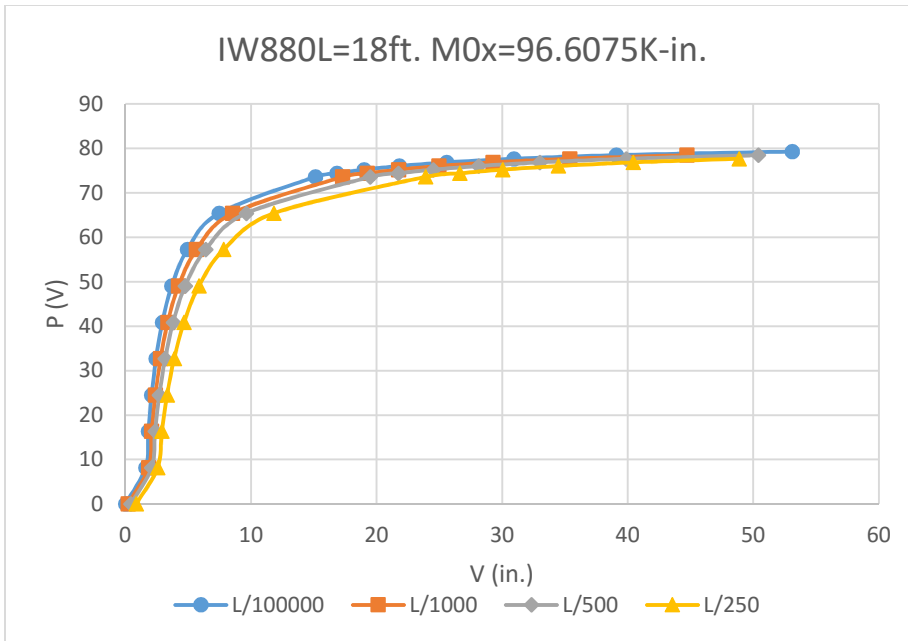


Fig. 93 Load vs. Deflection for uniaxial beam-column major axis response

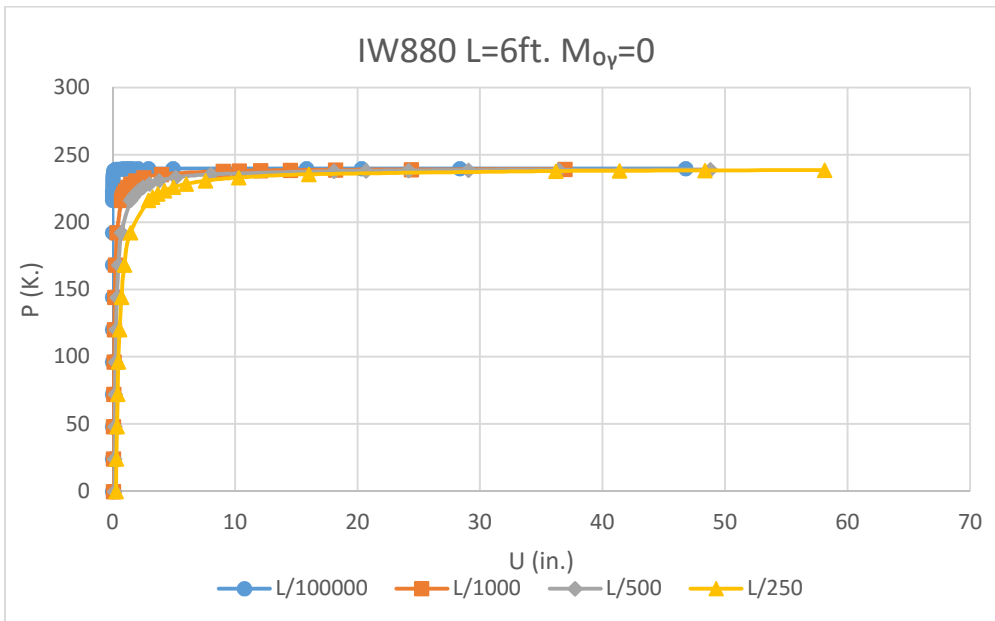


Fig. 94 Load vs. Deflection for uniaxial beam-column minor axis response

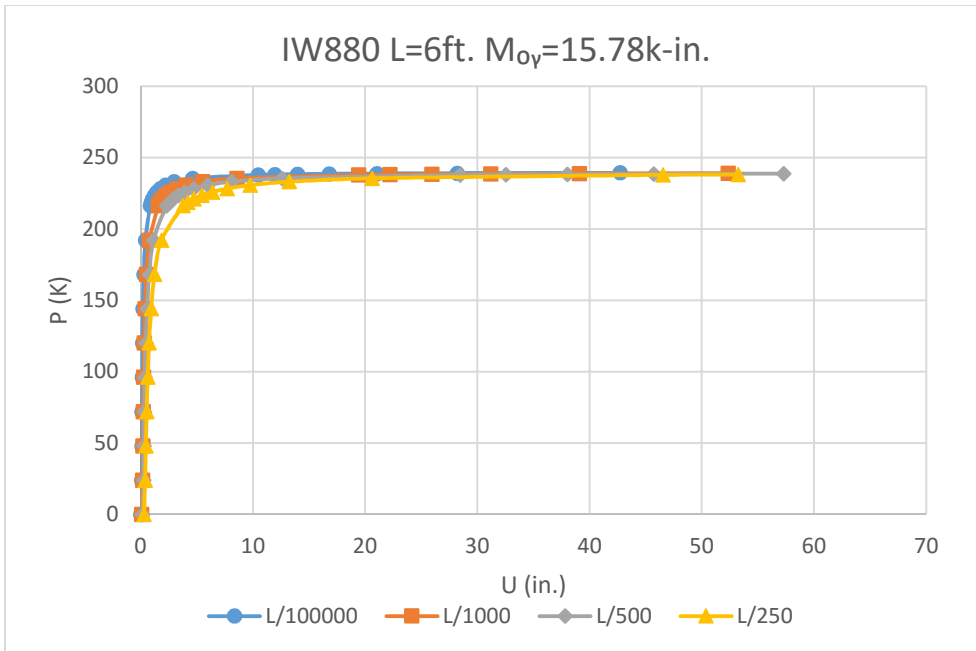


Fig. 95 Load vs. Deflection for uniaxial beam-column minor axis response

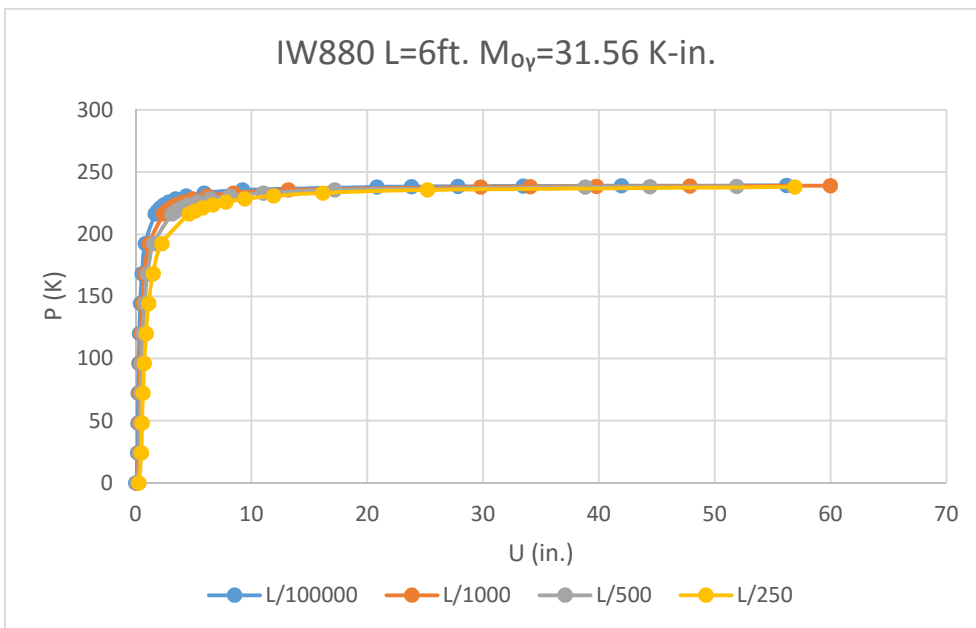


Fig. 96 Load vs. Deflection for uniaxial beam-column minor axis response

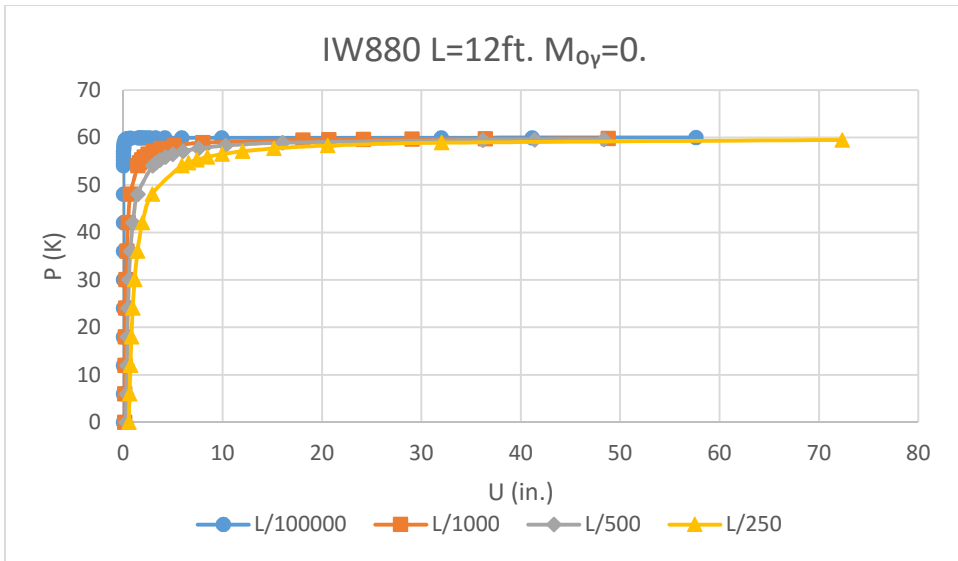


Fig. 97 Load vs. Deflection for uniaxial beam-column minor axis response

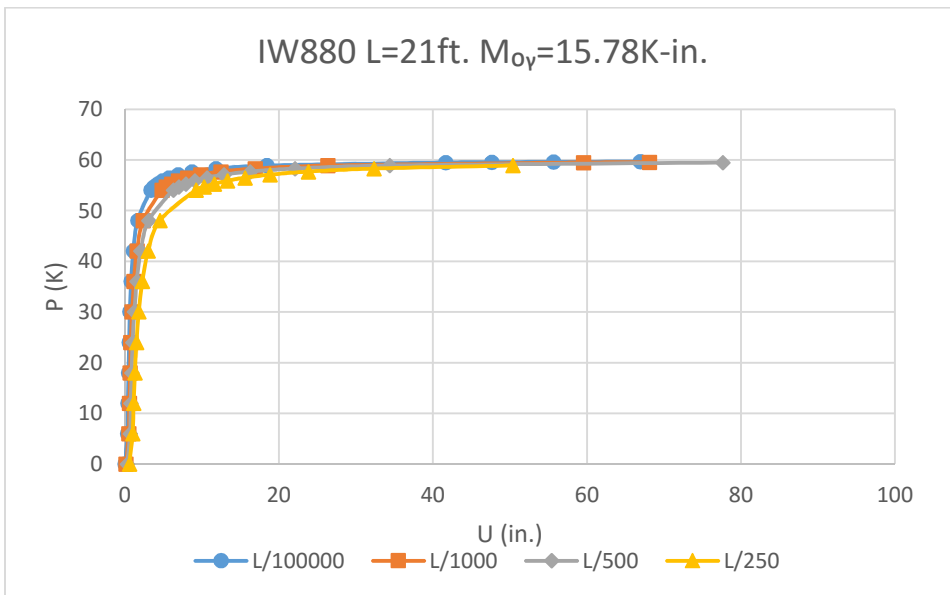


Fig. 98 Load vs. Deflection for uniaxial beam-column minor axis response

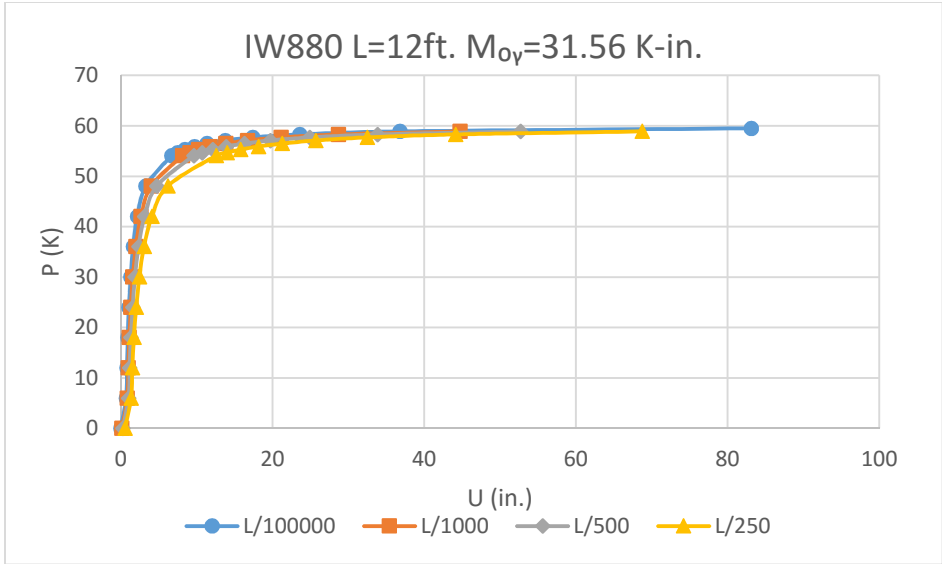


Fig. 99 Load vs. Deflection for uniaxial beam-column minor axis response

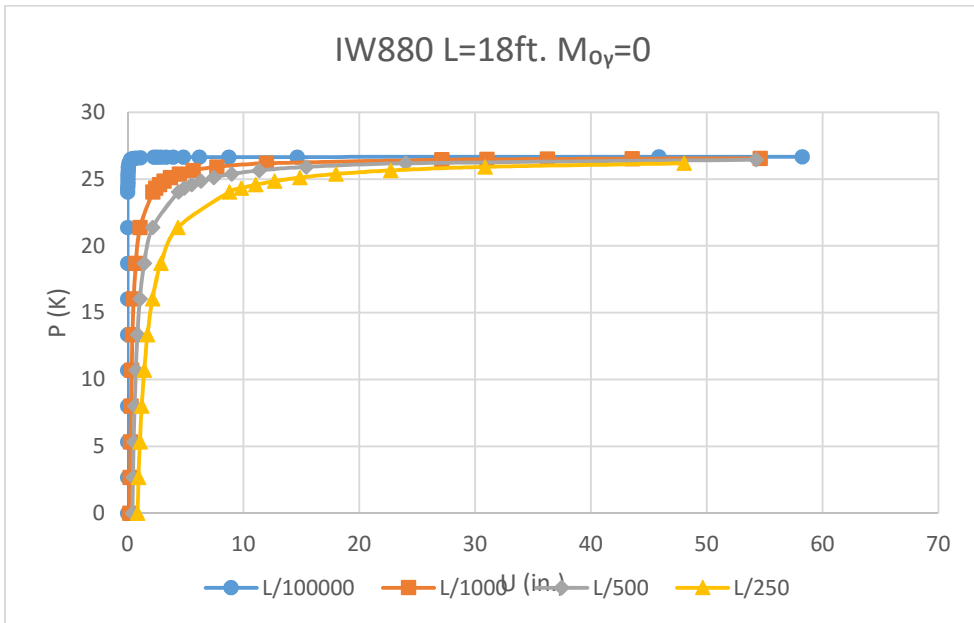


Fig. 100 Load vs. Deflection for uniaxial beam-column minor axis response

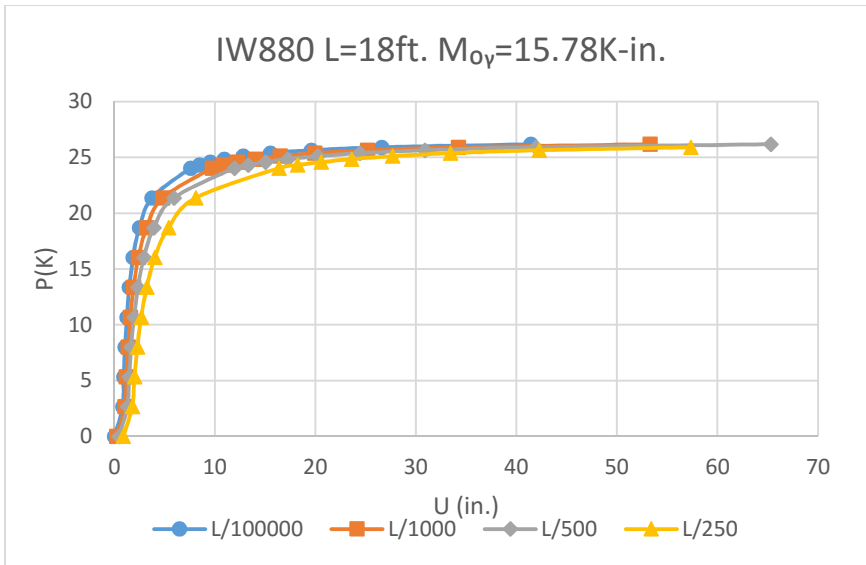


Fig. 101 Load vs. Deflection for uniaxial beam-column minor axis response

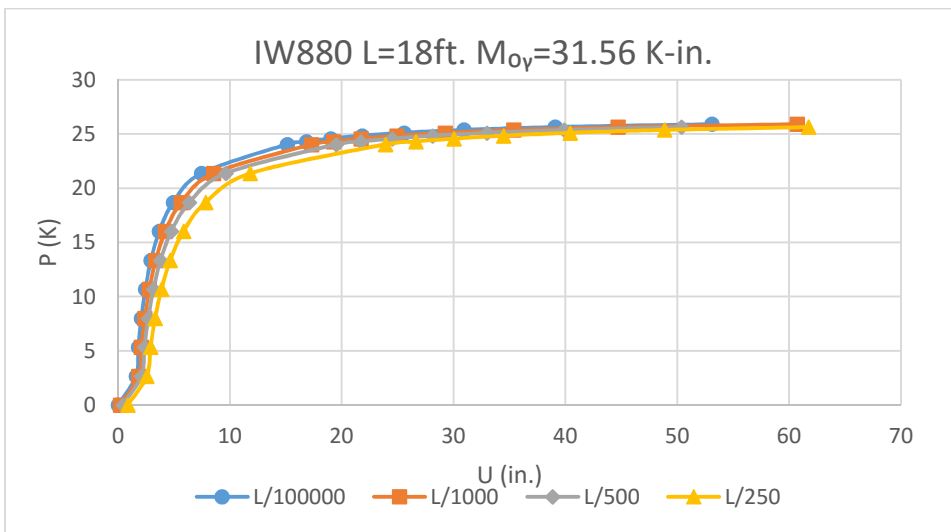


Fig. 102 Load vs. Deflection for uniaxial beam-column minor axis response

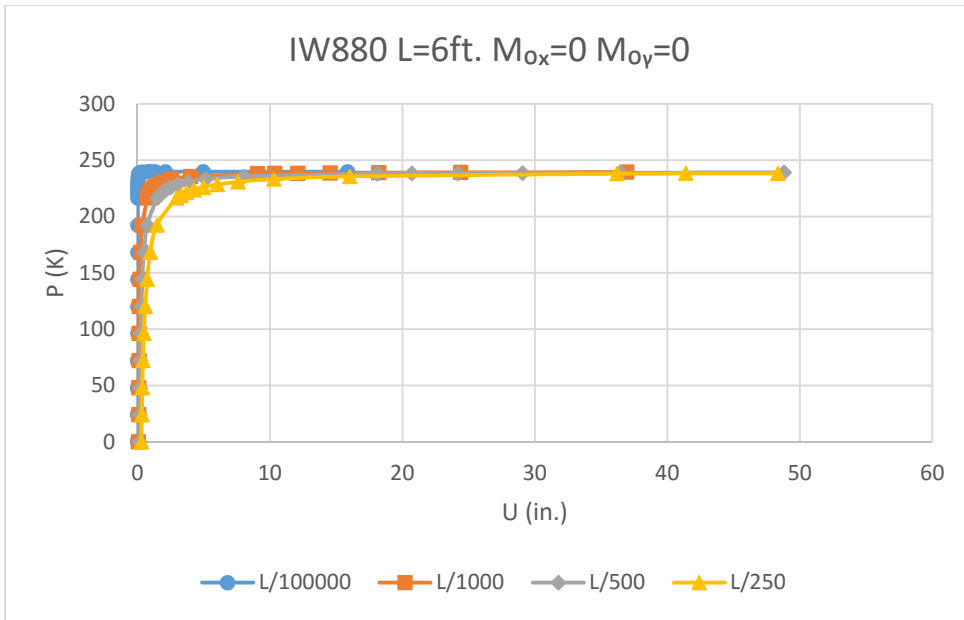


Fig. 103 Load vs. Deflection for biaxial beam-column response.

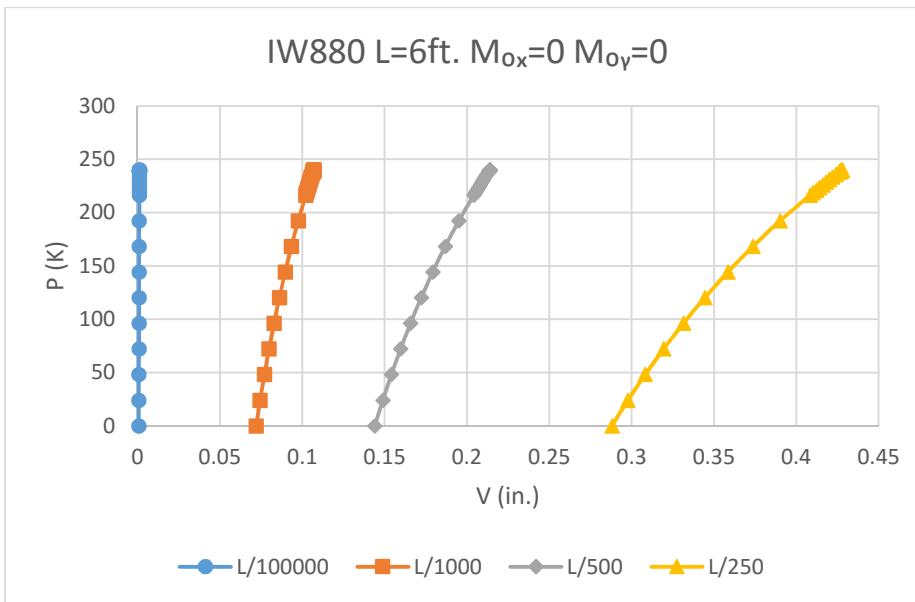


Fig. 104 Load vs. Deflection for biaxial beam-column response

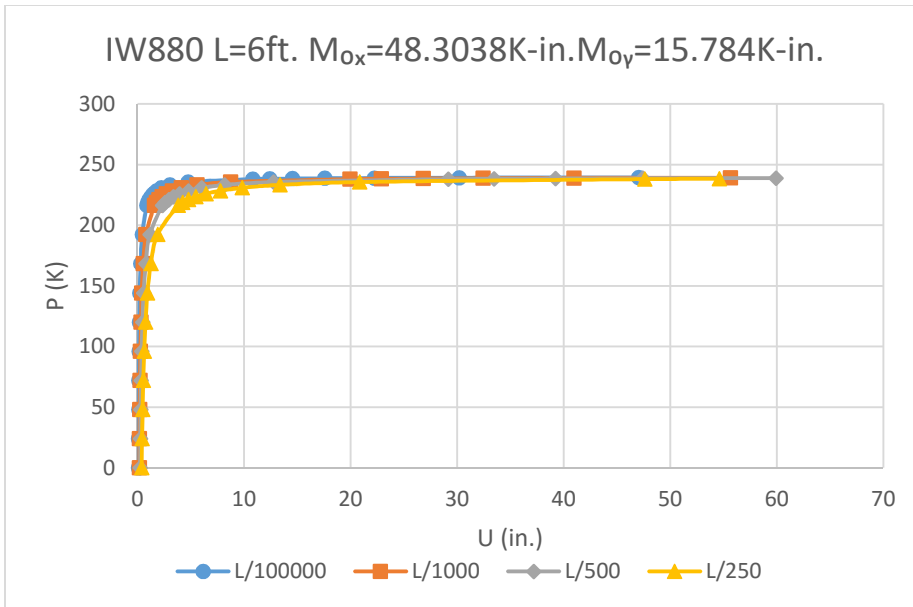


Fig. 105 Load vs. Deflection for biaxial beam-column response

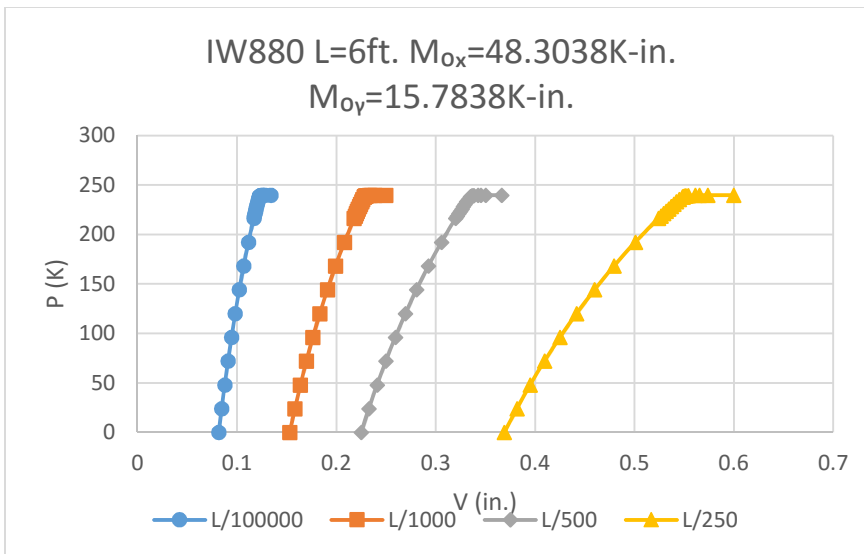


Fig. 106 Load vs. Deflection for biaxial beam-column response

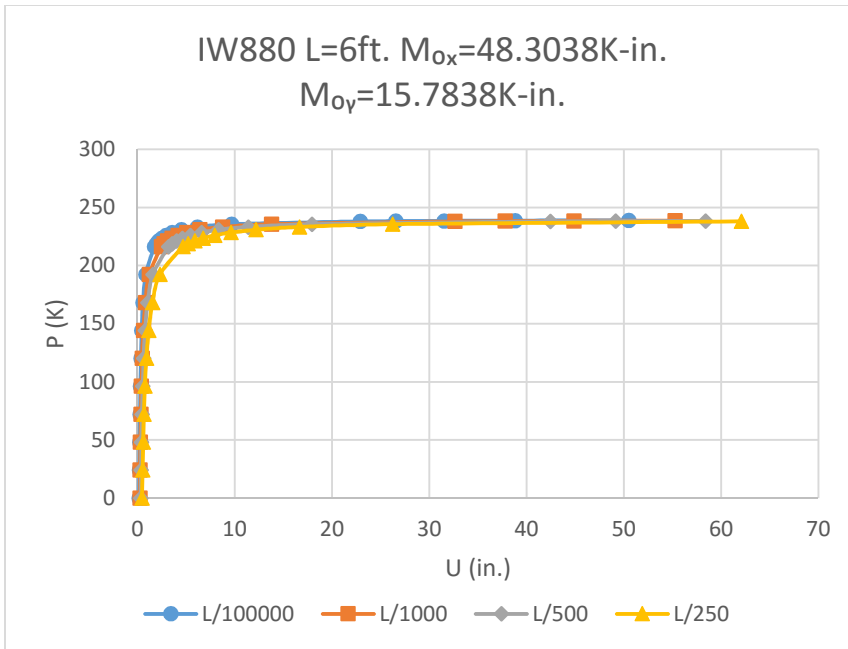


Fig. 107 Load vs. Deflection for biaxial beam-column response

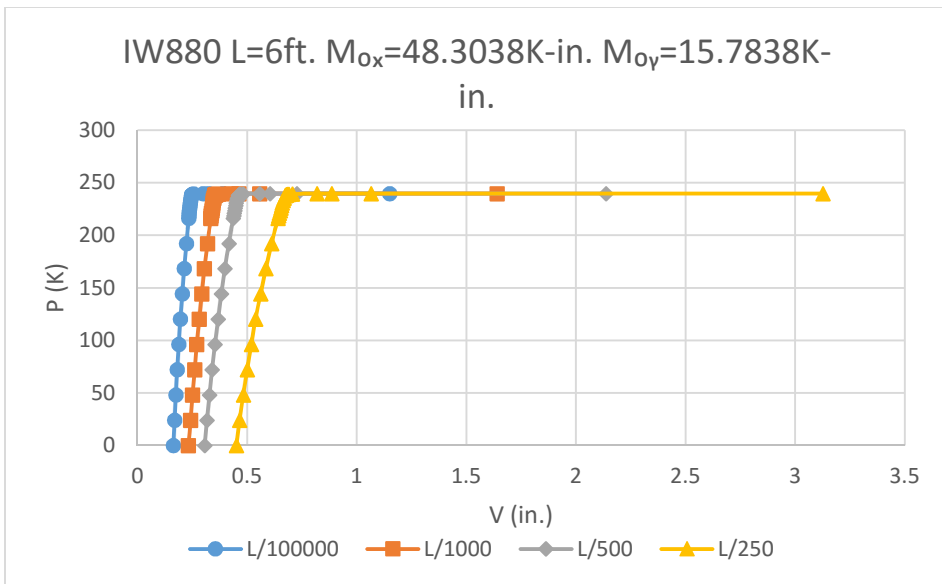


Fig. 108 Load vs. Deflection for biaxial beam-column response

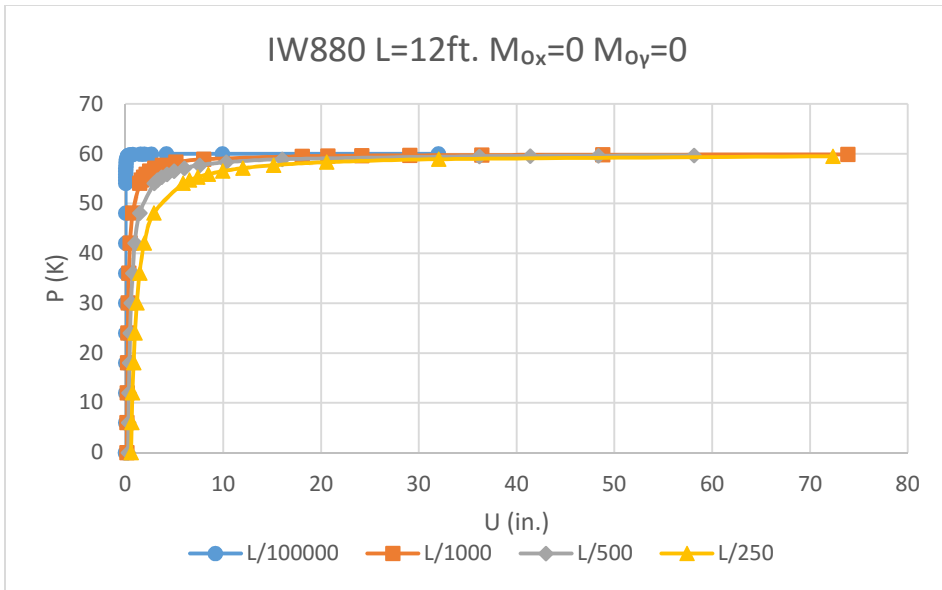


Fig. 109 Load vs. Deflection for biaxial beam-column response

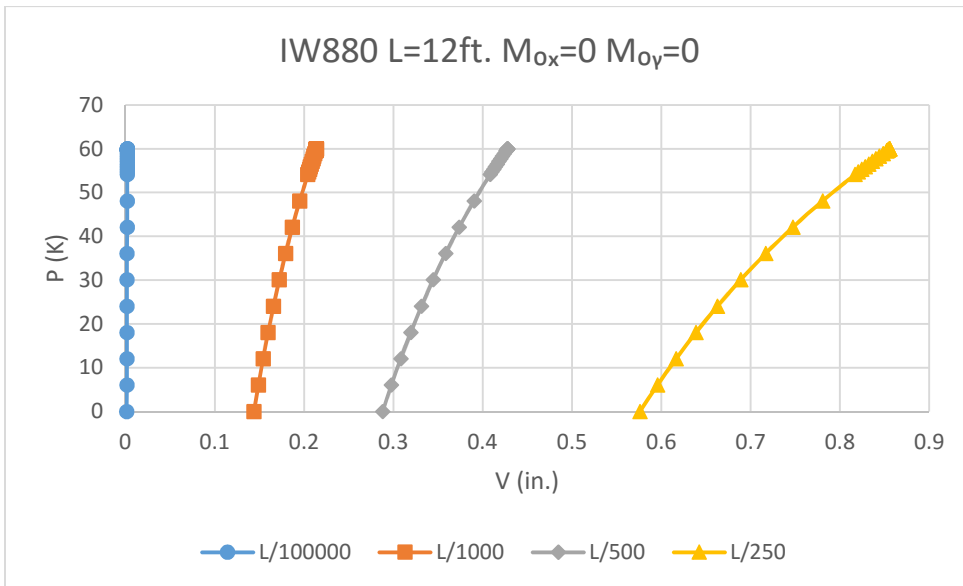


Fig. 110 Load vs. Deflection for biaxial beam-column response

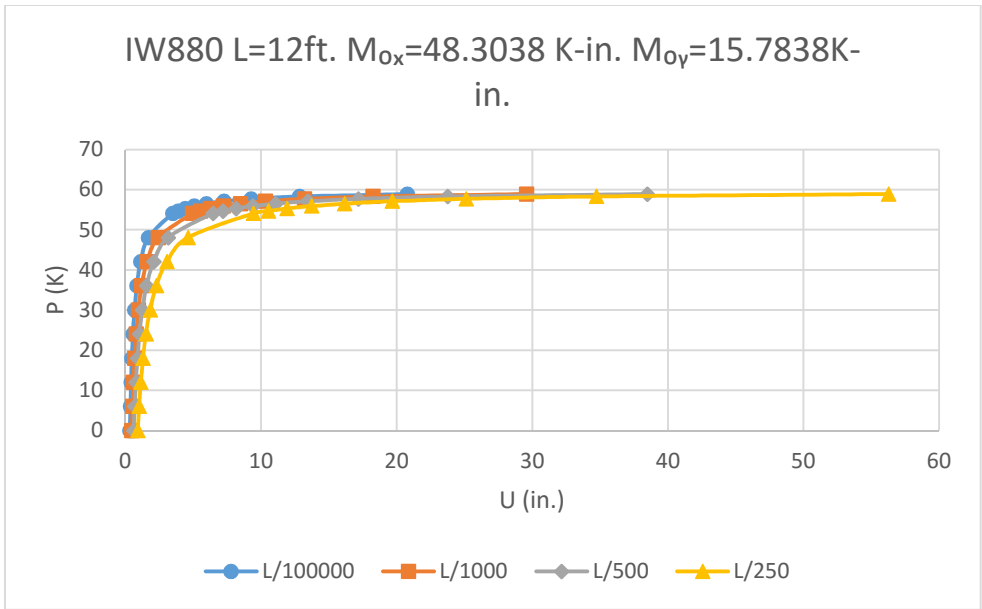


Fig. 111 Load vs. Deflection for biaxial beam-column response

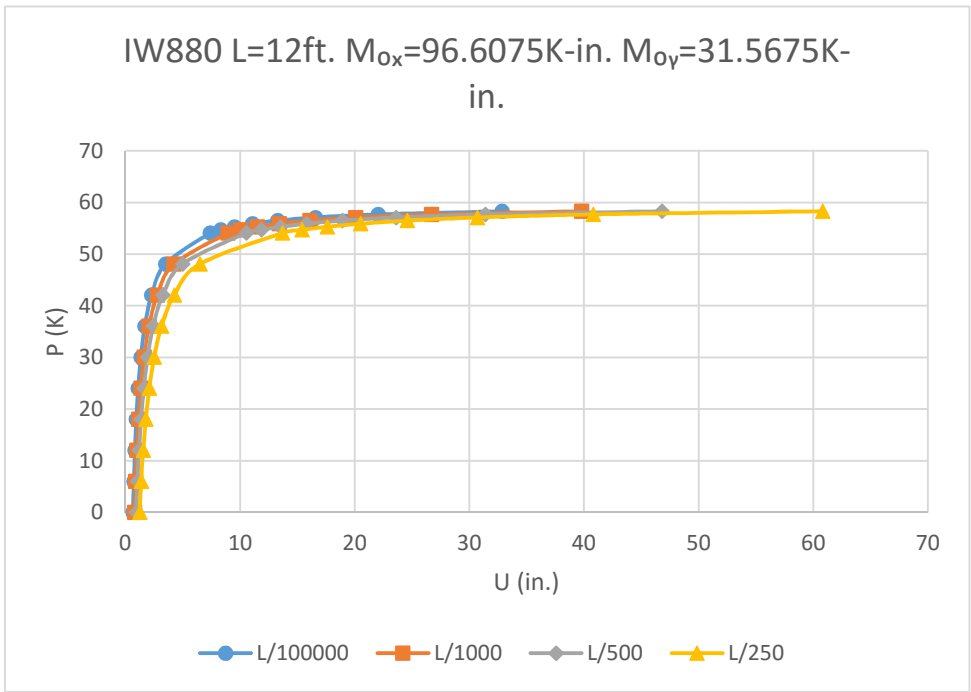


Fig. 112 Load vs. Deflection for biaxial beam-column response

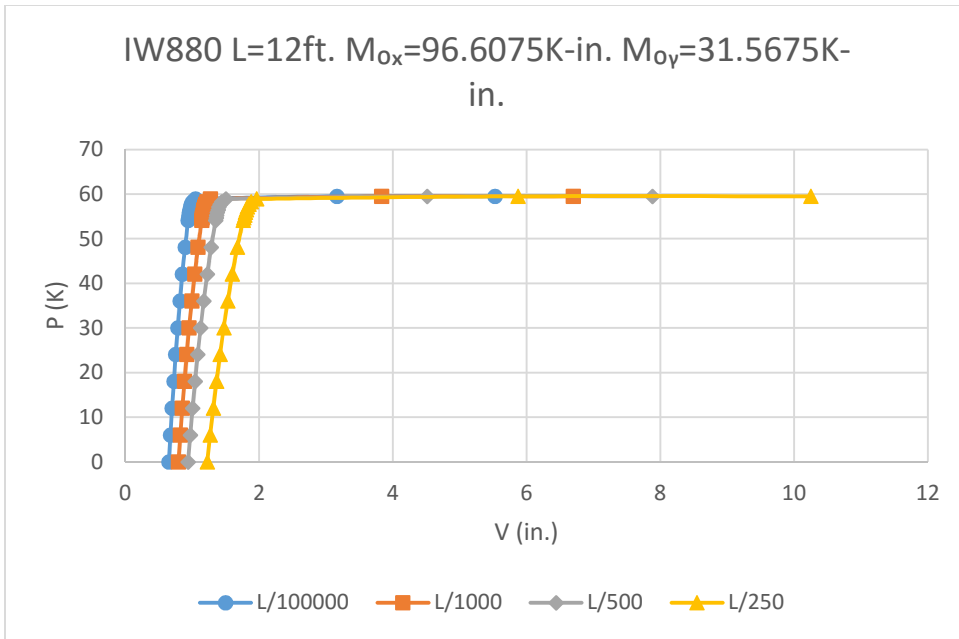


Fig. 113 Load vs. Deflection for biaxial beam-column response

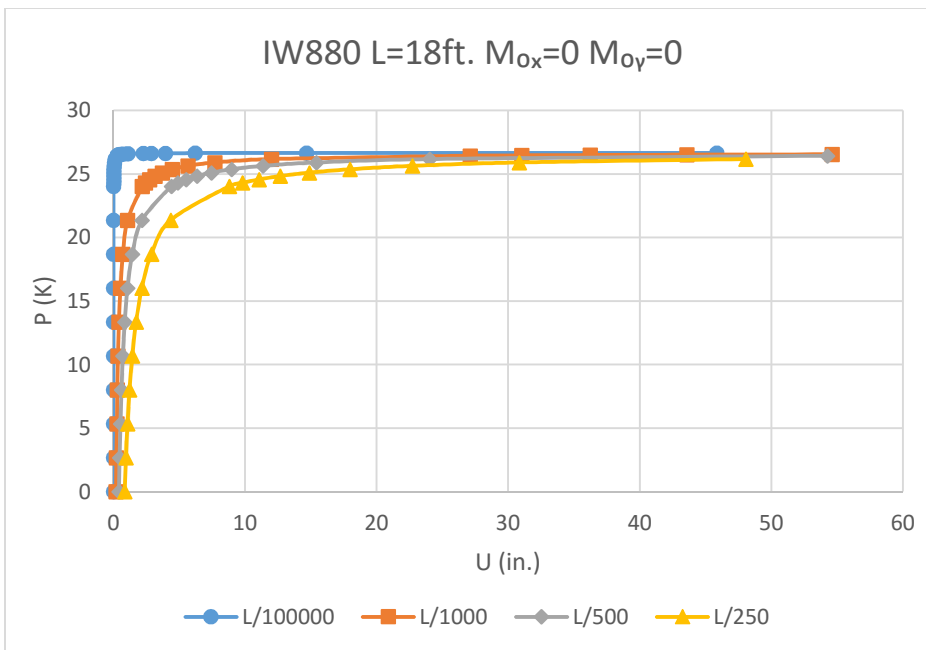


Fig. 114 Load vs. Deflection for biaxial beam-column response

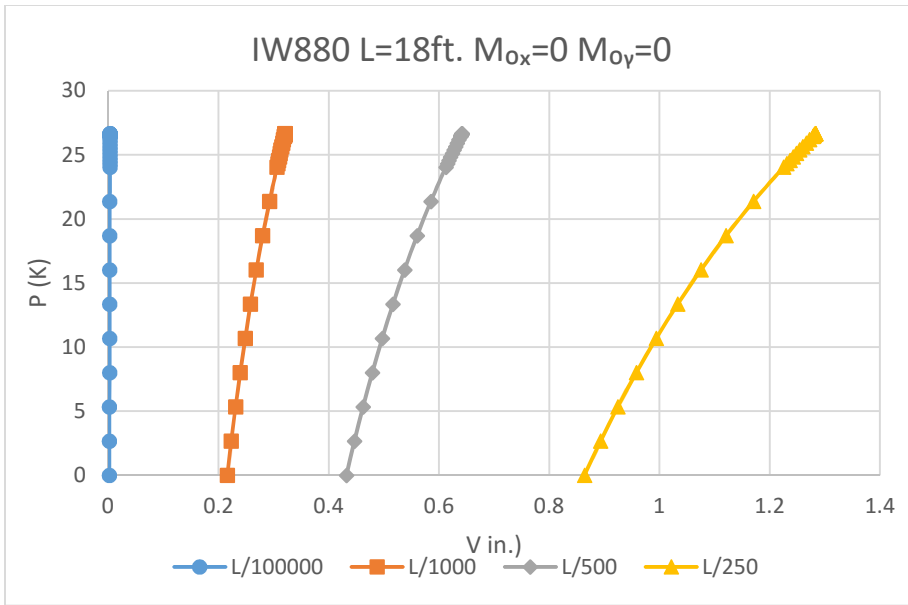


Fig. 115 Load vs. Deflection for biaxial beam-column response

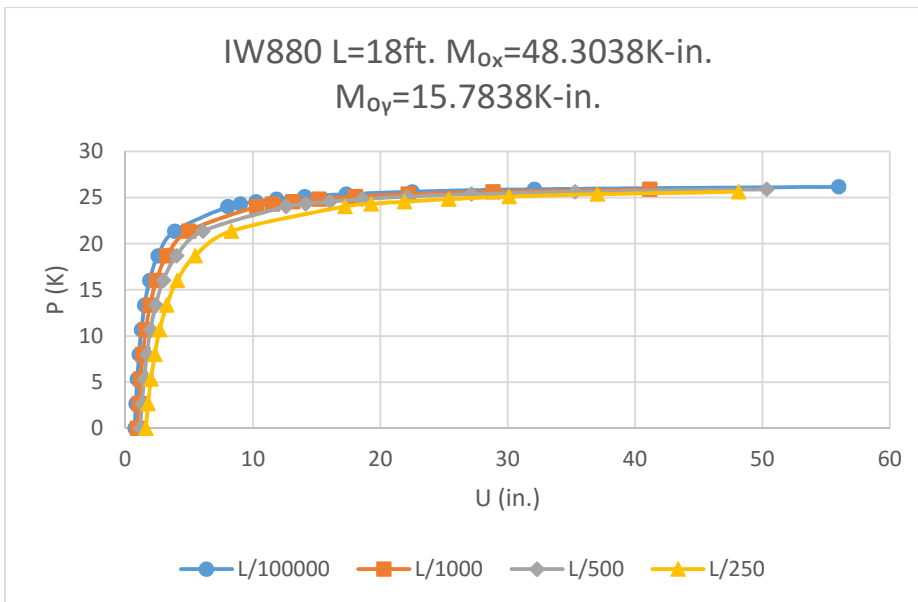


Fig. 116 Load vs. Deflection for biaxial beam-column response

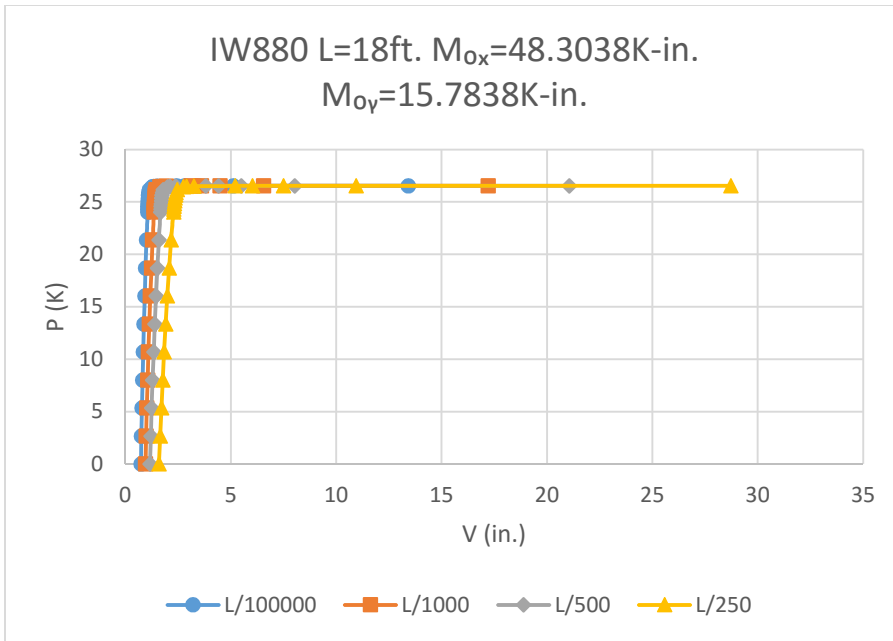


Fig. 117 Load vs. Deflection for biaxial beam-column response

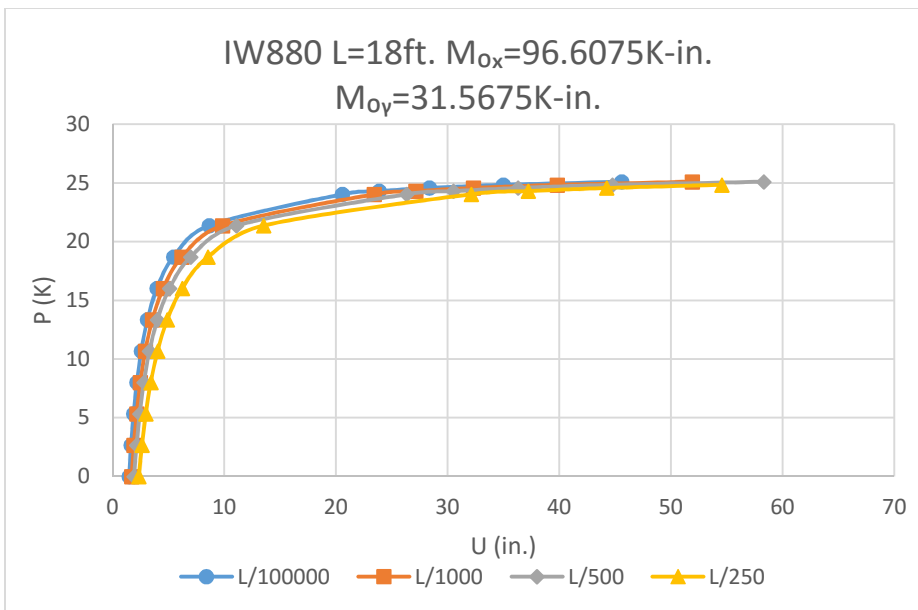


Fig. 118 Load vs. Deflection for biaxial beam-column response

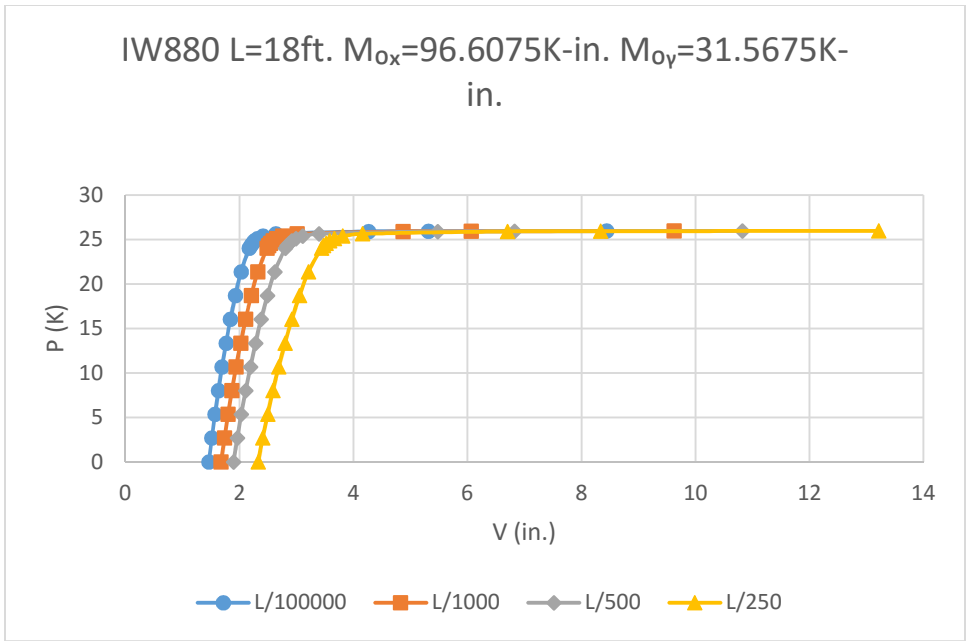


Fig. 119 Load vs. Deflection for biaxial beam-column response

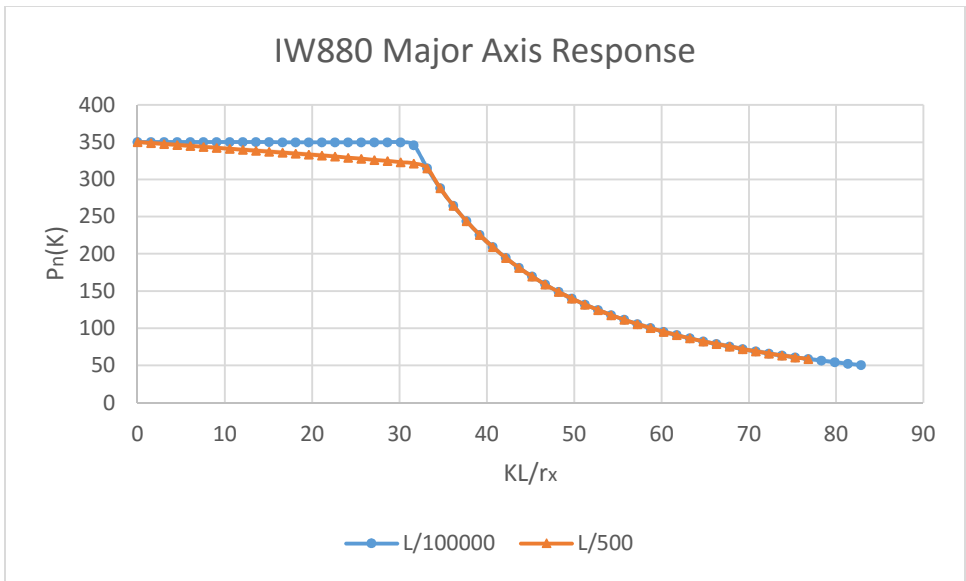


Fig.120 Load vs. slenderness ratio for FDM L/100000 vs. L/500. Major axis response IW880

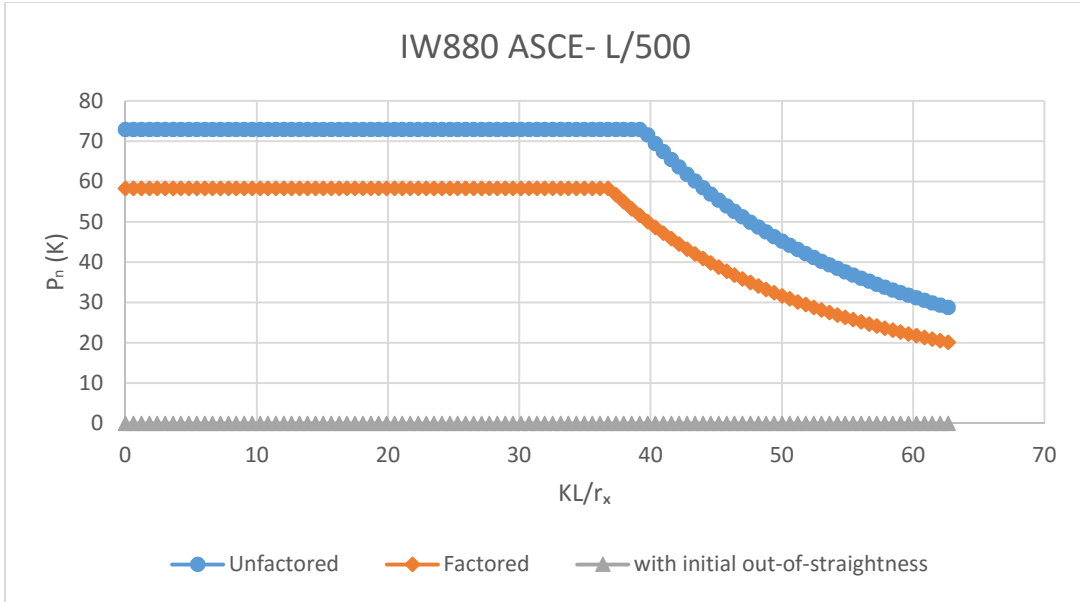


Fig.121 Load vs. slenderness ratio for ASCE Pre-Standard L/500.

Major axis

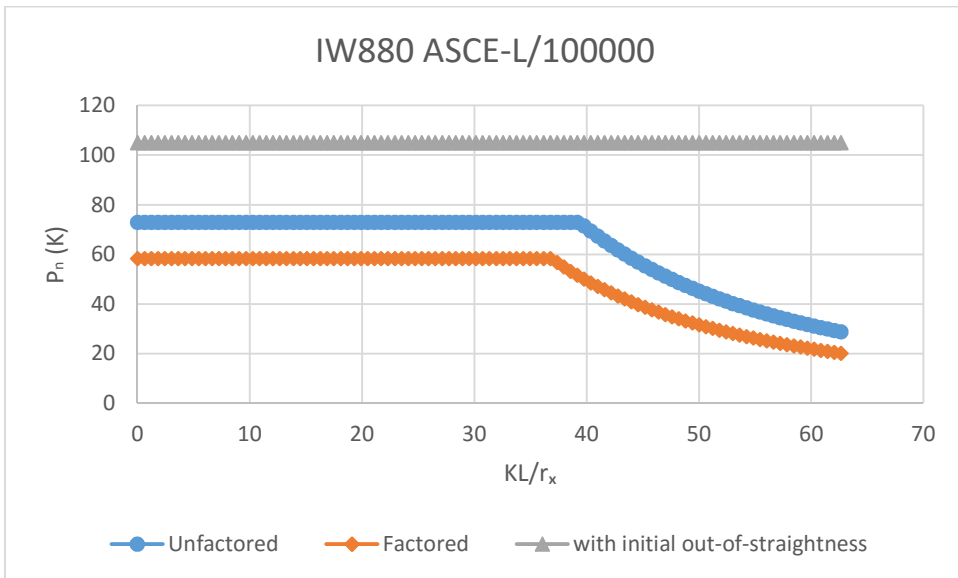


Fig.122 Load vs. slenderness ratio for ASCE Pre-Standard L/500.

Major axis

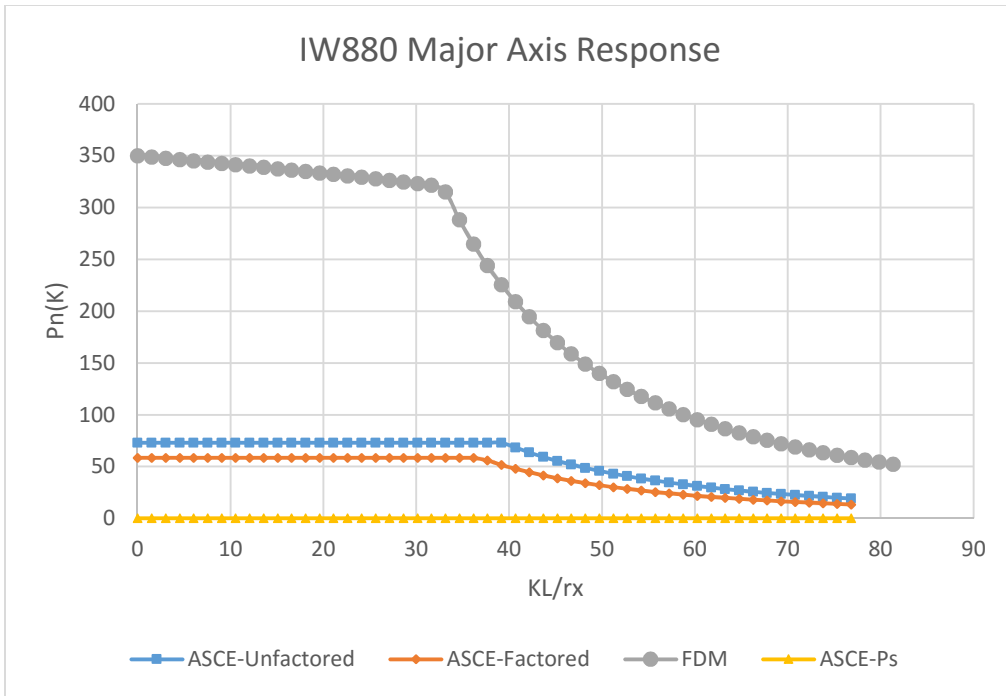


Fig.123 Load vs. slenderness ratio for ASCE LRFD Pre-Standard vs. FDM L/500. Major axis response.

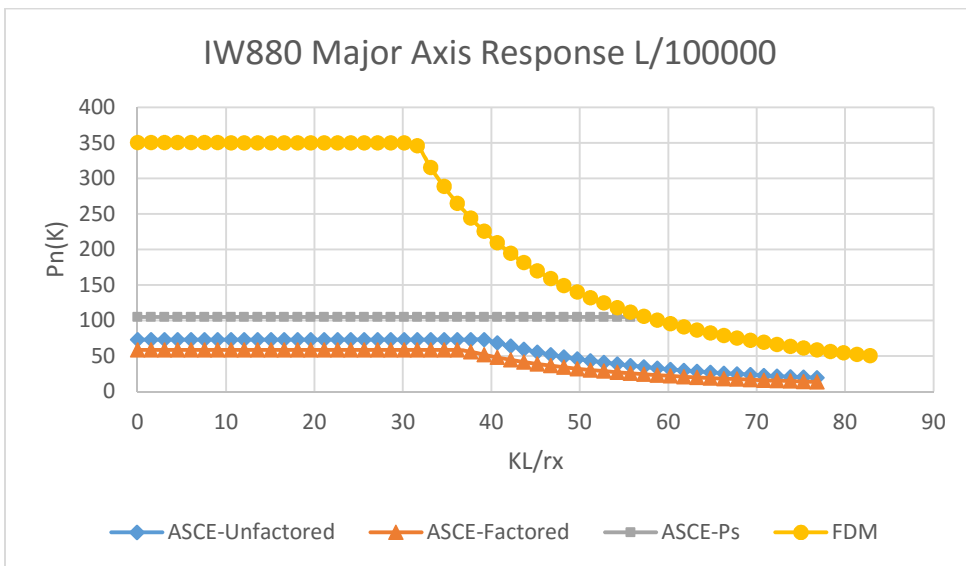


Fig. 124 Load vs. slenderness ratio for ASCE LRFD Pre-Standard vs. FDM L/100000 Major axis response

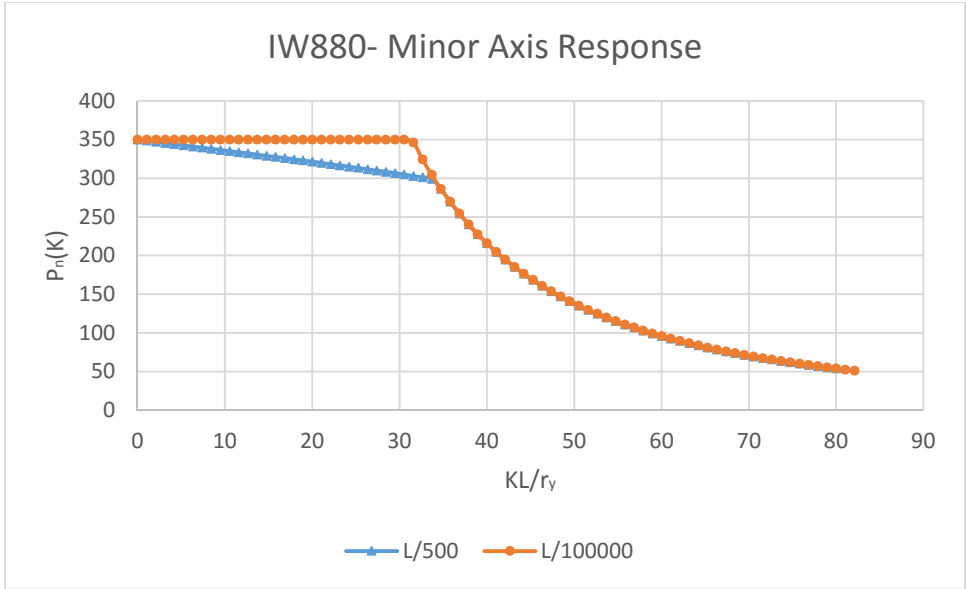


Fig. 125 Slenderness ratio vs. axial load $L/500$ vs. $L/100000$

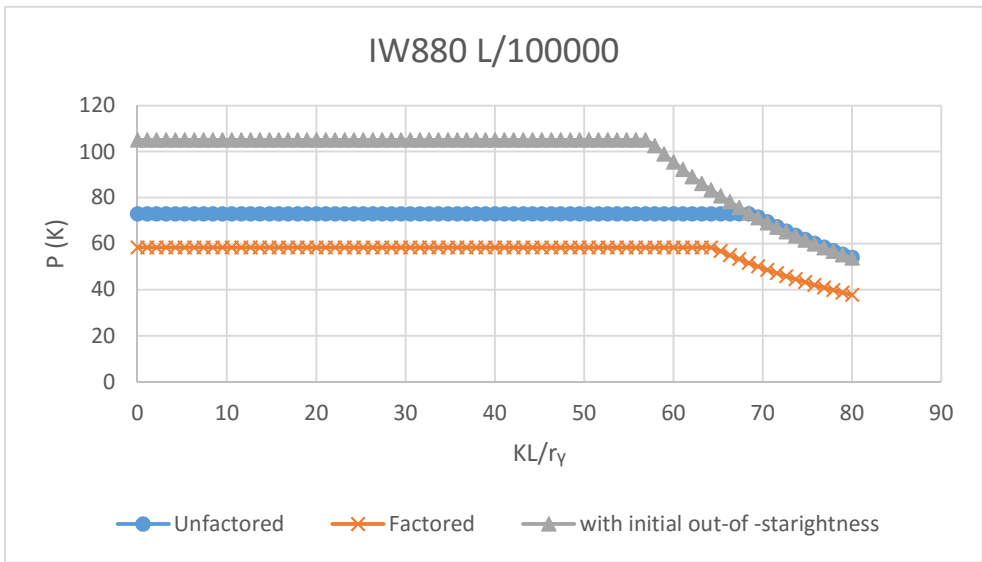


Fig.126 Load vs. slenderness ratio for ASCE LRFD Pre-Standard-minor axis $L/100000$

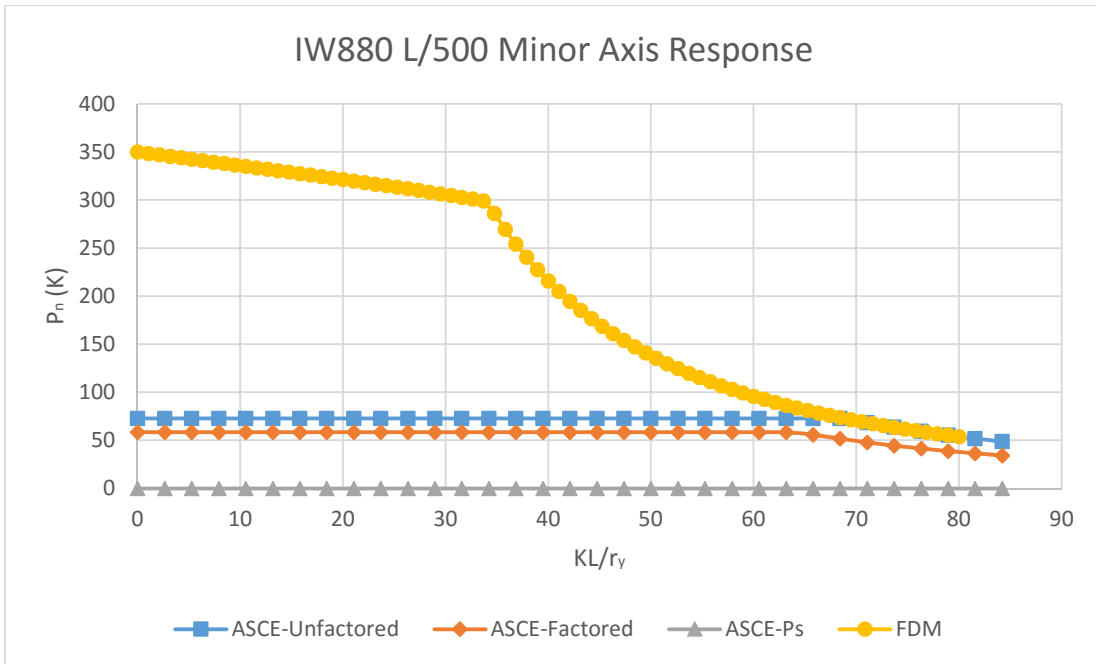


Fig. 127 Load vs. slenderness ratio for ASCE LRFD Pre-Standard vs. FDM- minor axis response L/500

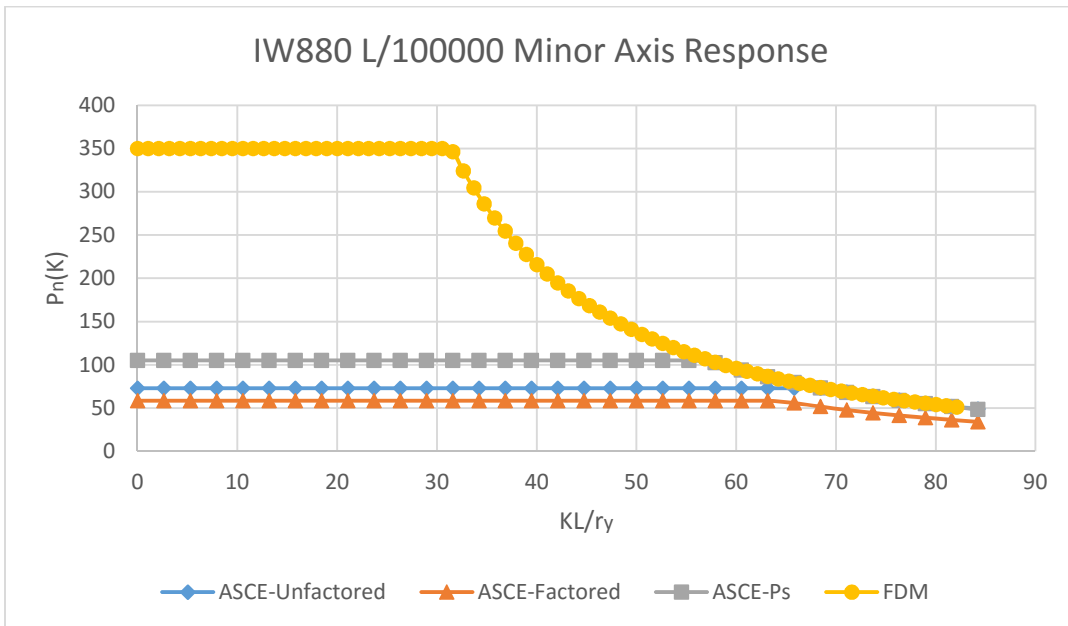


Fig. 128 Load vs. slenderness ratio for ASCE LRFD Pre-Standard vs. FDM- minor axis L/100000

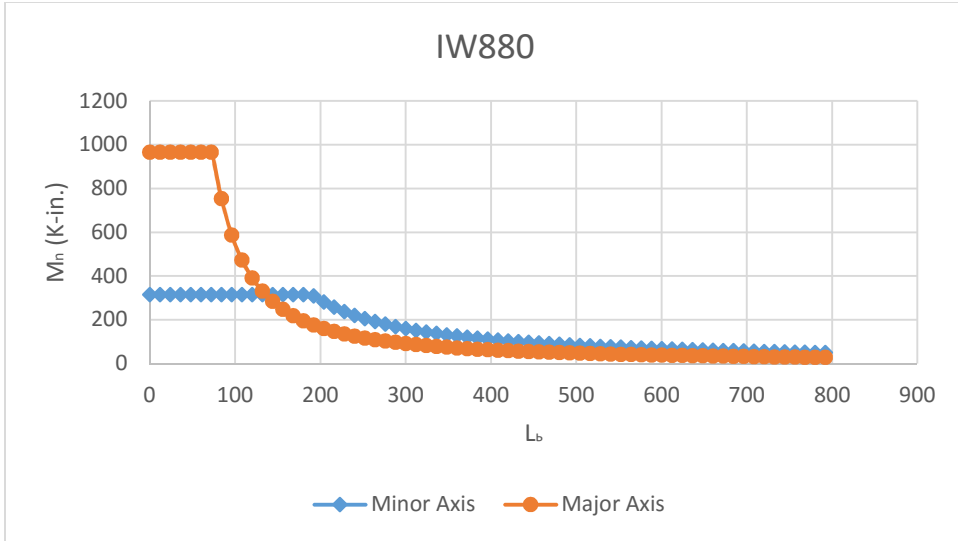


Fig. 129 Moment vs. Length for minor axis vs. Major axis

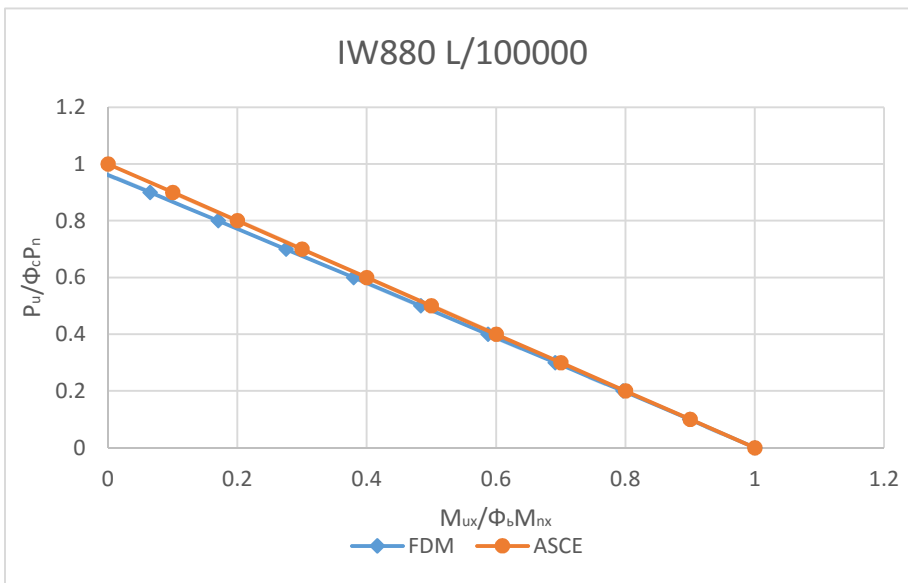


Fig. 130 Load- Moment Interaction for major axis. ASCE LRFD Pre-Standard vs. FDM

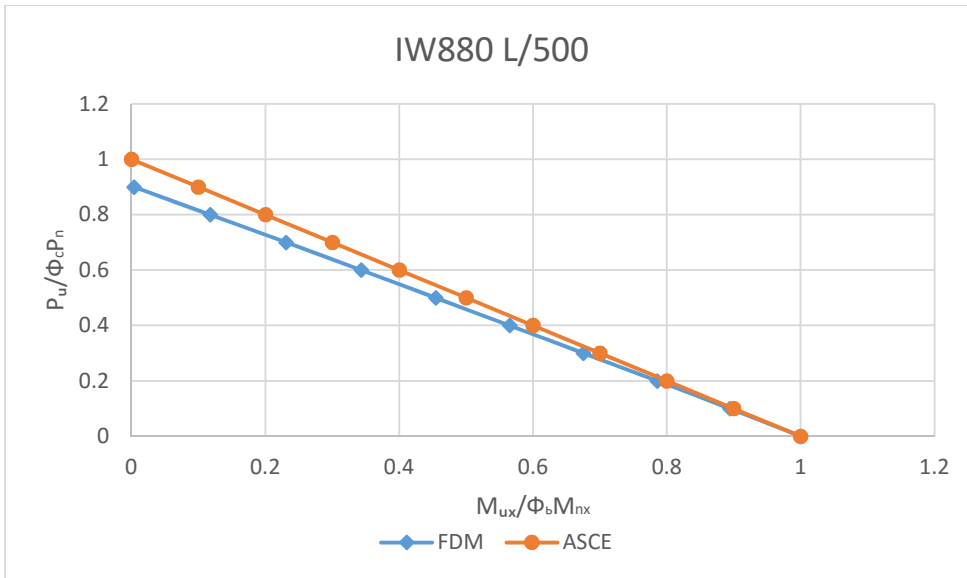


Fig. 131 Load- Moment Interaction for major axis. ASCE LRFD Pre-Standard vs. FDM

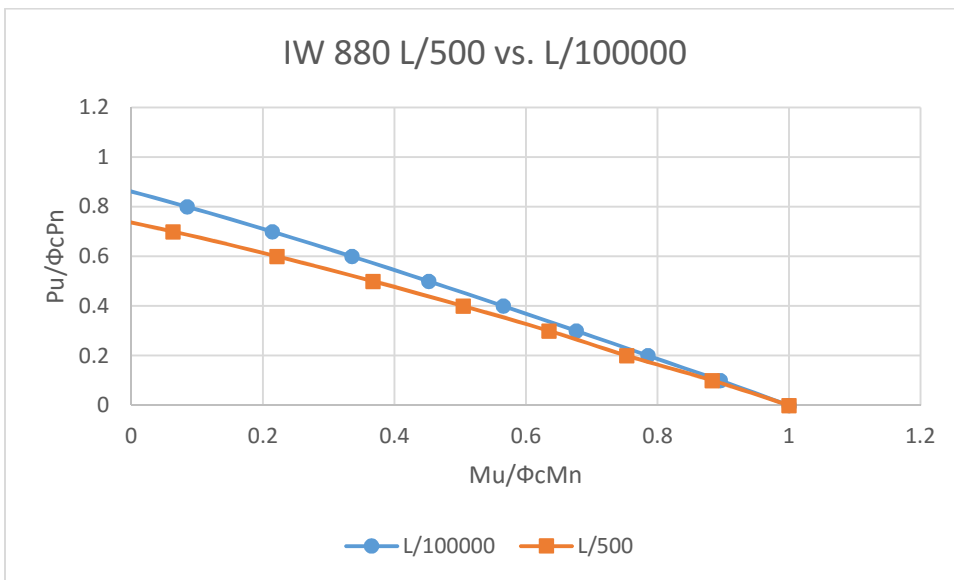


Fig. 132 Load- Moment Interaction for minor axis L/500 vs. L/100000

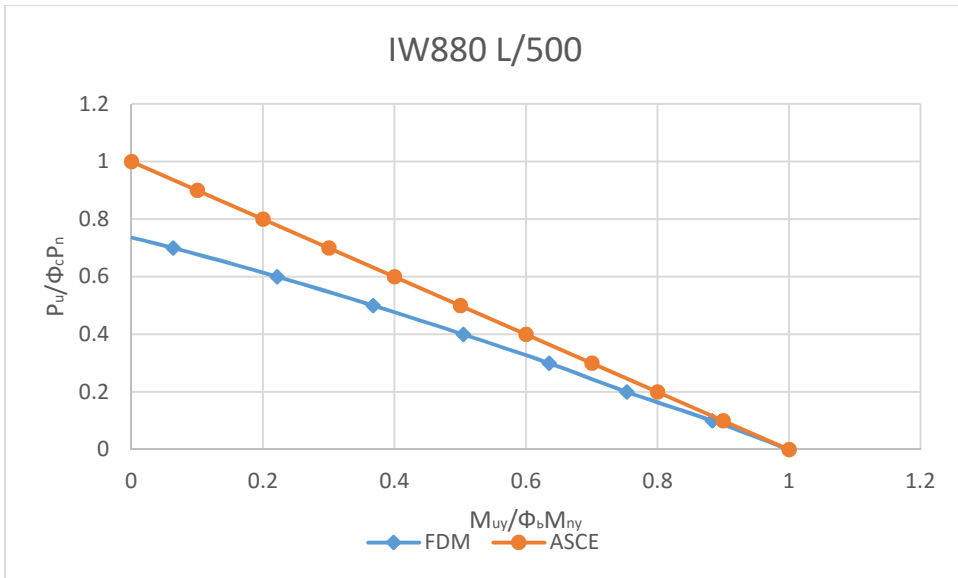


Fig. 133 Load- Moment Interaction for minor axis ASCE LRFD Pre-Standard vs. FDM

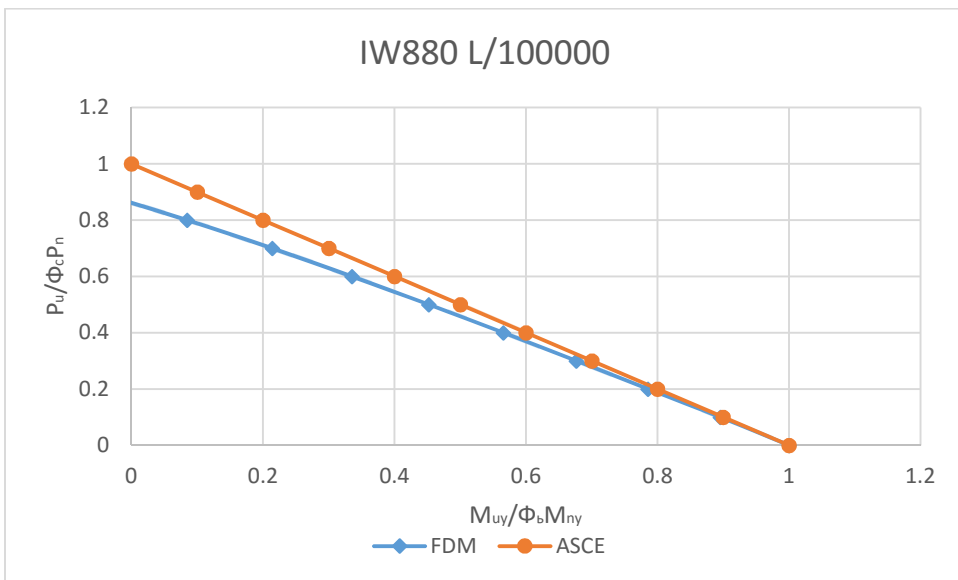


Fig. 134 Load- Moment Interaction for minor axis ASCE LRFD Pre-Standard vs. FDM.

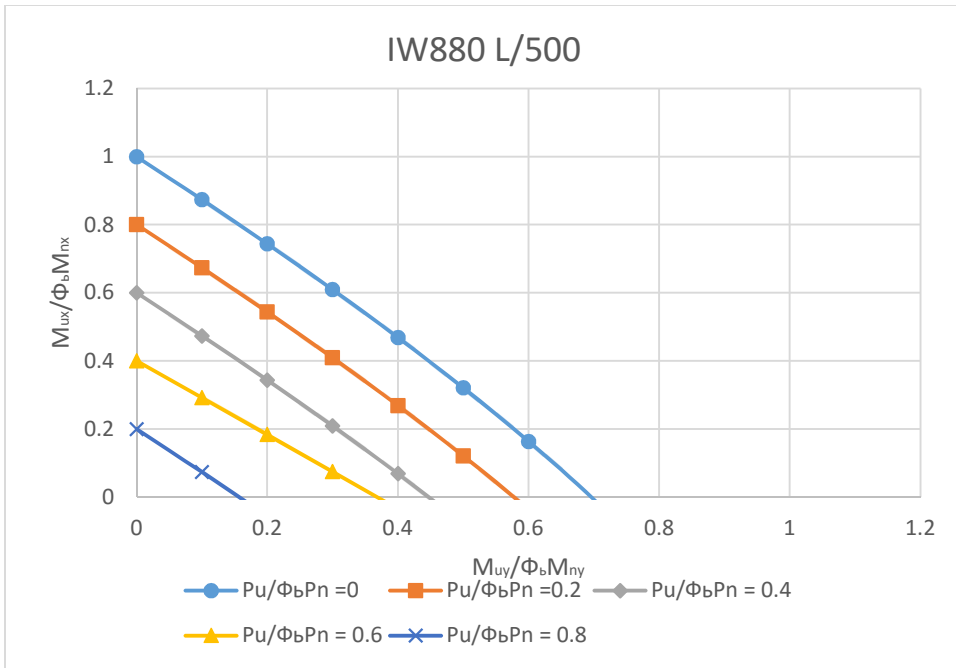


Fig. 135 Moment Interaction for biaxial response. FDM.

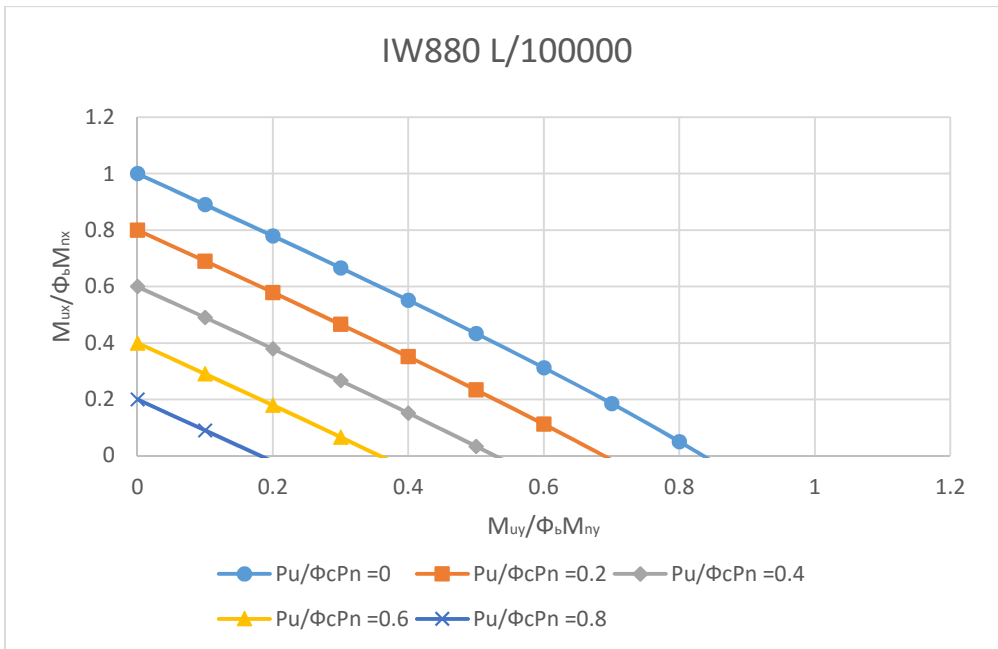


Fig. 136 Moment Interaction for biaxial response. FDM.

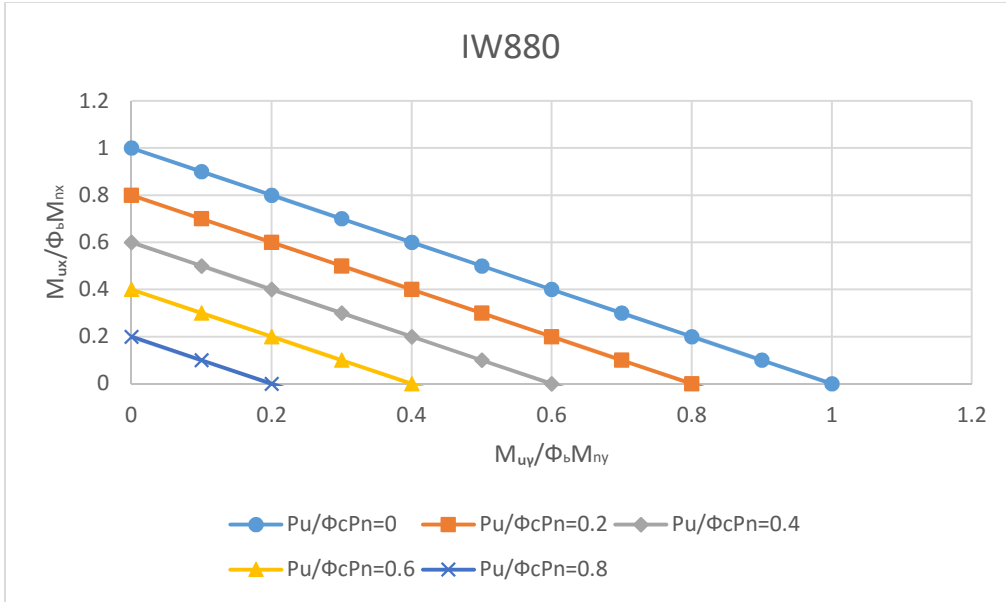


Fig. 137 Moment Interaction for biaxial response. ASCE LRFD Pre-Standard

APPENDIX C

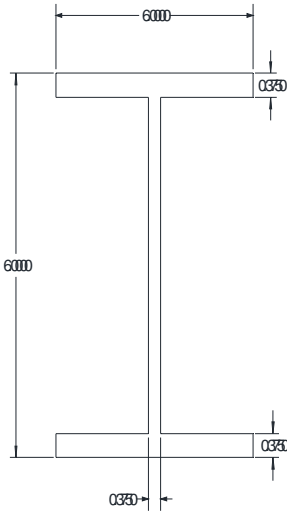


Fig. 1. IW660 Wide Flange Section



Fig. 2. IW880 Wide Flange Section

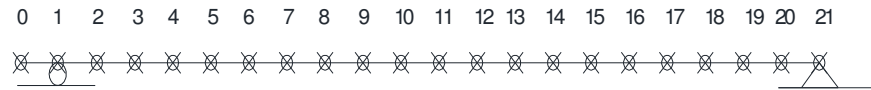


Fig. 3 Finite-Difference Method Nodes



Fig. 8 Case 3.3

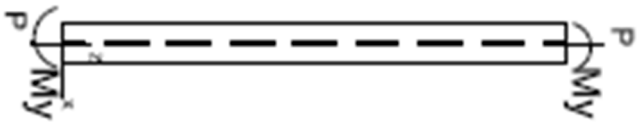
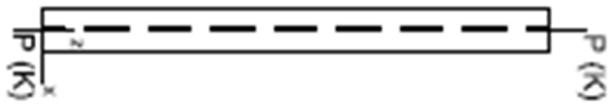


Fig. 4. Case 2.1.1 Fig. 5. Case 2.1.2 Fig. 6. Case 2.2.1 Fig. 7. Case 2.2.2

VITA AUCTORIS

The author received his Bachelor of Science in Civil Engineering from University of Technology – Baghdad in 1991. In 2008 he received Master of Business Administration (MBA) of Finance from South University. He started his Master of Science in Structural Engineering at Old Dominion University in August of 2013.

4313 Rose Glen Place,
Midlothian, VA 23112
(804) 647-5669
Emad.albayati@gmail.com